

A Thesis Submitted for the Degree of PhD at the University of Warwick

Permanent WRAP URL:

<http://wrap.warwick.ac.uk/110782>

Copyright and reuse:

This thesis is made available online and is protected by original copyright.

Please scroll down to view the document itself.

Please refer to the repository record for this item for information to help you to cite it.

Our policy information is available from the repository home page.

For more information, please contact the WRAP Team at: wrap@warwick.ac.uk

Block and Multi block Copolymers *via* SF-RAFT; utilising macromonomers as Chain Transfer Agents

Nikolaos Engelis

**A thesis submitted in partial fulfilment of the requirements of the
degree of
Doctor of Philosophy in Chemistry**

Department of Chemistry

University of Warwick

2018

Table of contents

List of figures.....	iv
List of tables.....	vii
List of schemes.....	ix
Abbreviations.....	x
Acknowledgements.....	xv
Declaration.....	xvii
Abstract.....	xviii
1.1 The “macromolecule” concept.....	1
1.2 Brief history of polymers.....	2
1.3 Free Radical Polymerisation (FRP).....	4
1.3.1 Sequence of events in FRP.....	4
1.3.2 Rate expression/Kinetics of FRP.....	7
1.4 Emulsion polymerisation.....	9
1.4.1 Sequence of events in an emulsion polymerisation.....	12
1.4.2 Kinetics of emulsion polymerisation.....	15
1.5 Catalytic Chain Transfer Polymerisation (CCTP).....	16
1.5.1 Brief History.....	17
1.5.2 Mechanism of CCTP.....	17
1.5.3 CCTP catalysts and their evolution.....	19
1.5.4 Monomers in CCTP.....	20
1.5.5 CCTP in emulsion.....	21
1.5.6 Uses of macromonomers.....	23
1.6 Living anionic Polymerisation.....	25
1.7 “Living”/Reversible Deactivation Radical Polymerisation.....	26
1.7.1 RDRP in emulsion.....	27
1.7.2 Nitroxide-mediated polymerisation (NMP).....	28
1.7.3 Atom transfer radical polymerisation (ATRP).....	29
1.7.4 Single Electron Transfer Living Radical Polymerisation (SET-LRP).....	30
1.7.5 Reversible-Addition-Fragmentation Chain-Transfer Radical Polymerisation (RAFT).....	31
1.7.6 Multi block copolymers and sequence-control.....	33
1.8 References.....	41
2.1 Introduction.....	47

2.2 Results and Discussion	51
2.3 Conclusions	68
2.4 Experimental	69
2.4.1 Materials and Methods.....	69
2.4.2 Instrumentation	69
2.4.3 General procedures	70
2.4.4 Numerical data.....	72
2.5 References	74
3.1 Introduction	78
3.2 Results and Discussion	82
3.2.1 Synthesis of macromonomers/macro chain transfer agents	82
3.2.2 Synthesis of methacrylic diblock copolymers using PMMA, PEMA, PBMA and PBzMA as macromonomers/macro chain transfer agents.....	91
3.2.3 Synthesis of sequence-controlled methacrylic copolymers using PMMA, PEMA, PBMA and PBzMA as macromonomers/chain transfer agents	96
3.2.4 Limitations of sulphur-free RAFT emulsion polymerisation towards narrow dispersity block copolymers.....	103
3.3 Conclusions	108
3.4 Experimental	108
3.4.1 Materials and Methods.....	108
3.4.2 Instrumentation	109
3.4.3 General procedures	110
3.4.4 Numerical data.....	111
3.5 References	114
4.1 Introduction	117
4.2 Initial Results.....	120
4.2.1 Attempts in organic solvent	120
4.2.2 Attempts in mineral oil	125
4.2.3 Kinetics of synthesis (feeding rate 0.1 mL min ⁻¹)	132
4.2.4 Kinetics of synthesis (feeding rate 0.25 mL min ⁻¹)	133
4.2.5 Kinetics of synthesis (feeding rate 0.5 mL min ⁻¹)	134
4.2.6 Summary for the kinetic studies (0.1, 0.25 and 0.5 mL min ⁻¹).....	136
4.3 Conclusions & future work.....	137
4.4 Experimental	137
4.4.1 Materials and Methods.....	137

4.4.1.1 Synthesis of Bis(boron difluorodimethylglyoximate)cobalt (CoBF)	138
4.4.1.2 Synthesis of Bis(boron difluorodimethylphenylglyoximate)cobalt [Co(MePh)BF]	139
Preparation of 4,4'-dimethylbenzyl glyoxime	139
4.4.2 Instrumentation	141
4.4.3 General procedures	142
4.4.3.1 Preparation of CCT agent stock solution for solution polymerisation.....	142
4.4.3.2 CCTP in solution for the synthesis of PMMA macromonomer	142
4.4.3.3 Comb copolymer synthesis in solution	143
4.5 References	143
Conclusions & Outlook.....	144

List of figures

Figure 1.1: History of the development of common industrial polymeric materials.	3
Figure 1.2: Schematic representation of the variation of conversion with time for an emulsion polymerisation system. t_I and t_{II} are the completion times for intervals I and II respectively.	14
Figure 2.1: Structure of multi block copolymers synthesised in this work. All multi block copolymers were prepared at 85 °C (in a 0.5 L reactor under monomer starved conditions) <i>via</i> the segregation approach of emulsion polymerisation utilising aqueous potassium persulfate (KPS) as initiator and PMMA ($\sim 2000 \text{ g mol}^{-1}$) as the initial chain transfer agent. (a) Structure of the heneicosablock homopolymer utilising BMA as the model monomer ($DP_n = 10$ per block, on average 2 h per block), (b) structure of the heneicosablock multi block copolymer consisting of BMA, BzMA, EHMA and MMA ($DP_n = 10$ per block, on average 2 h per block), (c) structure of higher molecular weight heptablock multi block copolymer consisting of BMA, BzMA, EHMA and MMA ($DP_n = 45$ per block) and (d) structure of the undecablock multi block copolymer altering the monomer sequence and composition throughout the polymerisation ($DP_n = i = 1105i$ per block).....	50
Figure 2.2: (a) ^1H NMR trace of the PMMA macromonomer obtained <i>via</i> CCTP in emulsion and (b) MALDI spectra of the of the PMMA macromonomer obtained <i>via</i> CCTP in emulsion.	52
Figure 2.3: Typical set up for the synthesis of macromonomers or multi block copolymers employing a double jacketed reactor and securing a constant monomer addition rate by the use of a syringe pump.	55
Figure 2.4: Synthesis and characterisation of model heneicosablock BMA homopolymer. (a) SEC traces of molecular weight distributions for consecutive cycles during the synthesis of the heneicosablock homopolymer, (b) ^1H NMR spectra for consecutive cycles, (c) hydrodynamic diameter evolution of the heneicosablock homopolymer, as obtained by Z-average measurements versus the number average molecular weight (M_n) as measured by DLS and (d) evolution of theoretical (black straight line) and experimental molecular weight M_n (\blacktriangle) and M_w (\blacksquare) determined by SEC and M_w/M_n (\bullet) versus the number of cycles during synthesis of heneicosablock homopolymer.	57
Figure 2.5: ^1H NMR traces of the of the PMMA macromonomer obtained <i>via</i> CCTP in emulsion and the residual MMA monomer.	59
Figure 2.6: Synthesis and characterisation of model heneicosablock BMA homopolymer. (a) SEC traces of molecular weight distributions for consecutive cycles during the synthesis of the heneicosablock copolymer, (b) ^1H NMR spectra for consecutive cycles, (c) hydrodynamic diameter evolution of the heneicosablock copolymer, as obtained by Z-average measurements versus the number average molecular weight (M_n) as measured by DLS and (d) evolution of dispersity (\mathcal{D}) values for consecutive cycles.	61
Figure 2.7: Scalable synthesis of the high molecular weight hexablock copolymer. (a) Image of the double jacketed 0.5 L reactor utilised for the high scale synthesis and (b) total amount of material/product obtained after 6 successive additions.	64
Figure 2.8: (a) hydrodynamic diameter evolution of the heptablock homopolymer, as obtained by Z-average measurements versus the number average molecular weight (M_n) as measured by DLS, (b) ^1H NMR traces for the synthesis of the heptablock copolymer following various patterns, (c) SEC and (d) dispersity (\mathcal{D}) as a function of the number of cycles for the heptablock copolymer The copolymer consists of BMA, BzMA, EHMA and MMA at 85 °C (in a 0.5 L reactor applying monomer starved	

conditions) <i>via</i> a segregation approach of emulsion polymerisation utilizing KPS as initiator and PMMA $\sim 2000 \text{ g mol}^{-1}$ as the initial chain transfer agent.	65
Figure 2.9: (a) SEC, (b) ^1H NMR traces for the synthesis of the undecablock copolymer following various patterns, (c) hydrodynamic diameter evolution of the undecablock homopolymer, as obtained by Z-average measurements versus the number average molecular weight (M_n) as measured by DLS and (d) dispersity (\mathcal{D}) as a function of the number of cycles for the undecablock copolymer The copolymer consists of BMA, BzMA, EHMA and MMA at 85 °C (in a 0.5 L reactor applying monomer starved conditions) <i>via</i> a segregation approach of emulsion polymerisation utilizing KPS as initiator and PMMA $\sim 2000 \text{ g mol}^{-1}$ as the initial chain transfer agent.	68
Figure 3.1: SEC chromatograms of the PMMA macromonomers synthesised by various amounts of CoBF.	84
Figure 3.2: ^1H NMR spectrum of the PMMA macromonomer synthesised <i>via</i> CCTP in emulsion and the MMA monomer.	84
Figure 3.3: (a) MALDI-ToF MS spectrum of the PMMA macromonomer synthesised <i>via</i> CCTP in emulsion and (b) Expanded MALDI-ToF MS spectrum of the PMMA macromonomer.	85
Figure 3.4: (a) MALDI-ToF MS spectrum of the PEMA macromonomer synthesised <i>via</i> CCTP in emulsion and (b) Expanded MALDI-ToF MS spectrum of the PEMA macromonomer.	86
Figure 3.5: SEC chromatograms of the PEMA macromonomers synthesised by various amounts of CoBF.	87
Figure 3.6: SEC chromatograms of the PBMA macromonomers synthesised by various amounts of Co(MePh)BF.	89
Figure 3.7: SEC chromatogram of the PBzMA macromonomers synthesised by various amounts of Co(MePh)BF.	89
Figure 3.8: (a) MALDI-ToF MS spectrum of the PBMA macromonomer synthesised <i>via</i> CCTP in emulsion and (b) Expanded MALDI-ToF MS spectrum of the PBMA macromonomer.	90
Figure 3.9: (a) MALDI-ToF MS spectrum of the PBzMA macromonomer synthesised <i>via</i> CCTP in emulsion and (b) Expanded MALDI-ToF MS spectrum of the PBzMA macromonomer.	90
Figure 3.10: SEC chromatograms of the samples taken during the free radical polymerisation of BMA in the presence of PMMA macromonomer.	92
Figure 3.11: SEC chromatograms of the samples taken during the free radical polymerisation of BMA in the presence of PBMA macromonomer.	93
Figure 3.12: (a) SEC traces of molecular weight distributions for the diblock macromonomers formed by different CTAs ($DP_n=80$ BMA) and (b) SEC traces of molecular weight distributions for the diblock macromonomers formed by different CTAs ($DP_n=400$ BMA).	95
Figure 3.13: SEC chromatograms of the PMMA macromonomer and the corresponding P(MMA $_n$ - <i>b</i> -BMA $_{80}$) diblock prepared in emulsion using tap water.	96
Figure 3.14: SEC traces of consecutive monomer additions for the preparation of the undecablock copolymer utilising PBMA macromonomer as CTA.	98
Figure 3.15: ^1H NMR spectra for consecutive cycles during synthesis of the undecablock copolymer utilising PBMA macromonomer as CTA.	98
Figure 3.16: (a) SEC traces of consecutive monomer additions for the preparation of the nonablock copolymer ($DP_n=25$ per block) utilising PEMA macromonomer as CTA and (b) ^1H NMR spectra for consecutive cycles during synthesis of the nonablock copolymer (values to the right indicate the number of sequential monomer additions carried out prior to collection of the spectrum).	100

Figure 3.17: ^1H NMR spectra for consecutive cycles during synthesis of the nonablock copolymer utilising PBzMA macromonomer as CTA.....	101
Figure 3.18: SEC traces of consecutive monomer additions for the preparation of the nonablock copolymer utilising PBzMA macromonomer as CTA.	102
Figure 3.19: SEC traces of consecutive monomer additions for the preparation of the tetrablock copolymer utilising high M_n PMMA macromonomer as CTA.	104
Figure 3.20: SEC traces of consecutive monomer additions for the preparation of the pentablock copolymer utilising high M_n PBMA macromonomer as CTA.	105
Figure 3.21: SEC traces of the PMMA macromonomer and the corresponding P(MMA $_n$ - b -iBMA $_{80}$) diblock prepared in emulsion.	106
Figure 3.22: THF SEC traces of the pMMA macromonomer and the corresponding P(MMA $_n$ - b -TFEMA $_{80}$) diblock prepared in emulsion.	107
Figure 4.1: SEC analysis of different MWt PLMA macromonomers, synthesised by diverse amounts of catalyst. The dot line shows the trace of the monomer.....	121
Figure 4.2: The 0.5 L reactor equipped with overhead stirrer, used for the synthesis of the methacrylic macromonomer in large scale.	123
Figure 4.3: SEC analysis of PLMA macromonomers, synthesised in 20 and 200 mL monomer scale using the same amount of catalyst.....	123
Figure 4.4: CHCl $_3$ SEC traces of the combs produced by different ratios of n -BA to macromonomer.	125
Figure 4.5: ^1H NMR spectrum of the reaction mixture of the macromonomer synthesis. Residual monomer peaks are visible.....	128
Figure 4.6: ^1H NMR spectrum of the final product of comb synthesis. The absence of peaks between 5 and 6.5 ppm indicate the complete conversion of all monomers and the macromonomer.	129
Figure 4.7: CHCl $_3$ SEC traces of comb copolymers synthesised in mineral oil. The low molecular weight, narrow peak is the mineral oil employed as solvent.	130
Figure 4.8: ^1H NMR spectrum of the reaction mixture during the addition of n -BA. The narrow peak at 6.21 ppm corresponding to the macromonomer allowed monitoring during the kinetic study. ..	131
Figure 4.9: CHCl $_3$ SEC traces showing the evolution of molecular weight during the addition of acrylate by 0.1 mL min $^{-1}$ rate.	133
Figure 4.10: CHCl $_3$ SEC traces showing the evolution of molecular weight during the addition of acrylate by 0.25 mL min $^{-1}$ rate.	134
Figure 4.11: CHCl $_3$ SEC traces showing the evolution of molecular weight during the addition of acrylic monomer by 0.5 mL min $^{-1}$ rate.	135
Figure 4.12: Evolution of \bar{D} in function with the eq of n -BA added for the three different addition rates. The cycles on the graph indicate the point where full macromonomer conversion was observed.	136

List of tables

Table 2.1: Summary of the multi block copolymers synthesised in this study.	51
Table 2.2: Characterisation data for the synthesis of the tetracosablock PBMA homopolymer in emulsion at 85 °C with potassium persulfate as initiator.....	58
Table 2.3: Characterisation data for the synthesis of the tetracosablock copolymer in emulsion at 85 °C with potassium persulfate as initiator.....	62
Table 2.4: Characterisation data for the synthesis of the heptablock copolymer in emulsion at 85 °C with potassium persulfate as initiator.	64
Table 2.5: Characterisation data for the synthesis of the undecablock copolymer in emulsion at 85 °C with potassium persulfate as initiator.	67
Table 2.6: Experimental conditions used for the preparation of the tetracosablock PBMA homopolymer in emulsion at 85 °C with potassium persulfate as initiator.	72
Table 2.7: Experimental conditions used for the preparation of the tetracosablock copolymer in emulsion at 85 °C with potassium persulfate as initiator.....	73
Table 2.8: Experimental conditions used for the preparation of the heptablock copolymer in emulsion at 85 °C with potassium persulfate as initiator.....	73
Table 2.9: Experimental conditions used for the preparation of the undecablock copolymer in emulsion at 85 °C with potassium persulfate as initiator.....	74
Table 3.1: Synthesis and characterisation data for the PMMA macromonomers synthesised in this study.....	83
Table 3.2: Synthesis and characterisation data for the PEMA macromonomers synthesised in this study.....	86
Table 3.3: Synthesis and characterisation data for the PBMA macromonomers synthesised in this study.....	88
Table 3.4: Synthesis and characterisation data for the PBzMA macromonomer synthesised in this study.....	88
Table 3.5: Data for the free radical polymerisation of BMA in emulsion in the presence of PMMA macromonomer.	91
Table 3.6: Data for the free radical polymerisation of BMA in emulsion in the presence of PBMA macromonomer.	93
Table 3.7: Synthesis and characterisation data for the diblock copolymers ($DP_n=80$) synthesised by the use of different CTAs.	94
Table 3.8: Data for the free radical polymerisation of BMA in emulsion in the presence of PMMA, PEMA, PBzMA and PBMA macromonomer ($DP_n=400$).	95
Table 3.9: Characterisation data for the free radical polymerisation of BMA in the presence of PMMA macromonomer ($DP_n=80$) in emulsion using tap water.	96
Table 3.10: Characterisation data for the synthesis of the undecablock copolymer in emulsion at 85 °C with potassium persulfate as initiator, utilising PBMA macromonomer as CTA.	99
Table 3.11: Characterisation data for the synthesis of the nonablock copolymer in emulsion at 85 °C with potassium persulfate as initiator, utilising PEMA macromonomer as CTA.	100
Table 3.12: Characterisation data for the synthesis of the nonablock copolymer in emulsion at 85 °C with potassium persulfate as initiator, utilising PBzMA macromonomer as CTA.	102

Table 3.13: Characterisation data for the synthesis of the tetrablock copolymer in emulsion at 85 °C with potassium persulfate as initiator, utilising high M_n PMMA macromonomer as CTA.	103
Table 3.14: Characterisation data for the synthesis of the pentablock copolymer in emulsion at 85 °C with potassium persulfate as initiator, utilising PBMA macromonomer as CTA.	105
Table 3.15: Characterisation data for the free radical polymerisation of <i>t</i> BMA in the presence of PMMA macromonomer ($DP_n=80$) in emulsion.	106
Table 3.16: Data for the free radical polymerisation of TFEMA in the presence of PMMA macromonomer ($DP_n=80$) in emulsion.	107
Table 3.17: Characterisation data for the macromonomers synthesised <i>via</i> CCTP in emulsion and subsequently employed as CTAs in free radical polymerisation of BMA ($DP_n=80$) in emulsion.	111
Table 3.18: Experimental conditions used for the preparation of the undecablock copolymer in emulsion at 85 °C with potassium persulfate as initiator, utilising PBMA macromonomer as CTA...	112
Table 3.19: Experimental conditions used for the preparation of the nonablock copolymer in emulsion at 85 °C with potassium persulfate as initiator, utilising PEMA macromonomer as CTA...	112
Table 3.20: Experimental conditions used for the preparation of the nonablock copolymer in emulsion at 85 °C with potassium persulfate as initiator, utilising PBzMA macromonomer as CTA.	113
Table 3.21: Experimental conditions used for the preparation of the tetrablock copolymer in emulsion at 85 °C with potassium persulfate as initiator, utilising high M_n PMMA macromonomer as CTA.	113
Table 3.22: Experimental conditions used for the preparation of the pentablock copolymer in emulsion at 85 °C with potassium persulfate as initiator, utilising PBMA macromonomer as CTA...	113
Table 4.1: Characterisation data for the synthesis of PLMA macromonomers in EMK.	121
Table 4.2: Summary of results for the synthesis of combs.....	125
Table 4.3: Summary of results for the synthesis of combs in mineral oil.....	129
Table 4.4: Summary of results for the synthesis of combs in mineral oil (feeding rate 0.1 mL min ⁻¹).	132
Table 4.5: Summary of results for the synthesis of combs in mineral oil (feeding rate 0.25 mL min ⁻¹).	133
Table 4.6: Summary of results for the synthesis of combs in mineral oil (feeding rate 0.5 mL min ⁻¹).	135
Table 4.7: Summary of results for the kinetic experiments. Characterisation data correspond to the samples taken at points of full macromonomer conversion.	137

List of schemes

Scheme 1.1: General conception of the CCTP of a α -methyl monomer leading to the formation of a vinyl terminated polymer (macromonomer).....	16
Scheme 1.3: d electron configurations of d^7 Co(II) in low (left) and high spin (right).....	19
Scheme 1.4: Structures of Co ^{II} hematoporphyrin tetramethyl ether and first and second generation Co ^{II} cobaloximes.....	20
Scheme 1.5: General properties for monomers of high and low CCTP activity	21
Scheme 1.6: The addition-fragmentation mechanism in the copolymerisation of methacrylic macromonomers with methacrylates. ²	24
Scheme 1.8: Proposed mechanism for NMP. ⁶²	28
Scheme 1.9: Widely accepted mechanism for ATRP. ⁵⁵	29
Scheme 1.10: Proposed mechanism for SET-LRP. ⁷⁸	31
Scheme 1.11: Proposed mechanism for RAFT polymerisation. ⁹³	32
Scheme 2.1: Proposed mechanisms of (a) CCTP and (b) addition-fragmentation reaction.....	53
Scheme 2.2: Conceptual scheme for the synthesis of multi block copolymers in emulsion.....	54
Scheme 3.1: Complete mechanism of SF-RAFT in emulsion. (a) Initial macromonomer formation <i>via</i> CCTP in emulsion (b) Compartmentalisation effect during the formation of primary radicals (c) Controlled chain extension in the polymer particles and (d) Sequential chain extensions <i>via</i> SF-RAFT.	81
Scheme 3.2: Schematic diagram showing the concept of the synthesis of sequence-controlled multi block copolymers by the use of macromonomers as macro chain transfer agents (CTA). Catalyst type and concentration are optimised as to provide macromonomers of the desired M_n which subsequently serve as CTA in the free radical polymerisation of methacrylic monomers.	82
Scheme 3.3: Proposed mechanism for CCTP. ⁴⁴	85
Scheme 4.1: Proposed mechanism for the graft copolymerisation of <i>n</i> -BA with methyl methacrylate macromonomer. ⁴	118
Scheme 4.2: Chemical structures of lauryl methacrylate (LMA) and mixture of methacrylic monomers used in industry.....	120
Scheme 4.3: Structures of the cobaloximes tested for solubility in mineral oil.....	126
Scheme 4.4: General scheme for the synthesis of CoBF.	139
Scheme 4.5: General scheme for the synthesis of Co(MePh)BF.	141

Abbreviations

°C	degrees Celsius
AIBN	a,a'-Azobisisobutyronitrile
ATRP	Atom transfer radical polymerisation
BA	Butyl acrylate
BMA	Butyl methacrylate
BzMA	Benzyl methacrylate
CCTP	Catalytic chain transfer polymerisation
CDCl₃	Deuterated chloroform
CHCl₃	Chloroform
CLRP	Controlled living radical polymerisation
CMC	Critical micelle concentration
CoBF	Bis[difluoroboryldimethylglyoximato] cobalt(II)
Co(MePh)BF	Bis[difluoroboryldimethylphenylglyoximato] cobalt(II)
Co(Ph)BF	Bis[difluoroboryldiphenylglyoximato] cobalt(II)
CTA	Chain transfer agent
CVA	4,4'-Azobis(4-cyanovaleric acid)
DLS	Dynamic light scattering
DMSO	Dimethyl sulfoxide
DNA	Deoxyribonucleic acid
DP_n	Degree of polymerisation
EHMA	2-Ethyl hexyl methacrylate
EMA	Ethyl methacrylate

EMK	Ethyl methyl ketone
FRP	Free radical polymerisation
H	Hours
<i>i</i>BMA	Isobutyl methacrylate
IUPAC	International union of pure and applied chemistry
k_d	Rate constant of initiator decomposition
k_i	Rate constant of initiation
k_p	Rate constant of propagation
KPS	Potassium Persulfate
k_t	Rate constant of termination
LMA	Lauryl methacrylate
MA	Methyl acrylate
MALDI-TOF	Matrix assisted laser desorption ionisation-time of flight
mCTA	Macrochain transfer agent
Me₆TREN	<i>N,N,N',N',N'',N''</i> -Hexamethyl-[tris(aminoethyl)amine]
Min	Minutes
MMA	Methyl methacrylate
M_n	Number-average molecular weight
M_w	Weight-average molecular weight
MWt	Molecular weight
NMP	Nitroxide mediated polymerisation
NMR	Nuclear magnetic resonance spectroscopy
PBMA	Poly(butyl methacrylate)
PBzMA	Poly(benzyl methacrylate)

PE	Poly(ethylene)
PEMA	Poly(ethyl methacrylate)
PLMA	Poly(lauryl methacrylate)
PMMA	Poly(methyl methacrylate)
PS	Poly(styrene)
PSD	Particle size distribution
PVC	Poly(vinyl chloride)
RAFT	Reversible addition fragmentation chain transfer
RDRP	Reversible deactivation radical polymerisation
RNA	Ribonucleic acid
SEC	Size exclusion chromatography
SET-LRP	Single electron transfer living radical polymerisation
SF-RAFT	Sulphur free reversible addition fragmentation chain transfer
TEMPO	(2,2,6,6-Tetramethyl-piperidin-1-yl)oxyl
TFEMA	2,2,2-Trifluoroethyl methacrylate
T_g	Glass transition temperature
VM	Viscosity modifier
VOC	Volatile organic content

*Το πόνημα αυτό αφιερώνεται στη μητέρα μου και την απέραντη εκτίμησή της στην
επιστήμη*

This piece of work is dedicated to my mother and her endless admiration of science

Put your hand on a hot stove for a minute, and it seems like an hour. Sit with a pretty girl for an hour, and it seems like a minute. That's relativity.

Albert Einstein

The whole of science is nothing more than a refinement of everyday thinking.

Albert Einstein

Research is what I'm doing when I don't know what I'm doing.

Wernher von Braun

Knowledge is of two kinds. We know a subject ourselves, or we know where we can find information upon it.

Samuel Johnson

Research is to see what everybody else has seen, and to think what nobody else has thought.

Albert Szent-Gyorgyi

Every revolutionary idea seems to evoke three stages of reaction. They may be summed up by the phrases: (1) It's completely impossible. (2) It's possible, but it's not worth doing. (3) I said it was a good idea all along.

Arthur C. Clarke

Perfection is achieved, not when there is nothing more to add, but when there is nothing left to take away.

Antoine de Saint-Exupery

Acknowledgements

First of all I want to thank Dave. Without his support this work would have not been completed. He has been willing to help with anything from the very first until the very last moment. Always encouraging me to try new things in the lab but also forgiving, even when the damages were too expensive. I still remember that during my MSc, when officially I was not a member of the Haddleton Group, he would often come in the lab to show me various things or demonstrate how things should be done. These three and a half years have been very intense and for all what was achieved during these years I will always be thankful to Dave. In parallel with my academic supervisor, I would also like to thank my industrial supervisors from Lubrizol (Dr. Tim Smith, Dr. Paul O'Hora) for being so patient and helpful with me.

Another key person during my PhD has been Athina Anastasaki. Apart from being a role model and an exemplary professional, demonstrating how a dedicated person should work, she has always been willing to provide assistance when things did not go right. I still remember the very first days of our cooperation, when she had to teach me almost everything, from basic lab techniques to reaction mechanisms! Recalling these days, I realise that she showed endless patience in my case! There have also been times that I did not agree with her advice. However, I soon realised that I was wrong as, up to date, all her advice has proved to be correct!

Many special thanks go to Gaspadin Nurumbetov! Apart from introducing me to emulsion and DLS, he was also willing to apply his great skills when repairs were necessary. Moreover, Gabit spent some time teaching me how vodka should be consumed. This is something I definitely failed to learn...

Next in the list is Vasiliki! Words are not enough as to describe the fact that she was ready to help with ANY issue in the lab. In addition, she spent endless hours teaching me how a nice powerpoint presentation is made and how an origin file should be plotted. However, her most important contribution was moral. Without her jokes ("a bit of water and we go on") and her always great mood, I would not have managed to keep on going when things were going wrong! Thanks kyra Vicky mou!

To be honest I should write a whole proper chapter about Glen, or just "M". Still wondering what I should mention first... Glen has been a great friend, always patient in order to overcome our massive cultural differences and always polite! At the beginning of our time in the Haddleton group he mentioned that in three years time he would convert me into a "proper English gentleman". Three years later, I would dare to say that Glen is thinking more as a Greek rather than English.

At the other end of English people is another great friend! Richard Whitfield! Always polite and friendly and always ready for a comment that would make me laugh. Whenever I face difficult situations I always remember him smiling and saying “Happy days” a phrase most of the times used ironically! It was really a pleasure to cooperate with him either in the lab or later on analysing the data!

Many thanks also go to Evelina! A great person that arrived at Warwick at the middle of my PhD but still managed to share with me thoughts, jokes and many cigarettes! Her contribution on my mood has been just irreplaceable! Thanks bro!

In parallel, I would like to thank all members of the Group with which I have shared a fumehood, a bench or just some time during the last three years! Namely, the great chemist Paul Wilson, Sam (who has a very particular set of skills), Patrick (who had always time to talk about F1), the great Scotsman Alan, the great footballer Nut, Alex Simula (who spoke french when no other language could describe the situation), Dan, Kristian, Carmelo, Tammy, Rachel, Atty, George, Sam, Arkadios, Danielle, Jong yu, Pawel, Beng zing, Fehaid, Alice, Greg, Ellis, Chloe, Tom, James, Jamie, Angela, Maria, Chris, Joji and Gavin. Apologies if someone is not included in the sequence of names!

Some very special thanks go to people outside the Haddleton Group. First of all my dear friend Panos for being a supportive and patient housemate for two years! He could always make me see things in a more positive way! I will definitely miss his special comments on football, cars and of course chemistry! Some special thanks to two French people that have been sources of inspiration, these were Segolene A. and Guillaume Gody. Also many thanks to all the members of the Terrace Bar mafia (Greek and not only) that shared with me time, drinks and thoughts, namely Karolos, “Kill Bill” Vasilis, Stavros the President, Ioanna, Giannis, Miltos, Christoforos, Daniele, Noe, Sofiem and Orestis. Moreover, I would like to thank all my friends that offered great support despite being far away. My great friend Elias and his wife Eleni, Maria (with all her other names), Tasos, Giannis K., Aimilia T., Varvara, Aimila N., Giorgos, Olga, Christos, Katerina, Ntina K, Frau Madlen and last but definitely not least, Darius Shemirani, a great chemist and even greater person.

At this point, I would like to thank my family; my mother, uncle Spilios, uncle Andreas and my grandmother Maria for their continuous support. Without their love, nothing would have been the same. Thank you!

Declaration

Experimental work contained in this thesis is original research carried out by the author, unless otherwise stated, in the Department of Chemistry at the University of Warwick, October 2014 and February 2018. No material contained herein has been submitted for any other degree, or at any other institution.

Date:

Nikolaos Engelis

Abstract

The objective of this work is to investigate and expand the use of methacrylic macromonomers as chain transfer agents. Although chain transfer activity had been demonstrated previously,^{1,2} the limits of the technique have not been fully explored. As such, a new approach for the efficient synthesis of methacrylic polymers in emulsion is presented, aiming at fully exploiting the vinyl end-group of the CCTP-derived macromonomers and consequently their chain transfer activity. Moreover, the preparation of higher MWt copolymers as well as more complex structures (*e.g.* triblocks etc) by this method will be investigated as research so far has only been focusing on certain degrees of polymerisation, mainly resulting in diblock copolymers of relatively low MWt. In addition, macromonomers based on diverse methacrylic monomers will be employed, as most studies to date have focused on a narrow monomer pool. In parallel, another aspect of radical polymerisation in the presence of macromonomers is the livingness of the system. Even though living-like characteristics have been observed,² previous studies did not reach definitive conclusions, according to the generally set criteria of livingness.

At the same time, the use of macromonomers as precursors for comb-like polymers will be described. Despite the technique being known and well-reported,³⁻⁵ the aim is to successfully employ solvents that satisfy the needs of automotive applications, such as mineral oil. In detail, both the macromonomer synthesis and the subsequent comb formation will be attempted in this solvent. A similar approach has not been reported so far. It needs to be noted, that this part is an ongoing work with the Lubrizol Corporation and as such it only demonstrates a few initial steps towards developing materials with interesting properties and applications.

1.1 The “macromolecule” concept

The term “polymer” derives from the Greek terms “πολύ” (“poly” meaning “many”) and “μέρος” (“meros” meaning “part”). Until the 1920s, it was a common belief that polymers consisted of physically associated aggregates of molecules. The German organic chemist Hermann Staudinger was the first to propose that polymers consist of large molecules containing sequences of small units, linked together by covalent bonds. In his paper “Über polymerization”,⁶ he described that polymers are formed *via* reactions linking together the repeat units in order to form high molecular weight molecules and called these reactions “polymerisations”. Moreover, he introduced the term “macromolecule” as to describe polymers. His conception, based on studies on polyoxymethylene and polystyrene, was initially disregarded by the scientific community. However, crystallographic studies performed by Herman Mark and Kurt Meyer along with the polyamide synthesis by Wallace Carothers managed to finally place polymer science on a sound basis. By the 1930s, the majority of scientists were convinced about the “macromolecule” concept. Staudinger’s contribution was finally recognised and he was awarded the Nobel Prize for chemistry in 1953. In 1974, Paul Flory was awarded the same prize for establishing fundamental principles of polymer chemistry.

1.2 Brief history of polymers

Although natural polymers count millions of years of contribution to life and evolution of species, synthetic polymers appeared only around one hundred years ago. Apart from biopolymers such as DNA or proteins, human kind has exploited several other natural polymers in order to obtain suitable materials for clothing, writing, weapons or many other uses. Nowadays, polymers, commonly referred to as “plastics” are the dominant material in all sorts of everyday life. The first application of polymers is attributed to the Mayans around 1500 BC when they made rubber balls by coagulation of the latex obtained from rubber trees. Many centuries later, in 1839, a polymer industry was born when Charles Goodyear discovered that the mechanical properties of the same material could be massively improved by heating with sulphur, a process to become known as “vulcanisation”. The first fully synthetic polymer is considered the synthetic rubber, known as “methyl rubber”, produced from 2,3-dimethylbutadiene in Germany, during World War I as a substitute for natural rubber for use in tank tracks developed as a consequence of the Allied forces dominating the rubber plantations in Malaysia. This is one of the first examples of a material being developed by the need for a material with specific properties.

Poly(vinyl chloride) (PVC) was first synthesised accidentally in 1872 by Eugen Baumann. In 1926 an efficient method of plasticising PVC was invented, allowing its use for many objects such as synthetic floor tiles, credit cards and pipes. Polystyrene (PS), was first manufactured in 1931 by I. G. Farben and nowadays is used in the construction of plastic cutlery, cups, rulers and toys. Two years later, in England polyethylene (PE) was synthesised industrially for the first time by Imperial Chemical Industries (ICI). Nowadays, it is the most common synthetic polymeric (and indeed chemical) material with an estimated production

of over 80 million tonnes per annum. Another important achievement was the preparation of Nylon-6,6 by the Du Pont company in USA, in 1938. Nylon fibres are widely applied in food packaging, textiles and carpets. In all, synthetic polymeric materials have substituted traditional materials such as metal or wood in all kinds of applications and have an omnipresent role in everyday life.

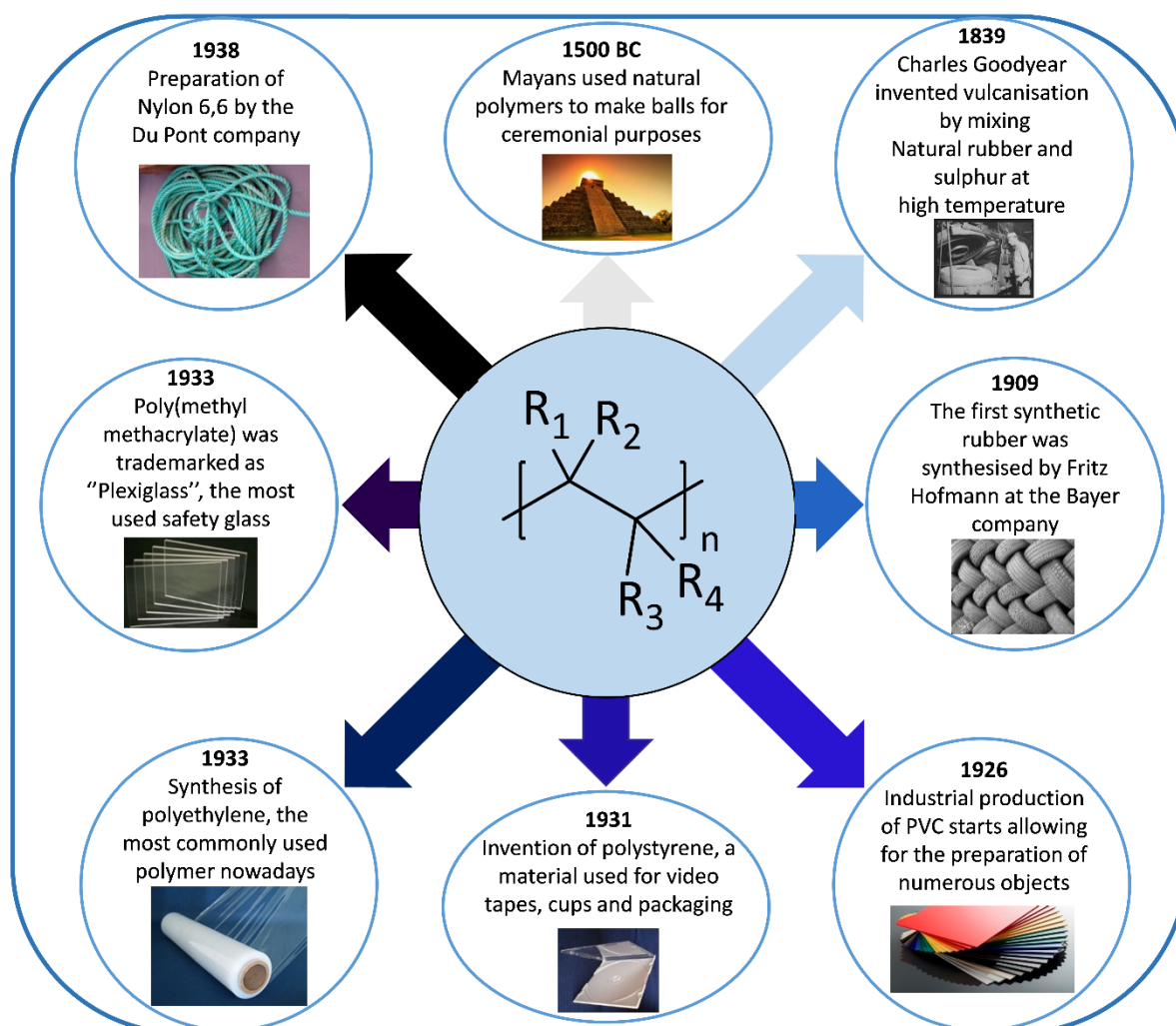


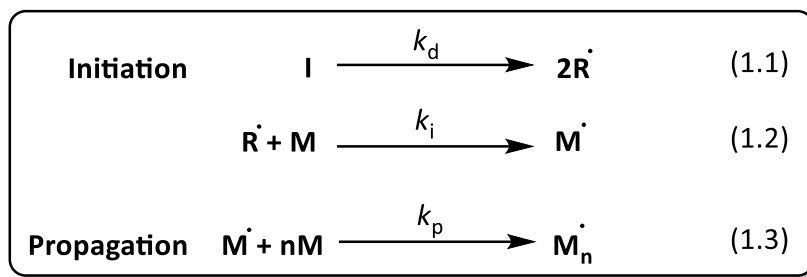
Figure 1.1: History of the development of common industrial polymeric materials.

1.3 Free Radical Polymerisation (FRP)

One of the most widely practised polymerisation method is free radical polymerisation (FRP), first reported by Flory in 1937.⁷ Many commercially available polymers are synthesised *via* FRP. Apart from the ability to synthesize high molecular weight polymers, FRP also offers the advantages of robustness and undemanding conditions. More specifically, FRP is tolerant towards impurities or traces of oxygen and does not always require removal of the stabilisers often added to most commercial monomers. Moreover, it can be applied in a wide range of solvents (including water) which do not need to be dried or purified *prior* to reaction. In addition, the technique can also be applied in bulk or in dispersed media. The following analysis of the stages of FRP refer to homogenous media such as bulk or solution. FRP can be divided into three main stages: initiation, propagation and termination.

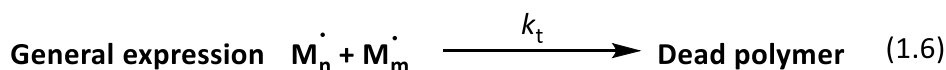
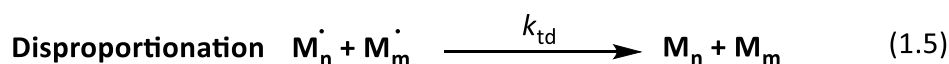
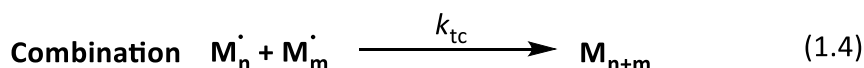
1.3.1 Sequence of events in FRP

Initiation is divided into two stages. During the first, radical species ($R\cdot$) are formed by the decomposition of a small molecule called "initiator" (I), Eq. 1.1, where k_d is the initiator decomposition rate constant. Most initiators undergo homolytical dissociation either by the application of heat (*thermal initiators*) or light (*photochemical initiators*). During the second stage of initiation, a free radical attacks the π -bond of a molecule of monomer (M) thus creating a new radical, sometimes referred to as "initiator radical" ($M\cdot$), as shown in Eq. 1.2, where k_i is the rate constant for the initiation step.

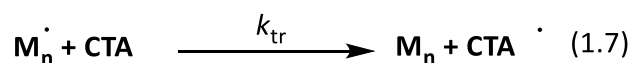


The later stage of polymerisation is termed propagation and includes all the reactions in which the free radical at the end of the growing chain (often called active centre) reacts with molecules of monomer thus further increasing the length of the chain (Eq. 1.3), where k_p is the rate constant for propagation. After every addition of monomer to the growing chain, the active centre is transferred to the newly-formed chain end.

An individual growing polymer chain does not keep propagating until total monomer consumption. Due to their highly reactive nature, radicals can lose their radical activity, mainly by reacting with another radical in an event called termination. There are two termination mechanisms. In the first, called combination, two radicals couple resulting in the formation of one dormant (dead) chain, Eq. 1.4. Alternatively, one of the radicals abstracts a hydrogen atom from the other chain thus forming two dormant chains in a disproportionation (Eq. 1.5). It has to be noted that the two modes of termination do not necessarily need to be distinguished and as a result termination can be expressed by Eq. 1.6 where k_t is the combined expression for k_{tc} and k_{td} . The term "dead polymer" is used as to describe permanently deactivated polymer chains. Termination rate coefficients vary from 10^6 to 10^8 L mol⁻¹ s⁻¹ while the corresponding values for k_p are 10^2 - 10^4 L mol⁻¹ s⁻¹.⁸

Termination

Apart from the two termination mechanisms mentioned above, there is also another kind of reaction producing dead polymer chains. This class of reactions, known as chain transfer reactions (or simply chain transfer) take place in most polymerisations and result in the transfer of the active centre from the growing chain to another species. The latter, generally referred to as chain transfer agent (CTA) may be a molecule of solvent, monomer, initiator or another polymer chain. The CTA can also be a deliberately added species. Chain transfer can be represented by Eq. 1.7, where k_{tr} is the corresponding rate coefficient.

Chain Transfer

Mechanistically, the reaction proceeds *via* the abstraction of an atom (usually hydrogen or halogen) from the CTA, causing homolytic scission of the bond and producing a dead chain as well as a new radical (CTA \cdot). This newly-formed radical may react with a molecule of monomer and reinitiate polymerisation, depending on its reactivity.

Chain transfer to polymer causes the formation of branched polymers and may considerably affect the properties of the final product. The reaction can be intramolecular (also known as "backbiting") resulting in the formation of short-chain branches or

intermolecular, giving rise to long-chain branches. The reaction may proceed *via* atom abstraction either from the backbone or from the side group of a repeat unit, depending on the monomer structure and the stability of the formed radical.

1.3.2 Rate expression/Kinetics of FRP

Although small size radicals are considerably more reactive than large propagating radicals, it is assumed that the rate coefficient k_p for propagation as well as the rate coefficient k_t for termination are independent of the chain length.

Monomer is being consumed during initiation and propagation, thus the rate of monomer disappearance is given by Eq. 1.8, where R_i and R_p stand for the rates of initiation and propagation respectively. However, the number of monomer molecules consumed during propagation is far higher than the number consumed in initiation. As a result, the term R_i can be neglected, resulting in the simplified Eq. 1.9.

$$-\frac{d[M]}{dt} = R_i + R_p \quad (1.8)$$

$$-\frac{d[M]}{dt} = R_p \quad (1.9)$$

The rate of polymerisation is summing all the individual propagation steps involving propagating radicals of diverse chain lengths and is expressed by Eq. 1.10.

$$R_p = k_p[M\cdot][M] \quad (1.10)$$

However, radical concentration is not measurable and remains very low during polymerisation ($\sim 10^{-8}$ M). The term $[M\cdot]$ can be considered as constant if the steady-state assumption is followed. According to this theory, which is applicable for most free radical polymerisations the rate of radical formation is equal to that of radical loss. As a result, the

net rate of change in $[M\cdot]$ is zero.⁹ As radicals are formed in the initiation stage and deactivated in termination, the steady state theory accepts that the rates of initiation and termination are equal (Eq. 1.11). The factor of 2 in the termination rate follows the general convention that radicals are deactivated in pairs.

$$R_i = R_t = 2k_t[M\cdot]^2 \quad (1.11)$$

By combining Eq. 1.10 and 1.11 and solving for $[M\cdot]$, we obtain Eq. 1.12:

$$[M\cdot] = \sqrt{\frac{R_i}{2k_t}} \quad (1.12)$$

Subsequently, by substituting Eq. 1.12 into 1.10, the rate of polymerisation will be given by Eq. 1.13:

$$R_p = k_p[M] \sqrt{\frac{R_i}{2k_t}} \quad (1.13)$$

For a thermal initiator the rate of radical production is expressed by Eq. 1.14 where $[I]$ is the initiator concentration and f is the initiator efficiency. This factor describes the fraction of radicals that successfully initiate polymerisation. The factor of 2 is entered if two radicals are formed from one molecule of initiator, which is the most common case. Between the two stages of initiation, the first (initiator decomposition, Eq. 1.1) is much slower than the second (addition of the primary radical to monomer, Eq. 1.2) and as a result is the rate determining step ($R_d=R_i$).

$$R_d = 2k_d f [I] \quad (1.14)$$

$$R_i = R_d = 2k_d f [I] \quad (1.15)$$

By substituting Eq. 1.15 into 1.13, we form Eq. 1.16:

$$R_p = k_p[M] \sqrt{\frac{k_d f[I]}{k_t}} \quad (1.16)$$

Equation 1.16 shows that the rate of polymerisation is proportional to the square root of the initiator concentration. The dependence had been studied and confirmed for several monomer-initiator systems.¹⁰⁻¹²

Although free radical polymerisation is a widely applied polymerisation protocol with extended use in industry, it still suffers from significant disadvantages, the most important being the lack of control over the molecular weight and the architecture of the resulting polymers.

1.4 Emulsion polymerisation

Apart from homogenous media (batch and solution), a polymerisation may also take place in heterogeneous media. Such a system consists of two phases, insoluble in each other. There are several methods of radical polymerisation in heterogeneous media, namely miniemulsion, microemulsion, precipitation, dispersion and suspension polymerisation. In a miniemulsion polymerisation, water, surfactant, monomer, a hydrophobe (usually hexadecane) and a water- or oil-soluble initiator undergo ultrasonication or microfluidisation in order to form monomer droplets. In this case, particle sizes vary between 60 and 200 nm, usually with broad distributions. A microemulsion is a thermodynamically stable emulsion formed by the mixing of an aqueous surfactant solution with monomer and possibly a cosurfactant. Microemulsion polymerisation results in even smaller particles (10 – 60 nm).

Precipitation polymerisation employs reagents that are initially soluble in the aqueous phase. However, as the polymer chains grow, a precipitation-critical chain length is reached, resulting in particles of 100 nm to 1 μm . A dispersion polymerisation is in fact a precipitation polymerisation in which a stabiliser is used. Finally, a suspension polymerisation employs water, emulsifier, monomer and an oil-soluble initiator.

The best known and most widely employed among dispersed polymerisations is emulsion polymerisation. Necessary reagents for its performance include water, a water-soluble initiator, monomer and emulsifier (usually referred to as surfactant) are required. Particle diameters vary between 40 nm and 1 μm . Emulsions consist of two phases. The aqueous phase, also referred to as the "continuous" phase and the organic, known as "dispersed". The necessary reagents for performing FRP in emulsion are a water-soluble radical initiator, a sparingly water-soluble monomer and a surfactant. The latter species is usually employed at levels of 1-5 wt % to monomer and consists of a long hydrophobic hydrocarbon chain, at the end of which there is a hydrophilic anionic head group, countered by a cation. Above a certain concentration, the critical micelle concentration (CMC), molecules of surfactant form aggregates, the "micelles". In these aggregates, the hydrophobic chains point inwards while the hydrophilic anionic heads are in contact with water. Thanks to this confrontation, micelles are able of absorbing water-insoluble species.

In an emulsion polymerisation mixture, before the reaction starts there are three phases. The continuous phase which contains the water-soluble initiator and in very small quantities, molecularly dissolved surfactant and monomer. The dispersed phase consists of the monomer droplets (1-10 μm) which remain in suspension thanks to agitation and to the absorption of molecules of surfactant. Droplets contain the largest amount of monomer

present in the system. Also part of the dispersed phase are the monomer-swollen micelles (5-10 nm).

Emulsion polymerisation has attracted great commercial interest thanks to some advantages over bulk and solution polymerisations. It is reported that 40-50 % of all free radical polymerisations performed in industrial scale, are in emulsion.^{8, 13, 14} The product of this process is a dispersion of polymer in water, with the appearance of a milky fluid, stabilised by surfactant and commonly known as “latex”. The use of water as solvent makes the whole system inexpensive, relatively odourless and non-flammable. The high heat capacity of the dispersion medium facilitates temperature regulation and guarantees efficient heat transfer. Moreover, the low organic volatile content (VOC) makes the method environmentally friendly. Important benefits by the use of the technique, also include high conversions and the low viscosity of the produced latex, independently of the molecular weight of the polymer. Interestingly, polymers synthesised by emulsion polymerisation can either be employed directly in the form of a latex (as for emulsion paints) or after isolation by removal of the water (*e.g.* synthetic rubbers), depending on the application targeted. However, emulsion polymerisation has also a few drawbacks, the main being the unavoidable presence of additives (surfactant) and the difficulties of water removal if required at the end of polymerisation.^{4, 15, 16}

1.4.1 Sequence of events in an emulsion polymerisation

At this point, classification of emulsion polymerisation processes is necessary. There are three types of processes. In batch emulsion polymerisation all ingredients are present in the reaction vessel from the beginning. Polymerisation starts when the initiator is activated, usually by the application of heat. In a semi-continuous process (also called semi-batch), one or more reagents (*e.g.* monomer) are fed into the reaction vessel throughout the polymerisation. Finally, in a continuous emulsion polymerisation, the components of the reaction system are continuously fed and removed from the vessel. Due to this particularity, special types of reactors are required for this process. Emulsion polymerisations are also classified according to the way of polymer particle formation. An emulsion polymerisation might start in a system where there are no formed loci of polymerisation (particles). In this case, the process is called "*ab initio*" emulsion polymerisation and particle formation (*nucleation*) needs to take place at an early stage of the process. In contrast, in seeded emulsion polymerisation, the loci of polymerisation have previously been formed in a separate process.

An *ab initio* emulsion polymerisation, is divided into three stages. The first stage, commonly referred to as Interval 1, is defined as the period during which particles are formed. There are three mechanisms for particle nucleation and the one that dominates is usually decided by the conditions. However, the first event is common in all of them and is the formation of oligomeric radicals *via* the decomposition of the water-soluble initiator and the subsequent addition of the primary radicals to molecules of monomer. The oligomeric radicals may reach two critical degrees of polymerisation, usually represented as z or j (for z -

mers and j -mers respectively, with $z < j$). Beyond the formation of z -mers and j -mers, the three nucleation mechanisms differentiate from each other.

In *micellar nucleation*, z -mers enter the existing monomer-swollen micelles thus, continuing polymerisation thanks to the molecules of monomer, already present there. Micelles that do not absorb a z -mer are subsequently ceased, releasing their monomeric content to the system while their molecules of surfactant get absorbed by newly-formed particles offering supplementary stability. Micellar nucleation stops when all micelles are consumed either by becoming particles or by having ceased. It needs to be noted that as the number of micelles is much higher than that of monomer droplets, oligomeric radicals almost entirely enter the first ones. Micellar nucleation takes place when CMC is exceeded.

Homogeneous nucleation occurs when oligomeric radicals keep on propagating until becoming j -mers. At that point, chains collapse and become particles while still retaining their active chain end. Subsequently, the newly-shaped particles absorb molecules of surfactant in order to secure their stability as well as molecules of monomer as to continue chain growth. *Coagulative nucleation* is similar to homogeneous nucleation. In this case, primary particles coagulate forming particle aggregates. The latter are colloidally stable and able of absorbing molecules of monomer in order to propagate. Another mechanism is the *droplet nucleation* which occurs when a z -mer enters a monomer droplet. This type of nucleation is considered unlikely in emulsion polymerisation. However it is the dominant mechanism in mini-emulsion polymerisation where ideally each monomer droplet becomes a particle. By the end of *Interval 1*, monomer conversion is about 10 % (Figure 1.2) and it is considered that the number of particles formed does not change until the end of the polymerisation reaction.

Interval 2 is considered the stage of particle growth and is oriented between 10 and 40 % conversion, Figure 1.2. During this stage, monomer droplets act as monomer reservoirs, containing molecules that reach the latex particles (where polymerisation takes place) *via* diffusion through the continuous phase. During *interval 2*, the monomer concentration in the particle ($[M]_p$) as well as the number of particles per unit of volume (N_p) are considered to be constant thus, resulting in a constant rate of polymerisation. It needs to be noted that the rate of monomer diffusion through the aqueous phase exceeds the rate of polymerisation and as a result, there is sufficient amount of monomer entering the particles in order to maintain propagation.

In *Interval 3*, the rate of polymerisation decreases due to the fact that monomer droplets are exhausted. As a result, polymerisation continues only with the molecules of monomer still present in the particles or the few dissolved in the continuous phase. The number of particles is also considered to remain constant during this stage.

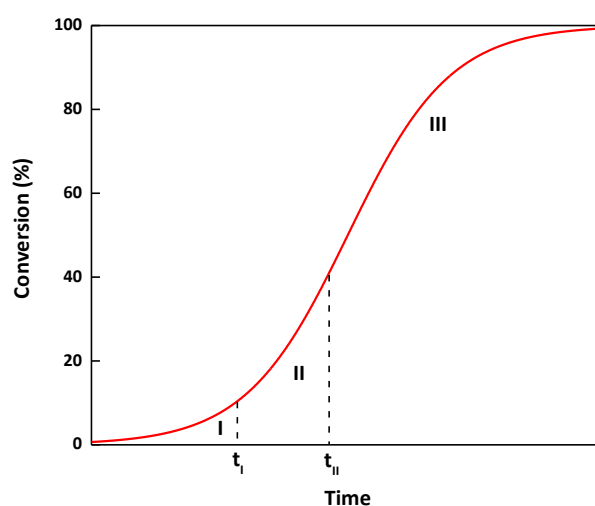


Figure 1.2: Schematic representation of the variation of conversion with time for an emulsion polymerisation system. t_I and t_{II} are the completion times for intervals I and II respectively.

1.4.2 Kinetics of emulsion polymerisation

The kinetics of emulsion polymerisation are governed by the compartmentalisation effect. While in solution or in bulk all radicals share the same overall space, in emulsion radicals are present in the latex particles. Notably, a radical may exit a particle and enter another or even terminate while being transferred through the aqueous phase. Overall, the chances of termination are much lower or, in other words, the rate of termination is considerably decreased when comparing to solution polymerisation. Consequently, the molecular weight of the produced polymer is higher. In detail, compartmentalisation is divided into two, more specific effects. The first is referred to as “segregation effect” and describes the inability of two chemical species, located in separate particles to react. The “confined” space effect refers to the reaction between two species located in the same particle. According to this, the smaller the particle size, the higher the rate of reaction between the two species. The rate of propagation is given by Eq. 1.17, where $[M]_p$ is the concentration of monomer within a particle, \tilde{n} is the average number of radicals per particle, N_A is the Avogadro constant and N_p is the number of particles per unit volume of latex. Notably, Eq. 1.17 is considered applicable to all stages of emulsion polymerisation.¹⁵

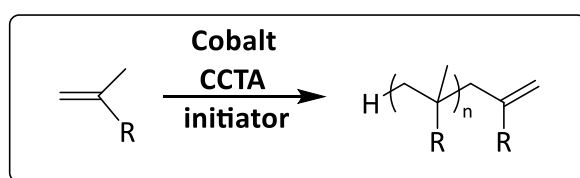
$$R_p = k_p [M]_p \frac{\tilde{n}}{N_A} N_p \quad (1.17)$$

Compartmentalisation occurs in the so-called *zero-one* systems and it is considered that termination takes place by the entry of a small mobile radical to a particle. In this case, due to small size and increased mobility, termination takes place instantly (*instantaneous termination*). In this case, it is widely accepted that a particle may contain either one or no radicals ($\tilde{n} \leq 0.5$). Thus, the rate of termination is dependent on the mobile small radical and independent of the chain length of the main propagating radical. However, for other systems

called *pseudo-bulk*, it is considered that more than one radical may be present at a particle ($\bar{n} > 1$). Thus, the compartmentalisation effect is neglected and termination is not rate determining.

1.5 Catalytic Chain Transfer Polymerisation (CCTP)

CCTP employs certain Co^{II} complexes as CTAs for the synthesis of low molecular weight functional polymers in free radical processes. The resulting polymers have a vinyl ω -end group and are known as “macromonomers” (Scheme 1.1).⁴ Thanks to their extremely high efficiency, Co^{II} catalysts are usually required in ppm levels and have attracted considerable interest by industry. Overall, the attraction of CCTP relies on the combination of the robustness of a FRP process with control over the molecular weight as well as introduction of functionality.



Scheme 1.1: General conception of the CCTP of a α -methyl monomer leading to the formation of a vinyl terminated polymer (macromonomer).

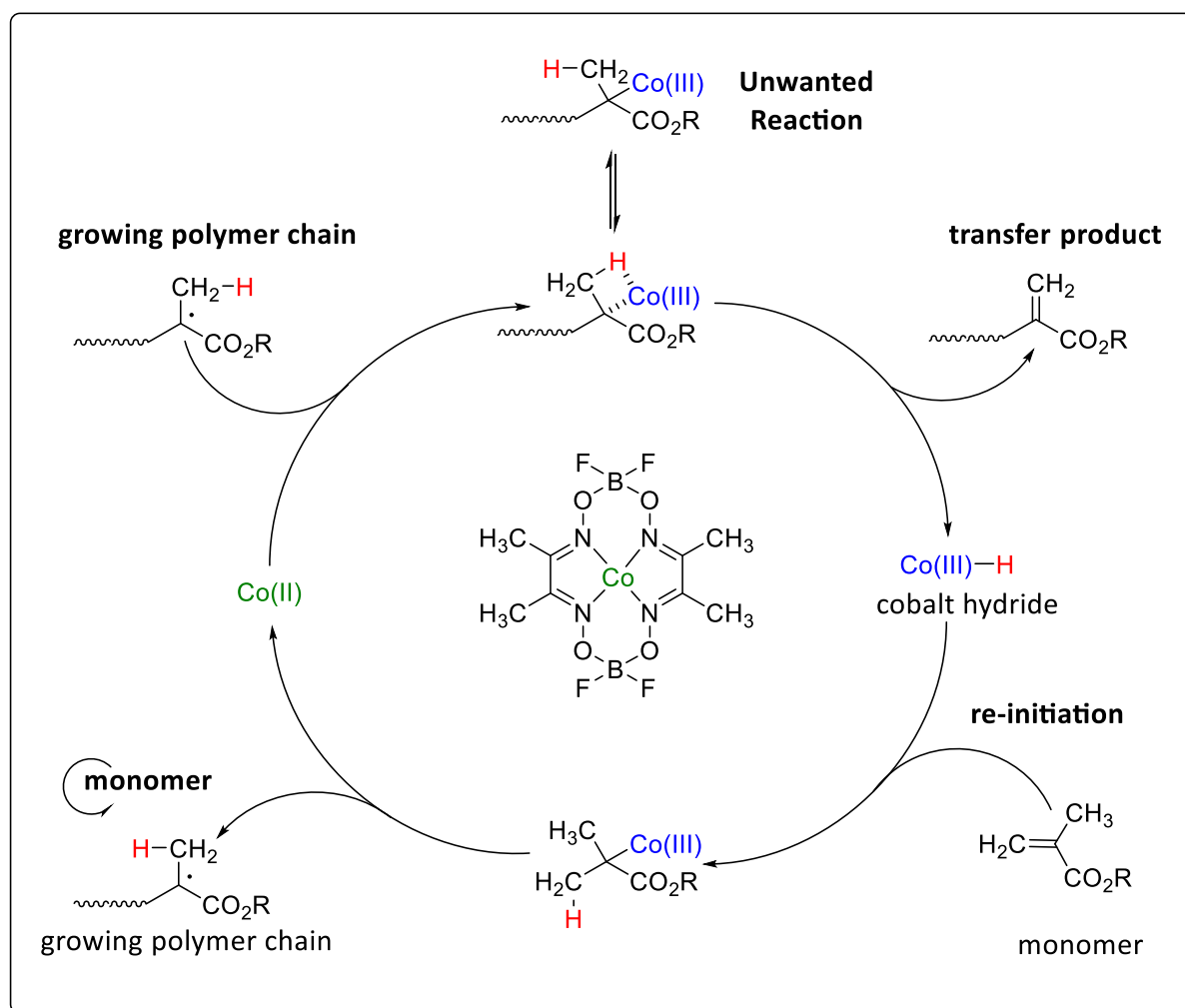
1.5.1 Brief History

CCTP initially came to attention in March 1975, in Moscow, where Boris Smirnov and Alexander Marchenko were investigating the potential of cobalt porphyrins as catalysts for the redox decomposition of peroxy initiators. Initial experiments showed that Co^{II} porphyrins were inhibiting polymerisation of methyl methacrylate (MMA) as the viscosity of the reaction mixture remained low. In contrast, calorimetric results demonstrated full conversion. Additional studies by Enikolopyan, Ponomarev and Gridnev lead to the establishment of CCTP as well as initial proposals about its mechanism. Chemical industries became interested a few years later and several companies, most notably the Glidden Paint company (parent cobaloxime)¹⁷⁻¹⁹ and DuPont (catalysts featuring BF₂ bridges),^{20, 21} contributed to the development of CCTP and to its commercial exploitation.

1.5.2 Mechanism of CCTP

According to all experimental evidence up to date, CCTP proceeds *via* a two-step radical process. In the first step, a β -hydrogen atom is abstracted from the growing radical by the Co^{II} complex. The abstraction results in the formation of a Co^{III}-H complex (or Co^{III} hydride) and a macromonomer. Subsequently, the Co^{III}-H complex reacts with a molecule of monomer, transferring to it the hydrogen atom. This second step yields back the initial Co^{II} catalyst and a monomeric radical. The catalyst may get involved in another catalytic cycle while the newly-formed radical starts propagating. Notably, it is considered that most of the chains in CCTP are initiated by the second step of the process thus, most chains possess a hydrogen atom as the α -end group.⁴ Despite this consideration, the presence of a radical initiator is necessary. Importantly, the initiator has to generate carbon centred radicals as oxygen-centred radicals

have been reported to deactivate the catalyst.²² In addition, peroxides²³ and redox systems²⁴ are also known for poisoning Co^{II} catalysts. The proposed mechanism for CCTP is presented in scheme 1.2.



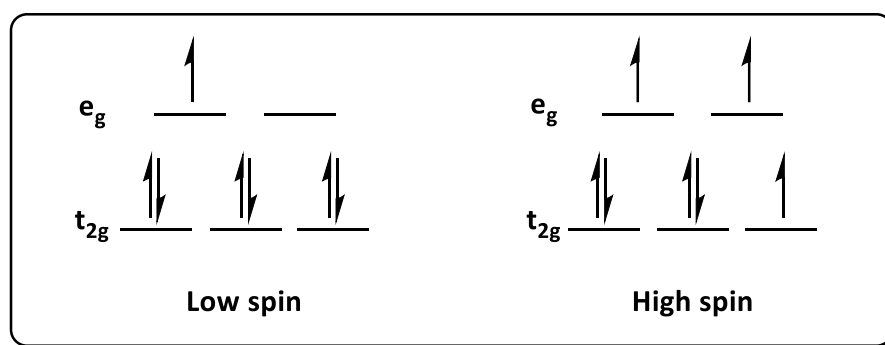
Scheme 1.2: Proposed mechanism for the CCTP of a methacrylic monomer.²⁵

The formation of a covalent bond between cobalt and carbon, Scheme 1.2 is an unwanted side reaction which results in the occupation of catalyst molecules and their elimination from the catalytic cycle. The Co-C bonding does not have a considerable effect in the polymerisations of methacrylates. In contrast, it is crucial in the polymerisation of monomers forming secondary radicals, in other words, for monomers such as styrene or

acrylates.²⁶⁻³² Interestingly, for such cases, even polymer chains with attached catalyst have been observed.³³ Higher concentrations of catalyst result in higher frequency of the catalytic cycle thus, shorter polymer chains to be formed.

1.5.3 CCTP catalysts and their evolution

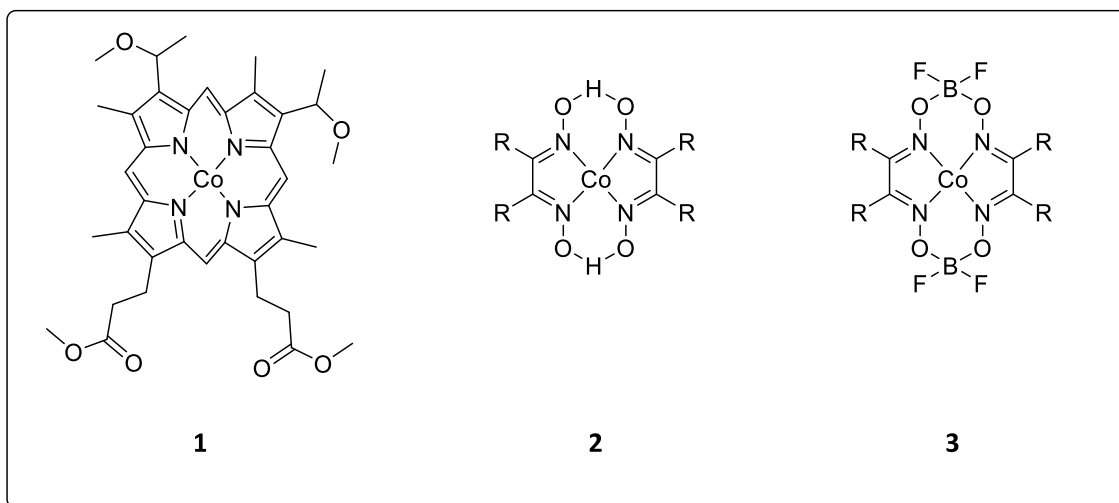
Active CCTP catalysts are low spin d^7 Co^{II} complexes with octahedral geometry. They possess a macrocyclic ligand of square planar geometry as well as two axial sites. Co^{II} has a d^7 configuration which may exist in low (with one unpaired electron) or high (with three unpaired electrons) spin (Scheme 1.3).



Scheme 1.3: d electron configurations of d^7 $\text{Co}(\text{II})$ in low (left) and high spin (right).

Initially, CCTP catalysts were Co^{II} porphyrin complexes such as hematoporphyrin ether (1, Scheme 1.4). This family of catalysts showed high activity. However, drawbacks including challenging isolation, limited solubility in organic solvents/monomers, intense colour and high cost prevented their industrial application. Later, the more active cobaloximes were introduced (2, Scheme 1.4), with their equatorial groups (R) being efficiently used in order to tailor solubility and activity.^{22, 25, 34, 35} Despite the important advantages compared to porphyrins, the new catalyst family was soon found to suffer from sensitivity to hydrolysis (by

acids) and oxidation (by peroxides and other oxygen-centred radicals). These drawbacks were bypassed by the introduction of BF_2 bridges between the axial oxygen atoms and the creation of the class of BF_2 bridged cobaloximes (3, Scheme 1.4). Notably, the new catalysts still show this sensitivity however, much less than initial cobaloximes. The latest cobaloxime complexes are known with the general name CoBF and are the most widely employed catalysts for CCTP.

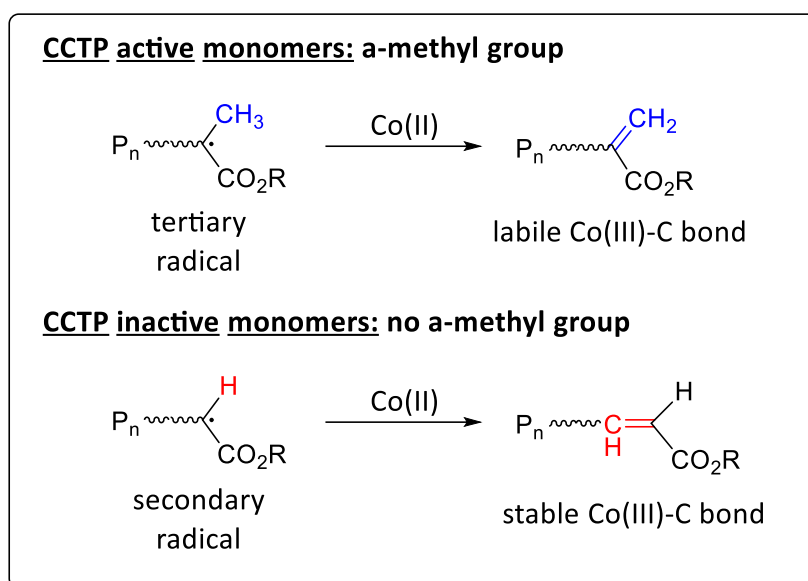


Scheme 1.4: Structures of Co^{II} hematoporphyrin tetramethyl ether and first and second generation Co^{II} cobaloximes.

1.5.4 Monomers in CCTP

Efficient monomers for CCTP are those facilitating the abstraction of a hydrogen atom. Functional methacrylates are the most widely used family of monomers for CCTP.⁴ As mentioned before, tertiary propagating radicals result in the formation of labile $\text{Co}^{\text{III}}\text{-C}$ bonds which allows higher catalytic efficiency. Apart from methacrylates, other monomers possessing an α -methyl group, such as α -methyl styrene and methacrylonitrile, also show high efficiency in CCTP. In contrast, monomers without a α -methyl group, like acrylates, styrenes and vinyl acetate show much lower activity, due to the secondary radical that allows a more

stable Co^{III}-C bond to be formed, thus taking catalyst out of the catalytic cycle. Notably, for such monomers, hydrogen abstraction takes place on the polymer backbone, Scheme 1.5.



Scheme 1.5: General properties for monomers of high and low CCTP activity.

1.5.5 CCTP in emulsion

The first report about performing CCTP in a dispersed system was introduced about ten years after the initial discovery.²¹ When performing CCTP in emulsion, the key difference is the lower catalyst efficiency compared to an equivalent solution process.³⁶⁻³⁸ This is demonstrated by the higher molecular weight observed for a specific catalyst to monomer ratio. The presence of the catalyst at the loci of polymerisation is a prerequisite for efficient control over the molecular weight. However, most of the widely used cobaloximes possess some solubility in both the continuous and the dispersed phase.^{25, 36, 39} As a result, these catalysts partition between the two phases. The extent of partitioning depends on the monomer hydrophobicity and the structure of the cobaloxime complex. It is expressed by the

partition coefficient, shown in Eq. 1.18, where $[Co]_{disp}$ is the catalyst concentration in the dispersed phase while $[Co]_{aq}$ is the corresponding value for the continuous phase.

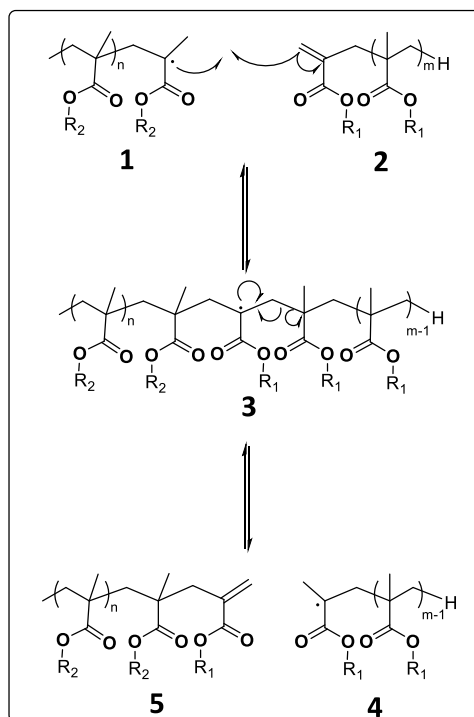
$$m_{Co} = \frac{[Co]_{disp}}{[Co]_{aq}} \quad (1.18)$$

Generally, the partition coefficient increases when the hydrophobicity of the R-group of the complex increases or the hydrophilicity of the monomer increases. Data reported for the partition coefficient of several monomers indicate that a considerable amount of catalyst may reside to the aqueous phase.⁴ Consequently, the concentration of catalyst at the loci of polymerisation (particles) is significantly lower than the overall concentration of catalyst in the system. When extremely hydrophobic cobaloximes are employed, transfer limitations may occur. For example, CoPhBF is insoluble in water thus, the necessary mass transport to polymer particles cannot take place *via* the continuous phase. In this case, mass transport is considered to occur through collisions between polymer particles.⁴⁰ Moreover, in dispersed media, cobaloximes still demonstrate the same sensitivity towards oxygen^{22, 41} and (peroxide) radicals.²²⁻²⁴ In order to circumvent these drawbacks, the application of oxygen-free conditions as well as the avoidance of peroxy initiators are suggested.

1.5.6 Uses of macromonomers

CCTP derived macromonomers have so far found direct use in thermoforming sheets for mould manufacturing and in road pavement manufacturing as additives.⁴² Moreover, macromonomers have attracted attention for the preparation of low VOC-high solids coatings, for example in automotive industry.⁴³ Direct application of CCTP in heterogeneous processes has also been reported, in pigment dispersants⁴⁴ and reactive surfactants in emulsion polymerisation.^{44, 45}

The vinyl ω -terminus of CCTP-derived macromonomers has also attracted attention for their application in copolymerisation. The copolymerisation of macromonomers with monomers generating secondary radicals, such as acrylates is known for leading to graft- and comb-like copolymers.⁴⁶ The copolymerisation of CCTP-derived methacrylic macromonomers with tertiary-radical generating monomers (*e.g.* methacrylates) is of particular interest as macromonomers have demonstrated CTA action themselves. In this case, copolymerisation involves an addition-fragmentation mechanism, Scheme 1.6. In detail, chain transfer occurs due to the susceptibility of the vinyl ω -end group on undergoing radical addition by a propagating radical (**1**). The addition results in the formation of a macromonomer-ended polymer radical (**3**) which is relatively unreactive but can undergo β -scission.⁴⁷ The latter reaction leads to a tertiary radical (**4**) generated *via* fragmentation of the adduct product. At the same time, a new macromonomer (**5**) is formed through combination of the initial growing radical with the vinyl end group of the initial macromonomer. The overall result of an addition-fragmentation process is the transfer of the vinyl ω -terminus from one polymeric chain to another. Thus, the newly formed vinyl-terminated polymer (**5**) can also act as CTA following the exact same reaction mechanism.



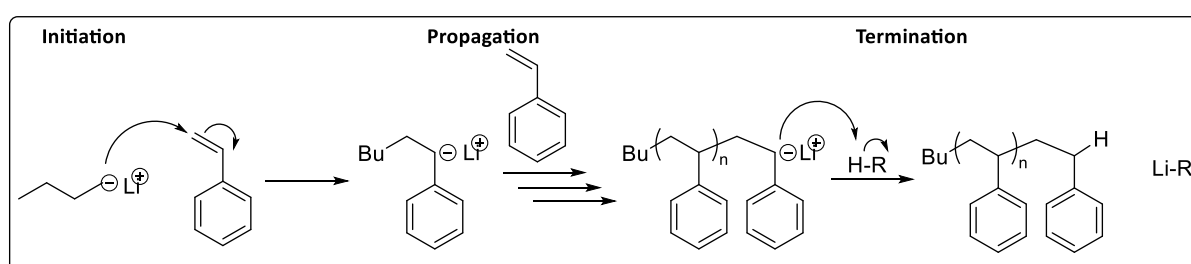
Scheme 1.6: The addition-fragmentation mechanism in the copolymerisation of methacrylic macromonomers with methacrylates.²

Initial studies reported the use of PMMA oligomers as CTAs for bulk polymerisations of MMA¹ while later reports also included polymerisations in solution⁴⁸ as well as in emulsion.² Notably, comparison of the chain transfer constants of the employed oligomers demonstrated little dependence to be attributed to the ester alkyl group of the monomer or the macromonomer.⁴⁸ The use of quantitative ¹H NMR, has demonstrated that the vinyl ω -end group content remains constant on a molar basis during reactions of this type.² Moad and co-workers, discovered that macromonomers employed as CTAs, may affect the polymerisation, allowing linear increase of the molecular weight with conversion and low dispersities, not expected for a free radical process. More specifically, by the employment of methyl methacrylate and phenyl methacrylate macromonomers as CTAs in the free radical emulsion polymerisation of butyl methacrylate (BMA), continuous increase of the molecular

weight, and narrow molecular weight distributions were observed throughout the BMA addition. It needs to be noted that in this study, monomer (BMA) addition was considered as low monomer concentration was required in order to limit propagation relative to chain transfer.

1.6 Living anionic Polymerisation

The first reports of anionic polymerisation was in 1956 by Szwarc and co-workers and referred to the controlled polymerisation of styrene, initiated by aromatic radical-anions.⁴⁹⁻⁵¹ In an anionic polymerisation, the initiation step is fast compared to the propagation. As such, all polymer chains initiate at time zero and grow equally fast, allowing access to well-defined materials. Carbanions, as propagating species are highly reactive towards oxygen, moisture and protic or carbanion-sensitive impurities, rigorous removal of such species is required. Under anionic polymerisation conditions termination is virtually absent and as such this technique is also considered as a living polymerisation.⁵²



Scheme 1.7: Anionic polymerisation of styrene with butyl lithium as initiator.

Anionic polymerisation has been mainly employed for the preparation of well-defined polystyrene. Moreover, most elastomeric block copolymers are commercially produced by anionic living polymerisation. However, the need of extensive purification of the reagents

(*e.g.* monomer, initiator) and the low temperatures employed usually (-78 °C), limit the attractiveness of the technique.

1.7 “Living”/Reversible Deactivation Radical Polymerisation

Conventional FRP is employed industrially and thousands of tons of polymeric materials are produced every year by this method. However, in most cases, the products of FRP do not have well-defined architectures as a result of termination and chain-transfer processes that take place beyond control. The lack of control over the architectures is also demonstrated by the molecular weight distribution that in most FRP reactions is close to 2. The concept of “living” radical polymerisation or later reversible deactivation radical polymerisation by IUPAC⁵³ revolutionised the field as, for the first time well defined architectures and control over the molecular weight were possible. Ideally, a living radical polymerisation comprises of chains growing at the same rate and results in polymers with narrow molecular weight distribution and end-groups dictated by the termination species employed. Moreover, no irreversible transfer or termination reactions should occur.⁵⁴ Despite the highly reactive nature of radicals, it was considered that a dynamic equilibrium between free/propagating and deactivated radicals would increase the overall lifetime of radicals thus allowing polymer chains to grow at similar rate. In order to achieve the dynamic equilibrium, two strategies have been reported. The first is based on the reversible deactivation of the growing radical to form dormant species while the second uses “degenerate transfer” between active and dormant chains.⁵⁵ However, in both cases conventional termination, as in FRP, may still occur thus questioning the “livingness” of the system. In order to address a successful living-radical polymerisation, Quirk and Lee proposed

a series of criteria⁵⁶: (1) Polymerisation proceeds until total monomer consumption. (2) Linear increase of the number-average molecular weight (M_n) with conversion. (3) The number of active centres being constant thus, maintaining a low concentration of active species. (4) The molecular weight (MWt) to be controlled by the stoichiometry of the reaction. (5) Low molecular weight distributions ($\mathcal{D}=M_w/M_n$), generally below 1.5. (6) Quantitative or near quantitative retention of chain-end functionality. (7) Ability to form block copolymers by sequential addition of monomer.

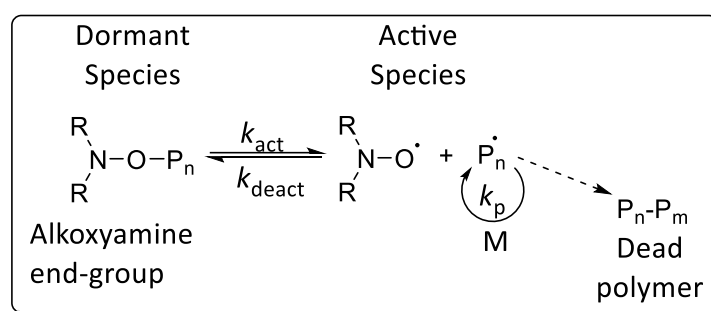
Over the last thirty years, a series of polymerisation techniques, all categorised as RDRPs have emerged. All these techniques allow the synthesis of well-defined polymeric materials while avoiding the highly demanding experimental conditions of living ionic polymerisation. These protocols, apart from securing control over MWt and \mathcal{D} , have also enabled the synthesis of complex structures such as well-defined multi block or star copolymers.

1.7.1 RDRP in emulsion

The main difference between RDRP in homogeneous (bulk/solution) and dispersed systems comprises issues related to the diffusion/partition of the CTA (also called control agent) between the phases.⁵⁷ Particle formation *via* self-assembly of amphiphilic living chains has emerged as an efficient method to circumvent such drawbacks.^{58, 59} A further limiting parameter is the occurrence of “superswelling”. This phenomena results in redistribution of the monomer between droplets/particles but not of the control agent. Consequently, the ratio of monomer to control agent differs in various loci/particles of the system, resulting in broad molecular weight distributions and poor livingness.⁵⁷

1.7.2 Nitroxide-mediated polymerisation (NMP)

Nitroxide-mediated polymerisation is one of the benchmarks of polymer science as it was the first controlled radical polymerisation technique to be applied. NMP takes advantage of the relatively stable nitroxide free radical which can react with the active centre of a propagating radical, forming an alkoxyamine.^{60, 61} NMP is based on an equilibrium between active and dormant species which limits undesired side reactions such as bimolecular termination. The first report on NMP was by Solomon and co-workers who used 2,2,6,6-tetramethylpiperidiny-1-oxy (TEMPO).⁶² The technique attracted more attention in 1993, when Georges *et al.* reported its application for the controlled polymerisation of styrene.⁶⁰



Scheme 1.8: Proposed mechanism for NMP.⁶²

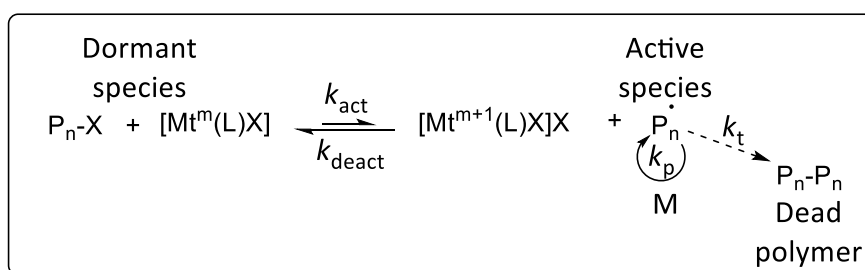
Scheme 1.8 shows the proposed mechanism for NMP. A stable radical mediates the reaction by capping with the active propagating radical. Overall, the concentration of the propagating radical is lower than that of the dormant species, resulting in controlled MWt and \mathcal{D} . Limitations of the technique include its successful application mainly on styrenic monomers⁶³⁻⁶⁵ as well as the long reaction times and high temperatures.⁸

NMP has also been attempted in emulsion, the key parameters proving to be the prevention of monomer droplet nucleation and the maintenance of a sufficient nitroxide concentration in the particles. Therefore, it is not surprising that reports on NMP in emulsion

employed either seeded emulsion⁶⁶ or self-assembly technique.^{67, 68} The latter method was successfully demonstrated by the employment of alkoxyamine macro-initiators by Dire *et al.*⁶⁹ Another interesting approach was followed by Maehata *et al.* who combined nitroxides of suitable hydrophobicity (in order to control partitioning between the two phases) and a hydrophobic inhibitor.⁷⁰

1.7.3 Atom transfer radical polymerisation (ATRP)

Atom transfer radical polymerisation (ATRP) was developed independently by Sawamoto⁷¹ and Matyjaszewski⁷² and reported in 1994 and 1995 respectively. This technique is based on a redox process. In detail, the exchange of a halide atom (either bromine or chlorine) between a metal complex and the propagating radical is taking place, thus governing the equilibrium between active and dormant species.^{73, 74} At first, Sawamoto *et al.* reported the use of a ruthenium (Ru^{II}) catalyst, assisted by the presence of phosphine ligands and aluminium Lewis acids for the controlled polymerisation of MMA. Matyjaszewski and co-workers used copper (Cu^I) complexes of 2,2'-bipyridine for the ATRP of acrylates and methacrylates. Nowadays, most ATRP systems are based on the employment of Cu complexes with nitrogen-based ligands.



Scheme 1.9: Widely accepted mechanism for ATRP.⁵⁵

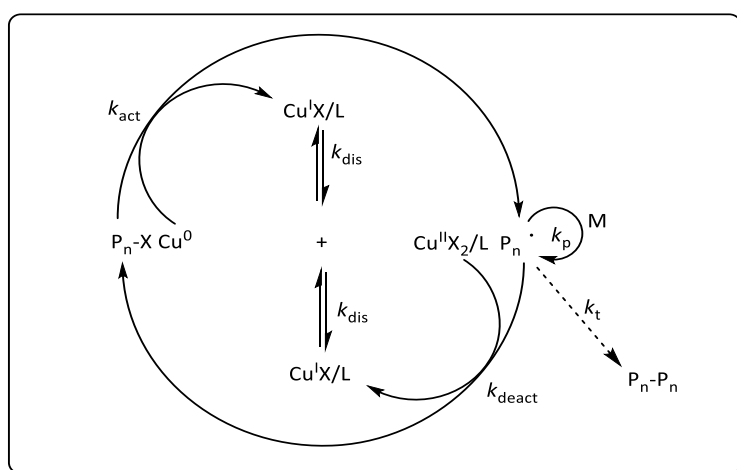
The very simplified proposed mechanism for ATRP is shown in Scheme 1.9. Control over the polymerisation is based on the reversible abstraction of the halide atom (X) from the dormant chain by the metal complex. The catalyst is also able to cap the active centre of the chain by transferring the halogen to it. Ideally, the equilibrium lies on the dormant species side thus, keeping the concentration of the propagating radicals low and securing control of the polymerisation. The existing active radicals propagate as in an FRP process consequently, conventional termination will also occur.

ATRP has also been successfully applied in emulsion both by *ab initio* and *seeded* approaches. In contrast to the application of NMP in emulsion, there has been very limited work on self-assembly approach for emulsion ATRP.⁷⁵ However, other novel methods have been demonstrated about ATRP, such as that by Rusen *et al.* who performed ATRP of styrene *via ab initio* emulsion polymerisation, using a water-soluble alkyl halide as initiator and two ligands, one for the continuous and the other for the dispersed phase.⁷⁶

1.7.4 Single Electron Transfer Living Radical Polymerisation (SET-LRP)

The concept of Single Electron Transfer Living Radical Polymerisation (SET-LRP or Cu⁰ mediated RDRP) was first introduced by Percec and co-workers in 2002⁷⁷ but became widely known in 2006 when the synthesis of ultrahigh molecular weight polymers using this method was reported.⁷⁸ In SET-LRP polar solvents such as water or dimethyl sulfoxide (DMSO) support the disproportionation of CuBr to Cu⁰ and CuBr₂ in the presence of N-containing ligands such as tris[2-(dimethylamino)ethyl]amine (Me₆-Tren). According to the proposed mechanism, Cu⁰ species (either in the form of copper wire or copper powder) activate alkyl halides, Scheme 1.10.⁷⁸⁻⁸⁰ Meanwhile, CuBr is considered to be “inactive” under these conditions due to its

disproportionation into Cu^0 and Cu^{II} species.^{81, 82} Notably, there is controversy about the mechanism of SET-LRP. According to the Matyjaszewski group and others, the process is catalysed by $\text{Cu}(\text{I})$ thus, belonging to the class of ATRP processes.^{83, 84} Whatever the exact mechanism might be, the method has demonstrated fantastic results for the synthesis of well-defined polymers. Dispersity values lower than 1.1 as well as near quantitative end-group fidelity have been achieved by the use of SET-LRP.⁸⁵⁻⁸⁷ Importantly, the technique has been successfully applied for the preparation of complex structures such as well-defined high molecular weight and star multi block copolymers.^{88, 89}

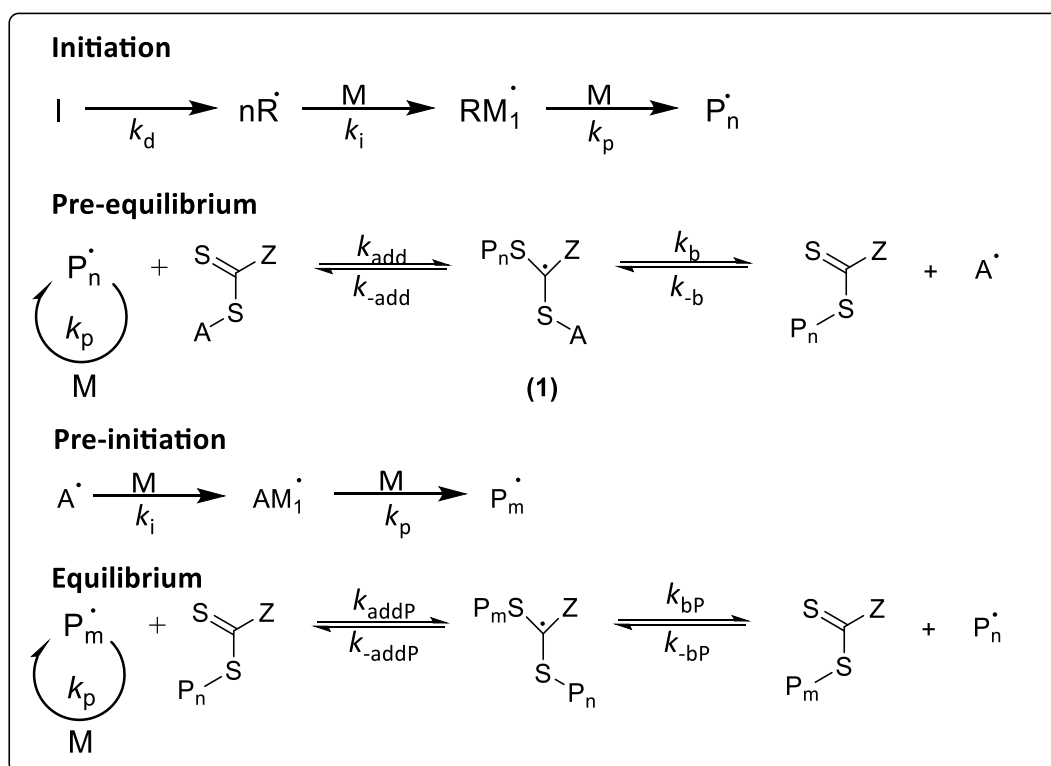


Scheme 1.10: Proposed mechanism for SET-LRP.⁷⁸

1.7.5 Reversible-Addition-Fragmentation Chain-Transfer Radical Polymerisation (RAFT)

RAFT was invented in 1998 at the Commonwealth Scientific and Industrial Research Organisation (CSIRO) of Australia by Le, Moad, Rizzardo and Thang;⁹⁰ together with ATRP they are the most widely applied methods of RDRP.¹⁵ RAFT utilises mainly dithiocarbonates $[\text{RSC}(\text{Z})=\text{S}]$ and trithiocarbonates $[(\text{RS})_2\text{C}=\text{S}]$ as CTAs (otherwise called RAFT agents) however, other thio-compounds may be used as well. In order to perform RAFT, a free-radical

initiator, a monomer, a solvent and the RAFT agent are needed. The choice of the latter is closely related to the reactivity of the chosen monomer.^{91, 92} Polymerisation starts with the decomposition of the initiator that provides the primary and ultimately the propagating radical species (P_n^\cdot), Scheme 1.11. Subsequently, the propagating radical is reversibly added to the RAFT agent (here a dithiocarbonate) to form the intermediate adduct product (1). The latter is then reversibly fragmented providing a new radical (A^\cdot) and a dormant polymer chain. These two steps (reversible addition and fragmentation) compose the RAFT pre-equilibrium. The newly-formed radical species then forms the new propagating chain (P_m^\cdot). The rapid equilibrium between dormant and active species is considered to be of vital importance for the synthesis of well-defined polymers as it governs the relative propagation rates of the propagating chains.⁹³



Scheme 1.11: Proposed mechanism for RAFT polymerisation.⁹³

RAFT can be employed for a large variety of monomers and in several reaction media (bulk, solution, emulsion, suspension). Moreover, it is a versatile technique and easy to perform. Conversely, most RAFT agents are not commercially available and their synthesis may be quite challenging. In addition, such reagents are malodorous and their employment results in coloured polymeric products (usually pink or yellow) which can only be removed through chemical modification of the end group, thus posing limitations for some kinds of applications (*e.g.* personal care).

The application of RAFT in emulsion polymerisation is also known in literature.⁹⁴⁻⁹⁷ However, it originally faced drawbacks similar to those mentioned for NMP. More specifically, poor colloidal stability and insufficient partitioning of the RAFT agents had to be overcome.⁵⁷ Thus, the employment of amphiphilic macroRAFT agents targeting on a self-assembly approach was initially the dominant technique.^{58, 59, 98} In detail, the technique was based on the in situ formation of the amphiphilic agent, typically employing poly(acrylic acid) as the hydrophilic and styrene or *n*-butyl acrylate as the hydrophobic block. However, the use of low MWt, oil-soluble RAFT agents was also reported later for ab initio RAFT polymerisations. This was enabled by the minimisation of superswelling (the main cause of colloidal instability) through the use of suitable surfactant combined with postneutralisation by NaOH.⁹⁹

1.7.6 Multi block copolymers and sequence-control

Chemists have always sought for synthetic macromolecules which would be capable of approaching or even replicating the precision over monomer sequence, as exemplified by natural biopolymers such as DNA, RNA and proteins. This extremely high level of precision allows the aforementioned structures to maintain life by regulating where and when cellular

reactions occur as well as fulfil complicated predefined functions.¹⁰⁰⁻¹⁰² Therefore, the ability to mimic these molecules would be a significant breakthrough with potential applications in a wide range of fields including materials science and nanomedicine. Towards that goal, the synthesis of polymers in which different monomer units are comprised in an ordered fashion, otherwise termed 'Sequence-controlled polymers' has attracted a lot of attention by academia. In spite of the considerable advances in the field of polymer chemistry over the last few decades, synthetic chemists have not yet reached the level of precision expressed by nature.

The development of the solid peptide synthesis by Merrifield in 1963 revolutionised the field.¹⁰³ Nowadays, automated peptide synthesisers are routinely employed in many laboratories, however, the synthesis is still time consuming, expensive due to multiple protection/deprotection steps and difficult to scale up. Moreover, the synthesis of higher molecular weight materials is challenging, if not impossible.

In order to circumvent these issues alternative approaches have been explored. These included single monomer insertion,¹⁰⁴ monomer addition and modification,^{105, 106} kinetic control,¹⁰⁷⁻¹⁰⁹ solution,^{72, 110-114} segregating templating and selected reactivities and sequential growth on soluble polymer supports. Despite the notable progress that has been made over the last few years to harness the potential of step-growth and chain-growth polymerisation in gaining synthetic control over the polymer primary sequence, the majority of the aforementioned methods are limited to the synthesis of low molecular weight materials.

However, the synthesis of sequence-controlled multi block copolymers is more scalable (tens of grams of materials can be routinely synthesised) and allows for the

production of higher molecular weight polymers. In addition, no specialised equipment is essential for the fabrication of these materials (in most cases, a vial is adequate and even deoxygenating the materials is not essential for some cases) in contrast with other sequence-controlled techniques such as templating strategies. Importantly, the synthesis of multi block copolymers can be achieved in 'one pot', meaning there is no requirement for tedious purification and/or protection/deprotection steps. This is of utmost importance as it saves both time and hassle and it also limits the consumption of materials. Finally, a wide range of functionalities with controlled physio-chemical properties can be incorporated along the polymer backbone that can lead to the formation of highly ordered materials exhibiting unique functions and properties.

Among the various polymerisation methods available in the literature, reversible deactivation radical polymerisation (RDRP) is one of the most popular families that allows for the synthesis of multi block copolymers, as it is easy to conduct, not requiring stringent reaction conditions such as tedious distillation of all compounds or specialised equipment (*e.g.* glovebox, sophisticated glassware) that would perhaps not be available in all laboratories or thorough deoxygenation of the reaction mixture. Although examples of multi block copolymers can be found using other polymerisation techniques such as anionic or ring opening polymerisations,¹¹⁵⁻¹¹⁸ RDRP is the most common to consider as it allows access to a wider range of functionalities, is tolerant to impurities and water and also exploitable by a broader range of scientific audience.

Radical polymerisation techniques need to satisfy four major criteria for the successful synthesis of sequence-controlled multi block copolymers, as described below:

- 1) Narrow molecular weight distributions for each block. Although dispersity strongly depends on the size exclusion chromatography (SEC) equipment and thus may not always be directly comparable among different laboratories, a final dispersity < 1.5 is considered indicative of a successful multi block synthesis. Ideally lower dispersities are preferred (< 1.3 or even less) although the effect of the dispersity is associated with the final application of the material.
- 2) High end group fidelity. This can be indirectly exemplified through multiple chain extensions/block copolymerisations and can also be assessed *via* post polymerisation modifications.
- 3) Quantitative or near quantitative conversion ($> 97\%$ and ideally $> 99\%$) for each block. It is essential that each block reaches very high or full monomer conversion otherwise the purity of the material is compromised as the remaining monomer will be copolymerised in the subsequent monomer addition, thus leading to statistical copolymerisation rather than sequential.
- 4) No purification step involved between each monomer addition. This requirement is closely related to the previous one and of utmost importance from an environmental perspective as it eliminates the waste of materials typically consumed during tedious purification steps (*e.g.* solvents). In addition, the one pot synthesis dramatically decreases the reaction time thus, allowing facile access to the synthesis of complex materials.

For many years in living radical polymerisation process was advised to be ceased prior to reach of full monomer conversion in order to ensure maximum end group fidelity. Even the inventors of ATRP and RAFT were suggesting to isolate the macroinitiator at moderate conversions ($\sim 40\text{-}60\%$) before performing chain extensions and/or block copolymerisations. This is not surprising, given that when full monomer conversion is reached the monomer concentration is depleting and hence the polymer end group radical is more likely to react

with another polymer radical or the solvent rather than the monomer and as such termination events occur. Hence, all multi blocks reported in the past, relied on extensive purification of each individual block prior to extension with the next monomer.¹¹⁹⁻¹²⁸ However, over the past few years new synthetic methodologies have been developed which allow the polymer chain to maintain high end group fidelity even at full monomer conversions thus paving the way for the synthesis of one pot sequence-controlled multi block copolymers.

It was in 2011 when Whittaker and co-workers exploited the high end group fidelity obtained *via* Cu(0)-RDRP (also known as single electron transfer living radical polymerisation or SET-LRP)^{88, 129, 130} to synthesise the first one pot highly ordered acrylic multi block copolymers comprising of very short blocks⁸⁵ and then expanded the scope of the work to include higher MWt multi block copolymers.¹³¹ Sugar-based multi blocks copolymers were also reported by the use of the same technique.¹³² Haddleton, Junkers and co-workers subsequently utilised novel photo-induced copper RDRP systems that allowed access to a wider range of functionalities and a higher number of blocks, although still limited in the synthesis of acrylic multi blocks.^{133, 134} As opposed to acrylates, the polymerisation of acrylamides is less established by ATRP mainly due to the complexation of the amide group at the chain ends which stabilised the propagating radicals.¹³⁵ In a further study, Anastasaki *et al.* focused on the optimisation of the amounts of Cu and ligand.⁸⁶ Those two parameters proved to be crucial for maintaining high rates of polymerisation without compromising the livingness. Later, Alsubaie *et al.* reported the preparation of a nonablock copolymer comprising of acrylamides within 3.5 h.¹³⁶ In parallel this study demonstrated that different monomers induce a different rate of chain-end loss.

RAFT has also arisen as a technique with great potential for the synthesis of multi block copolymers, mainly represented by the Perrier group. Gody *et al.* demonstrated the synthesis of complex hexablock, dodecablock and icosablock structures derived from acrylamides in dioxane.¹³⁷ Impressively, the latter structure represented the largest number of blocks seen at the time. However, it comprised of very short blocks ($DP_n = 3$ per block) and had a final molecular weight distribution of 1.36. In all cases, near quantitative conversions were observed, thus allowing for one-pot processes without purification steps. Subsequently, a study focusing on the retention of high end-group fidelity was conducted.¹³⁸ Parameters such as temperature, choice of initiator and solvent were carefully approached. Despite achieving impressive livingness (up to 93 % for a decablock), the study was limited in the synthesis of multi block homopolymers derived only from acrylamides, a monomer family with high k_p in water. Even so, chain extensions were carried out over 24 h. Notably, the authors mentioned that the technique was not expected to be equally efficient for monomer families with lower k_p , such as styrene or methacrylates. The same researchers managed to greatly reduce the reaction times (from 24 down to 2 h per block) by replacing the initially used initiator [4,4'-Azobis(4-cyanovaleric acid), (ACVA)] with VA-044 which decomposes faster thus, allowing optimum radical concentration and faster polymerisation rates.¹³⁹ Importantly, there was no compromise over the end-group fidelity or the quantitative conversions previously achieved. Moreover, this study also demonstrated the potential for higher molecular weight polymers as an octablock copolymer of $DP_n = 40$ and a pentablock of $DP_n = 100$ were synthesised. Following advances by the same research group included the preparation of complex structures without deoxygenation prior to monomer additions with parallel further reduction of the reaction times as to enable the synthesis of a heptablock homopolymer within 21 minutes.¹⁴⁰ Another interesting study focused on the application of aqueous RAFT for the

already tested range of monomers at room temperature.¹⁴¹ This allowed the incorporation of thermoresponsive blocks (*e.g.* PNIPAM) and also targeted on limiting the side reactions usually observed during the polymerisation of acrylic monomers at higher temperatures. Gody *et al.* also employed RAFT in order to investigate the limits of sequence-defined multi block copolymers.¹⁴² Despite the use of RAFT, the findings of this study were related to all kinds of chain growth polymerisation, as all of them are statistical processes, producing a distribution of products, in contrast to stepwise techniques. The authors tried to quantify the level of structural control by the use of the standard deviation of the distribution (σ), instead of utilising the fraction of chains that are in accord with the desired structure (yield). In parallel, they considered ideal living polymerisation conditions where the degree of polymerisation is obeying a Poisson distribution. Following those assumptions, they studied the absolute as well as the relative position of monomers within a polymeric chain. By expanding the scope on to the preparation of multi block copolymers, it was shown by mathematical equations that a minimum block length needs to be targeted in order to limit the amount of defective chains (chains not containing all the desired blocks). It was thus demonstrated that multi block copolymers containing many short blocks were more susceptible to containing defective chains. Specifically, when targeting an average DP_n of three (3), almost 5 % of the polymeric chains would be defective and a copolymer of eighteen blocks would majorly consist of defective chains. However, doubling the targeted average block length to six (6), would theoretically allow the preparation of an icosablock copolymer with only 5 % of defective chains. Overall, this work enlightened the limits of precision that can be achieved by chain polymerisation. Nevertheless, it was noticed that the findings do not equally apply to all controlled chain-growth polymerisation techniques as side reactions

and possible addition of more than one species of monomer during a reaction cycle may largely affect the results.

Despite the expected difficulties related to the relatively low k_p values of methacrylates, mentioned by Gody *et al.*, the preparation of such copolymers has been attempted. Matyjaszewski and his co-workers synthesised copolymers comprising between three and seven blocks with the targeted chain length varying between ten (10) and fifty (50).¹⁴³ As expected, the results were not as promising as for the corresponding attempts on acrylates and acrylamides. The synthesis was limited to seven blocks, thus limiting the molecular weight to 21000 g mol⁻¹ with a final dispersity of 1.29. Low MWt tailing was observed in all stages of the synthesis and was attributed to the need for adding extra initiator in each one. Moreover, the reaction times were longer than 24 h for each chain extension and even so, full conversion was not observed for any of the chain extensions (mostly around 95 %). It needs to be mentioned however that this study focused more on the self-assembly of the triblock copolymers rather than the optimisation of the synthesis of multi block copolymers derived from methacrylics.

Considering the studies on multi block copolymers described, it is evident that despite the remarkable achievements over the last years, there are still many challenges to be faced before even approaching the perfect sequence control achieved by nature. Limiting the unwanted side reactions can lead to narrower molecular weight distributions. The synthesis of longer blocks remains difficult in some cases while there is always the task of conducting all processes in environmentally benign solvents. Moreover, another challenge is the successful preparation of complex multi block structures by the employment of

methacrylates. As such, multi block copolymers may be considered as a way to explore as well as expand the potential and the limitations of a polymerisation technique.

1.8 References

1. C. L. Moad, G. Moad, E. Rizzardo and S. H. Thang, *Macromolecules*, 1996, **29**, 7717-7726.
2. J. Krstina, G. Moad, E. Rizzardo, C. L. Winzor, C. T. Berge and M. Fryd, *Macromolecules*, 1995, **28**, 5381-5385.
3. N. Hadjichristidis, M. Pitsikalis, S. Pispas and H. Iatrou, *Chem. Rev.*, 2001, **101**, 3747-3792.
4. J. P. A. Heuts and N. B. M. Smeets, *Polym. Chem.*, 2011, **2**, 2407-2423.
5. G. Moad, A. G. Anderson, F. Ercole, C. H. J. Johnson, J. Krstina, C. L. Moad, E. Rizzardo, T. H. Spurling and S. H. Thang, *J. Am. Chem. Soc.*, 1998, **685**, 332-360.
6. H. Staudinger, *Ber. deutsch. chem. Ges.*, 1920, **53**, 1073-1085.
7. P. J. Flory, *J. Am. Chem. Soc.*, 1937, **59**, 241-253.
8. G. Odian, *Principles of Polymerization*, 4th Edition. Wiley, 2004.
9. V. N. Kondratiev, *Comprehensive Chemical Kinetics*, Vol. 2, American Elsevier, 1969.
10. M. Kamachi, J. Satoh, S. and I. Nozakura, *J. Polym. Sci.: Polym. Chem.*, 1978, **16**, 1789-1800.
11. G. F. Santee, R. H. Marchessault, H. G. Clark, J. J. Kearny and V. Stannett, *Makromol. Chem.*, 1964, **73**, 177-187.
12. G. V. Schulz and F. Blaschke, *Z. physikal. Chem.*, 1942, **51**, 75.
13. R. G. Gilbert, *Emulsion polymerization: A mechanistic approach*, Academic Press, 1995.
14. P. A. Lovell and M. S. El-Aasser, *Emulsion Polymerization and Emulsion Polymers*, Wiley, 1997.
15. R. J. Young and P. A. Lovell, *Introduction to Polymers, Third Edition*, Taylor & Francis, 2011.
16. S. C. Thickett and R. G. Gilbert, *Polymer*, 2007, **48**, 6965-6991.
17. G. M. Carlson and K. J. Abbey, US 4526945, 1985.
18. J. C. Lin and K. J. Abbey, US 4680354A, 1987.
19. K. J. Abbey, D. L. Trumbo, G. M. Carlson, M. J. Masola and R. A. Zander, *J. Polym. Sci., Part A: Polym. Chem.*, 1993, **31**, 3417-3424.
20. A. H. Janowicz and L. R. Melby, US 4680352, 1987.
21. A. H. Janowicz, EP 222619, 1987.
22. A. A. Gridnev and S. D. Ittel, *Chem. Rev.*, 2001, **101**, 3611-3660.
23. D. A. Morrison, T. P. Davis, J. P. A. Heuts, B. Messerle and A. A. Gridnev, *J. Polym. Sci., Part A: Polym. Chem.* 2006, **44**, 6171-6189.
24. A. A. Gridnev, *Polym. J.*, 1992, **24**, 613-623.
25. K. G. Suddaby, D. M. Haddleton, J. J. Hastings, S. N. Richards and J. P. O'Donnell, *Macromolecules*, 1996, **29**, 8083-8091.
26. J. P. A. Heuts, D. J. Forster, T. P. Davis, B. Yamada, H. Yamazoe and M. Azukizawa, *Macromolecules*, 1999, **32**, 2511-2519.
27. R. Vollmerhaus, S. Pierik and A. M. van Herk, *Macromol. Symp.*, 2001, **165**, 123-131.
28. G. E. Roberts, C. Barner-Kowollik, T. P. Davis and J. P. A. Heuts, *Macromolecules*, 2003, **36**, 1054-1062.
29. F. T. T. Ng, G. L. Rempel, C. Mancuso and J. Halpern, *Organometallics*, 1990, **9**, 2762-2772.
30. B. de Bruin, W. I. Dzik, S. Li, and B. B. Wayland, *Chem. Eur. J.*, 2009, **15**, 4312-4320.
31. F. T. T. Ng and G. L. Rempel, *J. Am. Chem. Soc.*, 1982, **104**, 621-623.
32. S. C. J. Pierik, R. Vollmerhaus, A. M. van Herk and A. L. German, *Macromol. Symp.* 2002, **182**, 43-52.

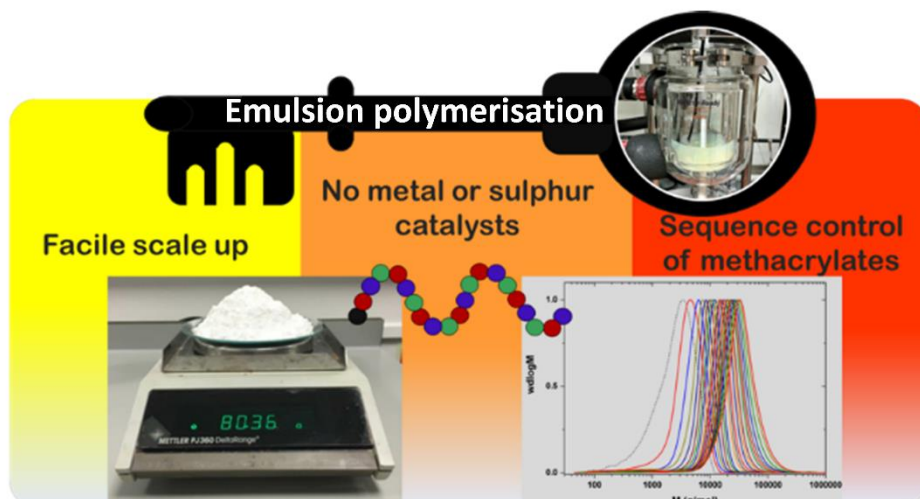
33. G. E. Roberts, J. P. A. Heuts and T. P. Davis, *Macromolecules*, 2000, **33**, 7765-7768.
34. A. Gridnev, *J. Polym. Sci., Part A: Polym. Chem.*, 2000, **38**, 1753-1766.
35. R. A. Sanayei and K. F. O'Driscoll, *J. Macromol. Sci., Part A: Chem.*, 1989, **26**, 1137-1149.
36. D. Kukulj, T. P. Davis, K. G. Suddaby, D. M. Haddleton and R. G. Gilbert, *J. Polym. Sci., Part A: Polym. Chem.*, 1997, **35**, 859-878.
37. D. M. Haddleton, D. R. Morsley, J. P. O'Donnell and S. N. Richards, *J. Polym. Sci., Part A: Polym. Chem.*, 1999, **37**, 3549-3557.
38. N. M. B. Smeets, J. P. A. Heuts, J. Meuldijk, M. F. Cunningham and A. M. Van Herk, *J. Polym. Sci., Part A: Polym. Chem.*, 2009, **47**, 5078-5089.
39. S. A. F. Bon, D. R. Morsley, J. Waterson, D. M. Haddleton, M. R. Lees and T. Horne, *Macromol. Symp.*, 2001, **165**, 29-42.
40. N. M. B. Smeets, T. G. T. Jansen, A. M. van Herk, J. Meuldijk and J. P. A. Heuts, *J. Polym. Chem.*, 2011, **2**, 1830-1836.
41. J. P. A. Heuts, G. E. Roberts and J. D. Biasutti, *Austr. J. Chem.*, 2002, **55**, 381-398.
42. G. D. Airey, J. Wilmot, J. R. A. Grenfell, D. J. Irvine, I. A. Barker and J. E. Harfi, *Eur. Polym. J.*, 2011, **47**, 1300-1314.
43. K. Adamsons, G. Blackman, B. Gregorovich, L. Lin and R. Matheson, *Prog. Org. Coat.*, 1998, **34**, 64-74.
44. J. Huybrechts, P. Bruylants, K. Kirshenbaum, J. Vrana and J. Snuparek, *Prog. Org. Coat.*, 2002, **45**, 173-183.
45. J. Huybrechts, P. Bruylants, A. Vaes and A. De Marre, *Prog. Org. Coat.*, 2000, **38**, 67-77.
46. P. Cacioli, D. G. Hawthorne, R. L. Laslett, E. Rizzardo and D. H. Solomon, *J. Macromol. Sci., Part A: Chem.*, 1986, **23**, 839-852.
47. D. M. Haddleton, D. R. Maloney and K. G. Suddaby, *Macromolecules*, 1996, **29**, 481-483.
48. L. Hutson, J. Krstina, C. L. Moad, G. Moad, G. R. Morrow, A. Postma, E. Rizzardo and S. H. Thang, *Macromolecules*, 2004, **37**, 4441-4452.
49. M. Szwarc, M. Levy and R. Milkovich, *J. Am. Chem. Soc.*, 1956, **78**, 2656-2657.
50. M. Szwarc, *J. Polym. Sci., Part A: Polym. Chem.*, 1998, **36**, IX-XV.
51. M. Szwarc, *J. Polym. Sci., Part A: Polym. Chem.*, 1998, **36**, v-xiii.
52. M. Szwarc, *Nature*, 1956, **178**, 1168-1169.
53. A. D. Jenkins, R. G. Jones and G. Moad, *Pure Appl. Chem.*, 2009, **82**, 483-491.
54. R. B. Grubbs and R. H. Grubbs, *Macromolecules*, 2017, **50**, 6979-6997.
55. K. Matyjaszewski, *Macromolecules*, 2012, **45**, 4015-4039.
56. R. P. Quirk and B. Lee, *Polym. Int.*, 1992, **27**, 359-367.
57. P. B. Zetterlund, Y. Kagawa and M. Okubo, *Chem. Rev.*, 2008, **108**, 3747-3794.
58. C. J. Ferguson, R. J. Hughes, B. T. T. Pham, B. S. Hawkett, R. G. Gilbert, A. K. Serelis and C. H. Such, *Macromolecules*, 2002, **35**, 9243-9245.
59. C. J. Ferguson, R. J. Hughes, D. Nguyen, B. T. T. Pham, R. G. Gilbert, A. K. Serelis, C. H. Such and B. S. Hawkett, *Macromolecules*, 2005, **38**, 2191-2204.
60. M. K. Georges, R. P. N. Veregin, P. M. Kazmaier and G. K. Hamer, *Macromolecules*, 1993, **26**, 2987-2988.
61. C. J. Hawker, *Acc. of Chem. Res.*, 1997, **30**, 373-382.
62. D. H. Solomon, E. Rizzardo and P. Cacioli, US 4581429, 1986.
63. C. J. Hawker, A. W. Bosman and E. Harth, *Chem. Rev.*, 2001, **101**, 3661-3688.
64. D. Benoit, V. Chaplinski, R. Braslau and C. J. Hawker, *J. Am. Chem. Soc.*, 1999, **121**, 3904-3920.
65. D. Benoit, S. Grimaldi, S. Robin, J.-P. Finet, P. Tordo and Y. Gnanou, *J. Am. Chem. Soc.*, 2000, **122**, 5929-5939.
66. J. Nicolas, B. Charleux, O. Guerret and S. Magnet, *Macromolecules*, 2005, **38**, 9963-9973.
67. B. Charleux and J. Nicolas, *Polymer*, 2007, **48**, 5813-5833.
68. G. Delaittre, J. Nicolas, C. Lefay, M. Save and B. Charleux, *Chem. Commun.*, 2005, **0**, 614-616.
69. C. Dire, S. Magnet, L. Couvreur and B. Charleux, *Macromolecules*, 2009, **42**, 95-103.

70. H. Maehata, X. Liu, M. Cunningham and B. Keoshkerian, *Macromol. Rapid Commun.*, 2008, **29**, 479-484.
71. M. Kato, M. Kamigaito, M. Sawamoto and T. Higashimura, *Macromolecules*, 1995, **28**, 1721-1723.
72. J.-S. Wang and K. Matyjaszewski, *J. Am. Chem. Soc.*, 1995, **117**, 5614-5615.
73. K. Matyjaszewski and J. Xia, *Chem. Rev.*, 2001, **101**, 2921-2990.
74. M. Kamigaito, T. Ando and M. Sawamoto, *Chem. Rev.*, 2001, **101**, 3689-3746.
75. P. B. Zetterlund, S. C. Thickett, S. Perrier, E. Bourgeat-Lami and M. Lansalot, *Chem. Rev.*, 2015, **115**, 9745-9800.
76. E. Rusen and A. Mocanu, *Colloid Polym. Sci.*, 2013, **291**, 2253-2257.
77. V. Percec, A. V. Popov, E. Ramirez-Castillo, M. Monteiro, B. Barboiu, O. Weichold, A. D. Asandeia and C. M. Mitchell, *J. Am. Chem. Soc.*, 2002, **124**, 4940-4941.
78. V. Percec, T. Guliasvili, J. S. Ladislav, A. Wistrand, A. Stjerndahl, M. J. Sienkowska, M. J. Monteiro and S. Sahoo, *J. Am. Chem. Soc.*, 2006, **128**, 14156-14165.
79. G. Lligadas, B. M. Rosen, C. A. Bell, M. J. Monteiro and V. Percec, *Macromolecules*, 2008, **41**, 8365-8371.
80. N. H. Nguyen, H.-J. Sun, M. E. Levere, S. Fleischmann and V. Percec, *Polym. Chem.*, 2013, **4**, 1328-1332.
81. M. E. Levere, N. H. Nguyen, X. Leng and V. Percec, *Polym. Chem.*, 2013, **4**, 1635-1647.
82. B. M. Rosen, X. Jiang, C. J. Wilson, N. H. Nguyen, M. J. Monteiro and V. Percec, *J. Polym. Sci., Part A: Polym. Chem.*, 2009, **47**, 5606-5628.
83. D. Konkolewicz, Y. Wang, P. Krysz, M. Zhong, A. A. Isse, A. Gennaro and K. Matyjaszewski, *Polym. Chem.*, 2014, **5**, 4396-4417.
84. D. Konkolewicz, Y. Wang, M. Zhong, P. Krysz, A. A. Isse, A. Gennaro and K. Matyjaszewski, *Macromolecules*, 2013, **46**, 8749-8772.
85. A. H. Soeriyadi, C. Boyer, F. Nyström, P. B. Zetterlund and M. R. Whittaker, *J. Am. Chem. Soc.* 2011, **133**, 11128-11131.
86. A. Anastasaki, C. Waldron, P. Wilson, C. Boyer, P. B. Zetterlund, M. R. Whittaker and D. M. Haddleton, *Acs Macro Lett.*, 2013, **2**, 896-900.
87. A. Anastasaki, V. Nikolaou, G. S. Pappas, Q. Zhang, C. Wan, P. Wilson, T. P. Davis, M. R. Whittaker and D. M. Haddleton, *Chem. Sci.*, 2014, **5**, 3536-3542.
88. C. Boyer, A. H. Soeriyadi, P. B. Zetterlund and M. R. Whittaker, *Macromolecules*, 2011, **44**, 8028-8033.
89. C. Boyer, A. Derveaux, P. B. Zetterlund and M. R. Whittaker, *Polym. Chem.*, 2012, **3**, 117-123.
90. J. Chiefari, Y. K. Chong, F. Ercole, J. Krstina, J. Jeffery, T. P. T. Le, R. T. A. Mayadunne, G. F. Meijs, C. L. Moad and G. Moad, *Macromolecules*, 1998, **31**, 5559-5562.
91. G. Moad, E. Rizzardo and S. H. Thang, *Aust. J. Chem.*, 2009, **62**, 1402-1472.
92. D. J. Keddie, *Chem. Soc. Rev.*, 2014, **43**, 496-505.
93. G. Moad, E. Rizzardo and S. H. Thang, *Aust. J. Chem.*, 2005, **58**, 379-410.
94. S. I. Ali, J. P. A. Heuts, B. S. Hawkett and A. M. van Herk, *Langmuir*, 2009, **25**, 10523-10533.
95. V. T. Huynh, D. Nguyen, C. H. Such and B. S. Hawkett, *J. Polym. Sci., Part A: Polym. Chem.* 2015, **53**, 1413-1421.
96. D. Nguyen, H. S. Zondanos, J. M. Farrugia, A. K. Serelis, C. H. Such and B. S. Hawkett, *Langmuir*, 2008, **24**, 2140-2150.
97. B. T. T. Pham, C. H. Such and B. S. Hawkett, *Polym. Chem.*, 2015, **6**, 426-435.
98. E. Sprong, J. S. K. Leswin, D. J. Lamb, C. J. Ferguson, B. S. Hawkett, B. T. T. Pham, D. Nguyen, C. H. Such, A. K. Serelis and R. G. Gilbert, *Macromol. Symp.*, 2006, **231**, 84-93.
99. Y. Luo, X. Wang, B.-G. Li and S. Zhu, *Macromolecules*, 2011, **44**, 221-229.
100. N. Badi and J.-F. Lutz, *Chem. Soc. Rev.*, 2009, **38**, 3383-3390.
101. J.-F. Lutz, *Polym. Chem.*, 2010, **1**, 55-62.
102. J.-F. Lutz, M. Ouchi, D. R. Liu and M. Sawamoto, *Science*, 2013, **341**, (6146).

103. R. B. Merrifield, *J. Am. Chem. Soc.*, 1963, **85**, 2149-2154.
104. J. Vandenberg, G. Reekmans, P. Adriaensens and T. Junkers, *Chem. Commun.*, 2013, **49**, 10358-10360.
105. K. Nakatani, T. Terashima and M. Sawamoto, *J. Am. Chem. Soc.*, 2009, **131**, 13600-13601.
106. K. Nakatani, Y. Ogura, Y. Koda, T. Terashima and M. Sawamoto, *J. Am. Chem. Soc.*, 2012, **134**, 4373-4383.
107. S. Pfeifer, Z. Zarafshani, N. Badi and J.-F. Lutz, *J. Am. Chem. Soc.*, 2009, **131**, 9195-9197.
108. M. Zamfir and J.-F. Lutz, *Nat. Commun.*, 2012, 1138.
109. D. Moatsou, C. F. Hansell and R. K. O'Reilly, *Chem. Sci.*, 2014, **5**, 2246-2250.
110. A. Marsh, A. Khan, D. M. Haddleton and M. J. Hannon, *Macromolecules*, 1999, **32**, 8725-8731.
111. A. Khan, D. M. Haddleton, M. J. Hannon, D. Kukulj and A. Marsh, *Macromolecules*, 1999, **32**, 6560-6564.
112. S. Ida, T. Terashima, M. Ouchi and M. Sawamoto, *J. Am. Chem. Soc.*, 2009, **131**, 10808-10809.
113. Y. Hibi, M. Ouchi and M. Sawamoto, *Angew. Chem. Int. Ed.*, 2011, **50**, 7434-7437.
114. Y. Hibi, S. Tokuoka, T. Terashima, M. Ouchi and M. Sawamoto, *Polym. Chem.*, 2011, **2**, 341-347.
115. C. Ntaras, G. Polymeropoulos, G. Zapsas, K. Ntetsikas, G. Lontos, A. Karanastasis, D. Moschovas, S. Rangou, C. Stewart-Sloan, N. Hadjichristidis, E. L. Thomas and A. Avgeropoulos, *J. Polym. Sci., Part B: Polym. Phys.*, 2016, **54**, 1443-1449.
116. S. Çakır, M. Eriksson, M. Martinelle and C. E. Koning, *Eur. Polym. J.*, 2016, **79**, 13-22.
117. A. M. Mannion, F. S. Bates and C. W. Macosko, *Macromolecules*, 2016, **49**, 4587-4598.
118. P. Olsén, K. Odelius, H. Keul and A.-C. Albertsson, *Macromolecules*, 2015, **48**, 1703-1710.
119. T. G. McKenzie, J. M. Ren, D. E. Dunstan, E. H. Wong and G. G. Qiao, *J. Polym. Sci., Part A: Polym. Chem.*, 2016, **54**, 135-143.
120. A. Mei, X. Guo, Y. Ding, X. Zhang, J. Xu, Z. Fan and B. Du, *Macromolecules*, 2010, **43**, 7312-7320.
121. T. Ren, X. Lei and W. Yuan, *Mater. Lett.* 2012, **67**, 383-386.
122. N. Beheshti, K. Zhu, A.-L. Kjøniksen, K. D. Knudsen and B. Nyström, *Soft Matter* 2011, **7**, 1168-1175.
123. L. Zhang, Z. Cheng, N. Zhou, R. Zhang and X. Zhu, *Macromol. Symp.*, 2008, **261**, 54-63.
124. K. A. Davis and K. Matyjaszewski, *Macromolecules*, 2001, **34**, 2101-2107.
125. A. Ramakrishnan and R. Dhamodharan, *Macromolecules*, 2003, **36**, 1039-1046.
126. W.-H. Chen, D.-J. Liaw, K.-L. Wang, K.-R. Lee and J.-Y. Lai, *Polymer*, 2009, **50**, 5211-5219.
127. E. Eastwood and M. Dadmun, *Macromolecules*, 2001, **34**, 740-747.
128. S. Kumar, J.-S. Lee and C. Murthy, *Macromol. Res.*, 2011, **19**, 1022-1028.
129. A. Anastasaki, V. Nikolaou, G. Nurumbetov, P. Wilson, K. Kempe, J. F. Quinn, T. P. Davis, M. R. Whittaker and D. M. Haddleton, *Chem. Rev.*, 2015, **116**, 835-877.
130. A. Anastasaki, V. Nikolaou and D. M. Haddleton, *Polym. Chem.*, 2016, **7**, 1002-1026.
131. A. Anastasaki, C. Waldron, P. Wilson, C. Boyer, P. B. Zetterlund, M. R. Whittaker and D. M. Haddleton, *ACS Macro Lett.*, 2013, **2**, 896-900.
132. Q. Zhang, J. Collins, A. Anastasaki, R. Wallis, D. A. Mitchell, C. R. Becer and D. M. Haddleton, *Angew. Chem. Int. Ed.*, 2013, **52**, 4435-4439.
133. A. Anastasaki, V. Nikolaou, N. W. McCaul, A. Simula, J. Godfrey, C. Waldron, P. Wilson, K. Kempe and D. M. Haddleton, *Macromolecules*, 2015, **48**, 1404-1411.
134. Y.-M. Chuang, A. Ethirajan and T. Junkers, *ACS Macro Lett.*, 2014, **3**, 732-737.
135. J. T. Rademacher, M. Baum, M. E. Pallack, W. J. Brittain and W. J. Simonsick, *Macromolecules*, 1999, **33**, 284-288.
136. F. Alsubaie, A. Anastasaki, P. Wilson and D. M. Haddleton, *Polym. Chem.*, 2015, **6**, 406-417.
137. G. Gody, T. Maschmeyer, P. B. Zetterlund and S. Perrier, *Nat. Commun.*, **2013**, **4**.
138. G. Gody, T. Maschmeyer, P. B. Zetterlund and S. Perrier, *Macromolecules*, 2014, **47**, 639-649.

139. G. Gody, T. Maschmeyer, P. B. Zetterlund and S. Perrier, *Macromolecules*, 2014, **47**, 3451-3460.
140. G. Gody, R. Barbey, M. Danial and S. Perrier, *Polym. Chem.*, 2015, **6**, 1502-1511.
141. L. Martin, G. Gody and S. Perrier, *Polym. Chem.*, 2015, **6**, 4875-4886.
142. G. Gody, P. B. Zetterlund, S. Perrier and S. Harrisson, *Nat. Commun.*, 2016, **7**.
143. S. M. Chin, H. He, D. Konkolewicz and K. Matyjaszewski, *J. Polym. Sci., Part A: Polym. Chem.* 2014, **52**, 2548-2555.

Sequence-controlled multiblock copolymers *via* sulphur-free RAFT emulsion polymerisation



Translating the precise monomer sequence control achieved by nature over macromolecular structure (for example DNA) to whole synthetic systems has been limited due to the lack of efficient synthetic methodologies. So far chemists have only been able to synthesise monomer sequence-controlled macromolecules by means of complex, time consuming and iterative chemical strategies. Here, a rapid and quantitative synthesis of sequence-controlled multi block polymers in discrete stable nanoscale compartments via an emulsion polymerisation approach in which a vinyl terminated macromolecule is used as an effective chain transfer agent is reported. This approach is environmentally friendly, fully translatable to industry (80 grams scale up), and thus represents a significant advance in the development of complex macromolecule synthesis, paving the way for a number of applications where a high level of molecular precision or monomer sequence control via an efficacious process confers potential for molecular targeting, recognition and biocatalysis, as well as molecular information storage.

2.1 Introduction

The timeline of evolution has given rise to diversity at all levels of biological organisation enabling the synthesis of complex, diverse, functional sequence-ordered macromolecules such as DNA and proteins in discrete compartments (*e.g.* cell's nuclei, cytoplasm and mitochondria). These sequence-controlled biomacromolecules play a vital role in the development, functioning and reproduction of all living organisms. Therefore, the ability to translate molecular precision, as demonstrated in nature, to highly organised sequence-controlled synthetic analogues would be a significant breakthrough with potential applications in many fields including nanomedicine and nanotechnology. Arguably, solid state peptide synthesis (Merrifield synthesis) revolutionised the field providing access to precisely controlled macromolecules.¹ However, the time consuming and iterative attachment/deprotection of monomers in solid state can be expensive, often results in poor yields, is difficult to scale up and often limited to the synthesis of relatively low molecular weight oligomers.

Synthetic chemical approaches in the homogeneous liquid phase have also been alternatively exploited in the last decade in order to allow access to a wider range of chemical functionalities as well as the synthesis of polymer-based sequence-controlled materials on a larger scale (g or kg rather than mg).²⁻⁵ More recently, diverse methodologies have been investigated that aim to more precisely control the sequence of monomers, including single monomer insertion,⁶⁻⁸ tandem monomer addition and modification,⁹⁻¹¹ kinetic control,¹²⁻¹⁴ solution,^{1,15-17} segregating templating,¹⁸ selected reactivities and sequential growth on soluble polymer supports.^{5,19-21} Importantly, the majority of these strategies remain limited to the synthesis of low molecular weight oligomers. In contrast, the synthesis of multi block

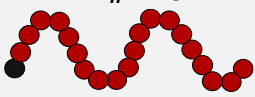
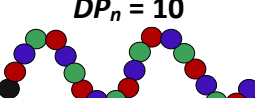

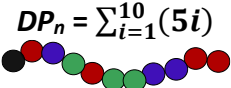
copolymers is more scalable, allows for the production of higher molecular weight polymers, while the incorporation of a wide range of functionalities along the polymer backbone with controlled physico-chemical properties can lead to the formation of highly ordered materials exhibiting unique functions and properties.

As such, improving the control of the synthesis of multi block copolymers dissolved in the solution phase has received considerable interest. Contributions by Whittaker, Haddleton, Junkers, Perrier and their co-workers have reported the impressive synthesis of acrylic and acrylamide multi block copolymers.²²⁻³³ However, because they made use of catalysts containing either transition metal (usually copper) or sulphur, multiple purification steps were required to isolate the final pure materials. In addition, the halide (as used in transition metal mediated approaches) and the reversible addition fragmentation chain transfer (RAFT) agents are typically attached to the polymer backbone even after purification and may be undesirable in certain applications. Further limitations of these approaches often include high dispersities (> 1.70 for a decablock copolymer), non-quantitative final conversions ($\sim 80\%$),^{23,34} extended reaction times per chain block (up to 48 h),²³⁻²⁵ undesirable hydrolysis²⁶ of the chain ends leading to architectural heterogeneity. Importantly, these systems have so far proved either incompatible with monomers exhibiting relatively low rates of propagation, k_p , such as methacrylates, or exhibit undesirable termination or chain transfer events.^{23,34} This limitation has a detrimental effect on a wide range of applications that require higher glass transition temperatures (T_g), as methacrylic polymers exhibit significantly higher values than their acrylic counterparts.

Inspired by nature's ability to synthesise structurally 'pure' complex biomolecules, the segregation strategy was employed in an attempt to address the aforementioned limitations.

Indeed, the well-established emulsion polymerisation (used industrially to make many coatings, adhesives and personal care products) represents a widely employed efficient synthetic application of this approach, where monomers and catalysts are isolated in nanoscale micelles dispersed in a continuous aqueous phase.^{35,36} This isolation provides spatial separation of individual growing macromolecules and can significantly reduce unwanted side reactions such as termination seen in radical polymerisations and can control chemistry *via* a kinetic approach. In this study, it is demonstrated for the first time that well-defined, sequence-controlled multi block copolymers can be synthesised in a facile, rapid, quantitative and scalable manner by developing a novel both 'transition metal' and 'sulphur' free polymerisation approach combined with an emulsion biomimetic segregation strategy. Catalytic chain transfer polymerisation (CCTP) as carried out in emulsion is exploited in the first stage in order to synthesise a vinyl terminated poly(methyl methacrylate) (PMMA) macromolecule which is subsequently (no purification involved) used *in situ* as a chain transfer agent for the reversible addition-fragmentation chain transfer polymerisation of various methacrylic monomers.

Table 2.1: Summary of the multi block copolymers synthesised in this study.

Block composition	No of blocks	Conv. ^a (%)	$M_{n,th}^b$ (g.mol ⁻¹)	$M_{n,SEC}$ (g.mol ⁻¹)	\bar{D}	Particle Diameter (nm)	\bar{D}_{DLS}
 $DP_n = 10$	21	>99	29800	27800	1.20	330	0.117
 $DP_n = 10$	21	>99	36400	29500	1.35	360	0.112
 $DP_n = 45$	7	98	48200	41300	1.24	400	0.125
 $DP_n = \sum_{i=1}^{10} (5i)$	11	>99	44100	42000	1.25	450	0.250

^a Overall monomer conversion for all additions characterised by ¹H NMR, CDCl₃:Acetone-d₆ (3:2 v/v). ^b $M_{n,th} = [M]_0 \times p \times M_M / [CTA]_0 + M_{CTA}$. Each coloured sphere represents one block with the black sphere representing the CTA, the red, blue and green representing BMA, BzMA and EHMA blocks respectively.

2.2 Results and Discussion

Butyl methacrylate (BMA) was first selected as the building block of the sequence-controlled macromolecules (Figure 2.1 a) to test whether the segregation approach of emulsion polymerisation is suitable for the synthesis of well-defined multi block polymers *via* multi-sequential monomer addition. Previous investigations have been directed towards the polymerisation of monomers with higher k_p (such as acrylamides and acrylates). However, the main focus of this study is on the methacrylic monomer family which have proved challenging as they exhibit significantly higher rates of termination relative to chain propagation due to relatively low values of k_p . A PMMA oligomer with $M_n \sim 2000$ g mol⁻¹ ($\bar{D} \sim 1.7$) was synthesised in a 0.5 L double-jacketed reactor *via* CCTP emulsion polymerisation^{37,38} and the presence of

the terminal vinyl protons was confirmed by both ^1H NMR and MALDI-ToF-MS (Figures 2.2 a & b).

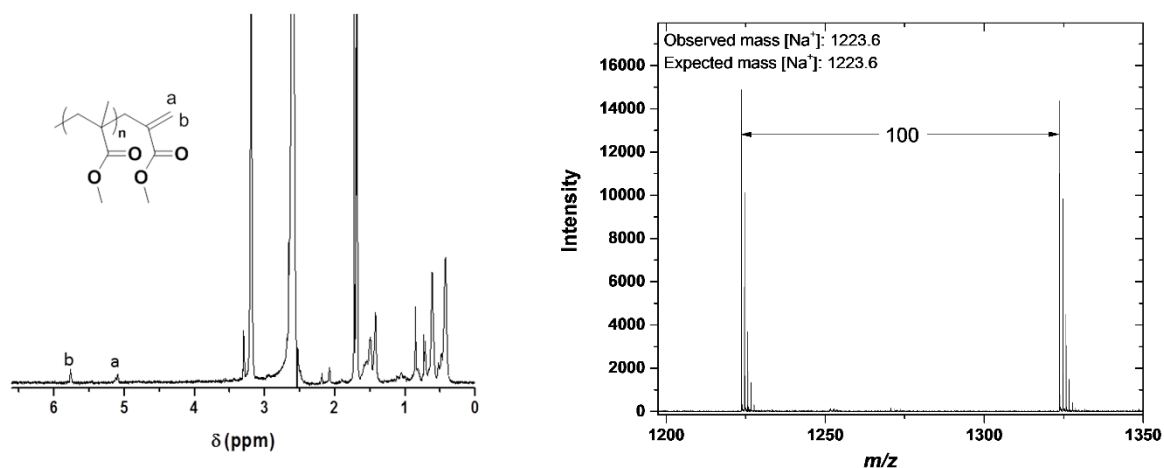
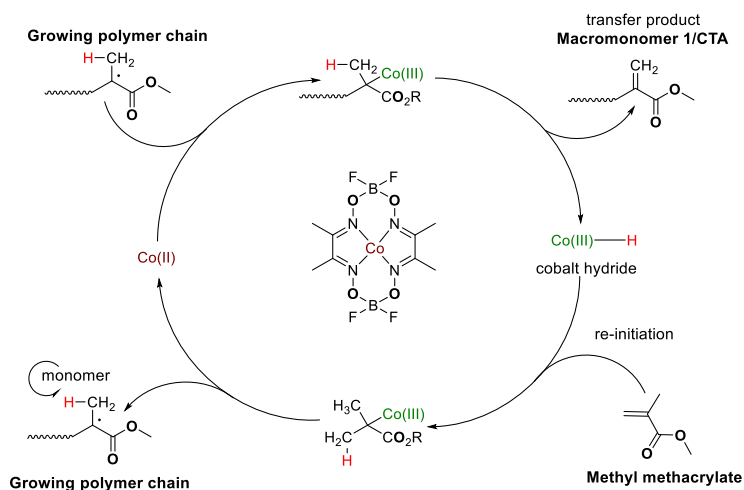


Figure 2.2: (a) ^1H NMR trace of the PMMA macromonomer obtained *via* CCTP in emulsion and (b) MALDI spectra of the of the PMMA macromonomer obtained *via* CCTP in emulsion.

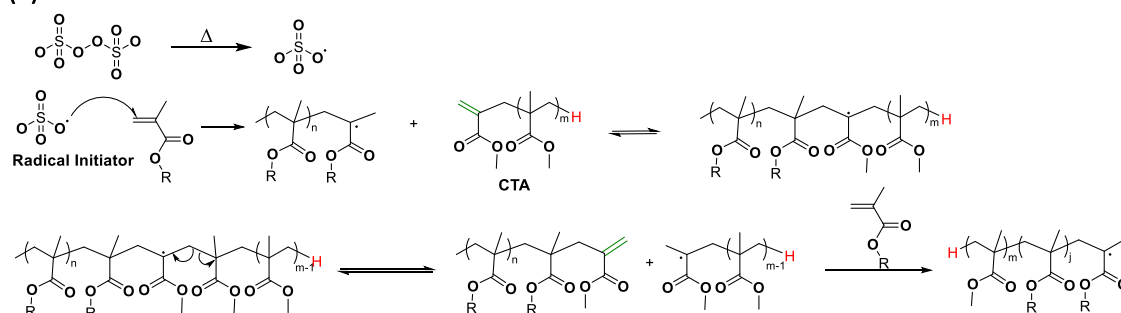
The mechanism of CCTP is depicted in Figure 2.3 and utilises appropriate low spin d^6 Co(II) complexes (cobaloximes), abstracting a hydrogen from a propagating methacrylic radical to yield a Co(III)-H intermediate and an oligomer with a terminal vinyl group. These unsaturated macromolecules have been found to exhibit chain transfer activity in the radical polymerisation of methacrylates.³⁹ The chain transfer mechanism proceeds *via* chain transfer followed by fragmentation to give a macroradical which is able to initiate the second monomer, ultimately leading to block copolymers. Fragmentation is favoured over chain growth as the rate of chain growth from the sterically hindered macroradical is greatly reduced relative to a normal methacrylic radical, while the rate of unimolecular fragmentation is unaffected by the increased steric constraints. The new chain propagates *via* repeated addition of monomer. The propagating block copolymer chain can again react with

the macromonomer resulting in an addition fragmentation process not unlike RAFT, mediated by sulphur containing chain transfer agents (Figure 2.3 b).

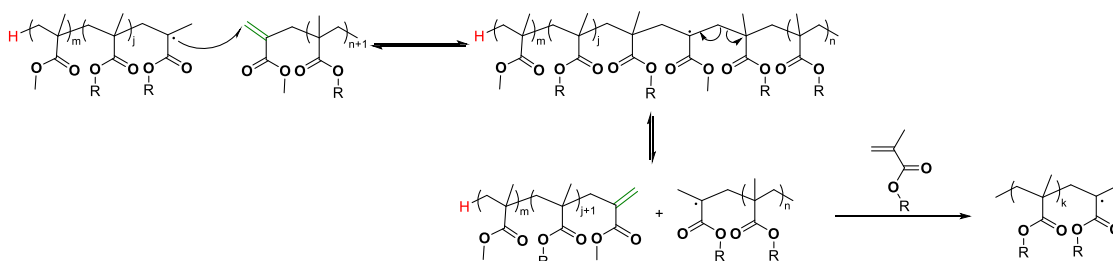
(a) Macromonomer formation



(b) Chain extension with second monomer

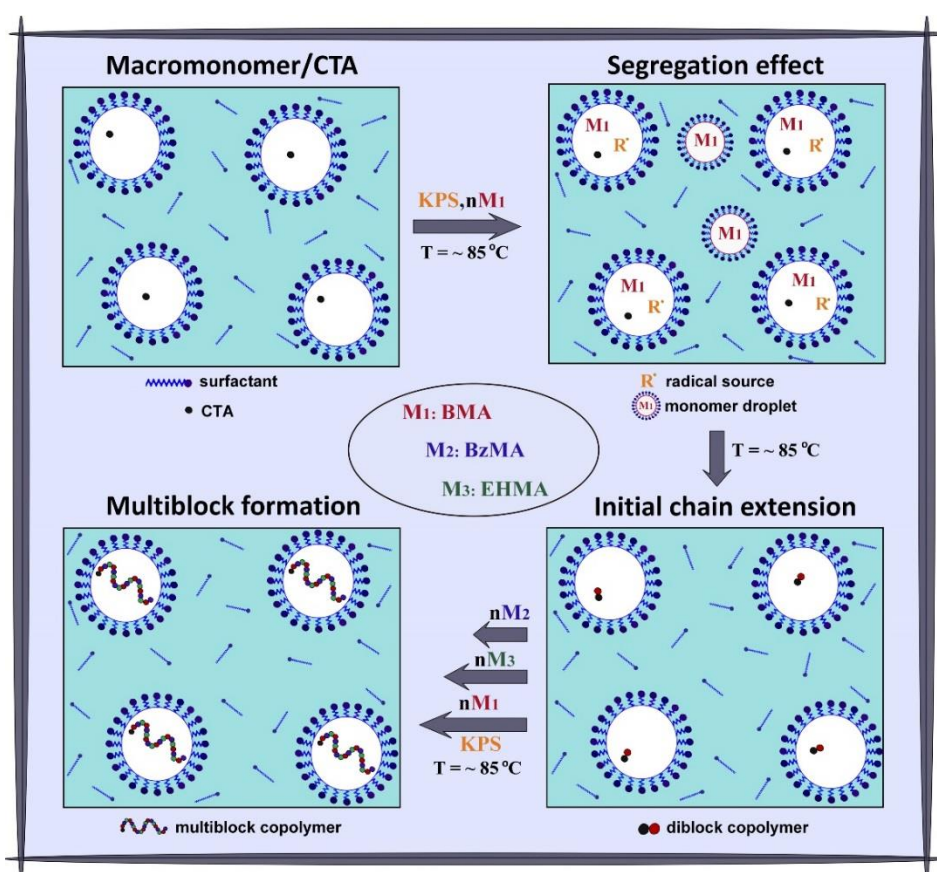


Block copolymer formation



Scheme 2.1: Proposed mechanisms of (a) CCTP and (b) addition-fragmentation reaction.

The PMMA ‘macromonomer’ is subsequently utilised as the chain transfer agent (without purification) to facilitate the synthesis of multi block copolymers employing an initial ratio of $[CTA]:[Monomer]:[Initiator]=[1]:[10]:[0.03]$ *via* reversible addition fragmentation chain transfer emulsion polymerisation. This approach can be summarised in Figure 2.4. BMA was used as the second monomer and each block was designed to be $DP_n = 10$ (Figure 2.1 a). It is noted that a targeted DP_n of 10 for each chain extension has been selected in order to minimise the proportion of missing blocks (percent of defective chains) for the final multi block material, which will be minimal according to a recently published paper by Harrison and co-workers.⁴⁰ Under the aforementioned conditions, degassed mixtures of (i) monomer and (ii) initiator in water were fed into the reactor *via* a syringe pump (Figure 2.5).



Scheme 2.2: Conceptual scheme for the synthesis of multi block copolymers in emulsion.



Figure 2.3: Typical set up for the synthesis of macromonomers or multi block copolymers employing a double jacketed reactor and securing a constant monomer addition rate by the use of a syringe pump.

It should be noted that an oxygen centred radical initiator (potassium persulfate) is used at this step to deactivate, *in situ* the bis[(difluoroboryl) dimethylglyoximato]cobalt(II) (CoBF) catalyst (used in the first step for the formation of macromonomer) *via* radical addition to the unsaturated groups with ligand “bleaching”, thus precluding the need for purification of the CTA prior to the subsequent block formation.⁴¹ This second stage of polymerisation resembles a typical RAFT polymerisation. The following components are included: (i) a free radical initiator (potassium persulfate in this case) to generate the radical source and at the same time deactivate CoBF, (ii) a CTA (vinyl terminated PMMA in this case) and (iii) a monomer (BMA in this case). On completion of the monomer addition to the reaction

mixture, the reaction was allowed to proceed for 1 h (giving a total of 2.5 h, including the feeding time), after which a sample was taken for further analysis. ^1H NMR spectroscopy confirmed high monomer conversion ($> 99\%$) while SEC showed the molecular weight distributions (MWDs) shifting to higher molecular weights with an observed decrease in dispersity ($\mathcal{D} \sim 1.3$) and excellent agreement between the theoretical and the experimental molecular weights (Figure 2.6). This confirmed the potential of this technique to support the synthesis of low dispersity multi block copolymers from methacrylates. When a second aliquot of BMA was subsequently added, a further reduction in dispersity was evident ($\mathcal{D} \sim 1.25$), which decreased further upon addition of each subsequent monomer aliquot, reaching a quasi hexablock multi block copolymer with $M_n \sim 10400 \text{ g mol}^{-1}$ and a final dispersity 1.10 (see Tables 2.2 and Section 2.4.4, Table 2.6 for synthetic details). This sequential addition was performed with success 20 times resulting in a heneicosa (21) quasi multi block copolymer (including the CTA as the CTA itself is also a polymer with $M_n = 2000 \text{ g mol}^{-1}$) exhibiting relatively narrow molecular weight distribution ($\mathcal{D} \sim 1.20$) and high degree of control, as demonstrated both by the good control over the MWDs and the satisfactory correlation between theoretical and experimental values, despite 20 cycles of sequential monomer addition. Throughout all of the monomer additions, SEC showed monomodal distributions that shifted to higher molecular weights, while ^1H NMR confirmed $> 99\%$ monomer conversion in each step (Figure 2.6 a & b and Table 2.2). Following additional chain extensions, no compromise over control of the molecular weight distributions was observed, and the dispersity of the resultant tetracosia (24) multi block remaining as low as 1.21 (Figure 2.6 d, Table 2.2). These data confirm the capacity of the segregation approach of emulsion polymerisation to successfully synthesise well-defined sequence-controlled multi block copolymers from the challenging methacrylic monomers.

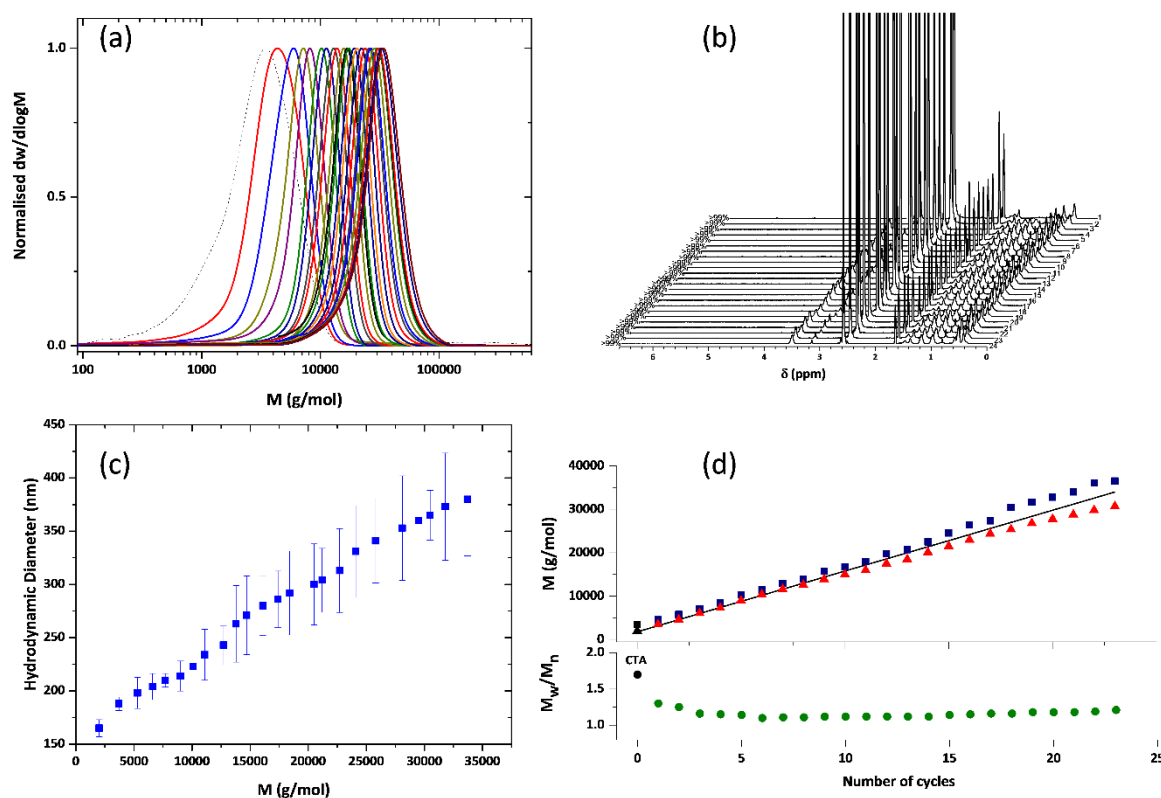


Figure 2.4: Synthesis and characterisation of model heneicasoblock BMA homopolymer. (a) SEC traces of molecular weight distributions for consecutive cycles during the synthesis of the heneicasoblock homopolymer, (b) ^1H NMR spectra for consecutive cycles, (c) hydrodynamic diameter evolution of the heneicasoblock homopolymer, as obtained by Z-average measurements versus the number average molecular weight (M_n) as measured by DLS and (d) evolution of theoretical (black straight line) and experimental molecular weight M_n (\blacktriangle) and M_w (\blacksquare) determined by SEC and M_w/M_n (\bullet) versus the number of cycles during synthesis of heneicasoblock homopolymer.

Table 2.2: Characterisation data for the synthesis of the tetracosablock PBMA homopolymer in emulsion at 85 °C with potassium persulfate as initiator.

Entry	Cycle	Conv. (%)	$M_{n,th}$ (g.mol ⁻¹)	$M_{n,SEC}$ (g.mol ⁻¹)	\bar{D}	Particle Diameter (nm)	\bar{D}_{DLS}
1	CTA	>99	1800	2000	1.7	166	0.072
2	1	>99	3200	3500	1.3	190	0.041
3	2	>99	4600	4600	1.25	200	0.073
4	3	>99	6000	6100	1.16	209	0.067
5	4	>99	7400	7300	1.15	213	0.096
6	5	>99	8800	9000	1.14	220	0.091
7	6	>99	10200	10400	1.10	232	0.096
8	7	>99	11600	11600	1.11	244	0.110
9	8	>99	13000	12600	1.11	250	0.109
10	9	>99	14400	13900	1.12	258	0.118
11	10	>99	15800	15000	1.12	265	0.137
12	11	>99	17200	16000	1.12	279	0.131
13	12	>99	18600	17500	1.12	285	0.103
14	13	>99	20000	18500	1.12	289	0.111
15	14	>99	21400	20100	1.12	296	0.105
16	15	>99	22800	21500	1.14	302	0.123
17	16	>99	24200	23000	1.15	309	0.109
18	17	>99	25600	24400	1.16	315	0.106
19	18	>99	27000	25400	1.16	320	0.117
20	19	>99	28400	26800	1.18	325	0.089
21	20	>99	29800	27800	1.18	329	0.117
22	21	>99	31200	28800	1.18	334	0.109
23	22	>99	32600	29800	1.19	341	0.112
24	23	>99	34000	30700	1.21	347	0.120

It is noted that in the ¹H NMR results, the remaining vinyl peaks observed between 5.5 and 6.6 ppm correspond to the terminal double bond from the CTA, as the monomer vinyl peaks appear at a slightly different chemical shift (Figure 2.7). This allows for the calculation of the monomer conversion and also shows that the residual vinyl peaks in the spectrum of the final product correspond to the CTA rather than any remaining unreacted monomer.

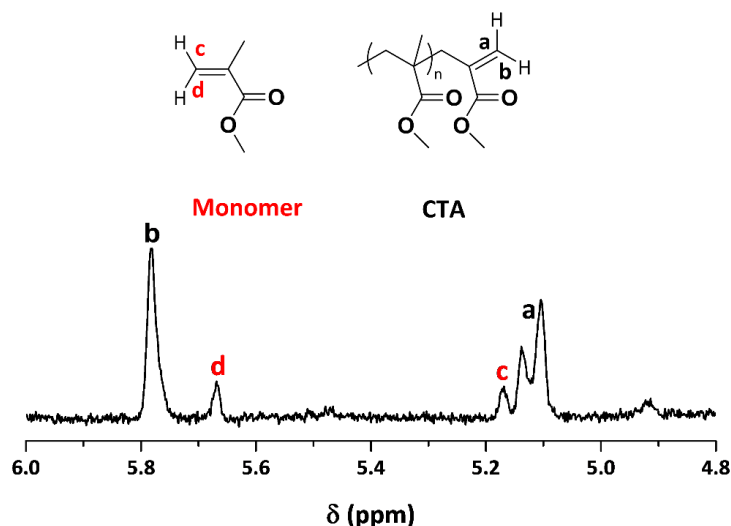


Figure 2.5: ^1H NMR traces of the of the PMMA macromonomer obtained *via* CCTP in emulsion and the residual MMA monomer.

An important consideration for the successful synthesis of this quasi multi block copolymer is to maintain the reaction solid content of the emulsion in relatively low/moderate levels in order to stabilise it and avoid coagulation which would limit the final yield and increase the structural heterogeneity of the final product. To circumvent this, the system was further diluted prior to the addition of each monomer batch (See Section 2.4.4, Table 2.6). It is remarkable that when comparing the first 10 methacrylate block homopolymers ($\mathcal{D} \sim 1.12$) with the fully optimised acrylamide decablock homopolymer reported in the literature ($\mathcal{D} \sim 1.15$), not only do they exhibit similar level of control ($\mathcal{D} \sim 1.12$ *versus* 1.15), but the overall polymerisation rates are also similar (~ 2 h per block), despite the methacrylates having such a low k_p (between 1000 and $1500 \text{ L mol}^{-1} \text{ s}^{-1}$; acrylates: 40000 - $60000 \text{ L mol}^{-1} \text{ s}^{-1}$).^{30,42-44} Of course, this is only possible due to the compartmentalisation effects of emulsion polymerisation, which result in an acceleration of the polymerisation rate while maintaining low termination levels due to the low concentrations of the radicals in the particle.^{45,46} Further evidence for the high control of the system can be seen from the plot of

the evolution of the number average molecular weight (M_n) with each monomer addition, where both M_n and M_w increase linearly with time, with very little deviation from the theoretical values (Figure 2.6 d). In addition, dynamic light scattering (DLS) was also employed to characterise this multi block homopolymer, demonstrating an increase in the hydrodynamic diameter with increasing M_n , which supports the gradual growth of the material (Figure 2.6 c).⁴⁵

Having tested the conditions for the synthesis of a quasi-multi block homopolymer, the fabrication of more complex multi block materials was subsequently investigated, as the inclusion of different monomers imparts a wide range of physico-chemical properties to the final materials. Apart from the PMMA macro CTA, which was used as the first (or the last) block, a family of three additional methacrylic monomers was employed, including benzyl methacrylate (BzMA), 2-ethyl hexyl methacrylate (EHMA) and BMA. The inclusion of different monomers (see Table 2.3 and Section 2.4.4, Table 2.7 for further synthetic details) resulted in a heneicosablock (21) multi block copolymer exhibiting relatively narrow molecular weight distributions ($\mathcal{D} \sim 1.35$) for such a complex structure (Figure 2.1 b). It is noted that when an icosablock (20) multi block copolymer was synthesised by Perrier and co-workers utilising a much more quickly propagating monomer family (acrylamides), a similar level of control was attained ($\mathcal{D} \sim 1.35$ for both systems).³⁰ SEC again confirmed complete shifts to higher molecular weight following each monomer addition (Figure 2.8 a), DLS showed an increase of the hydrodynamic diameter of the particles with increasing M_n (Figure 2.8 c) while ^1H NMR revealed very high conversions (> 99%) throughout the block copolymerisation cycles (Figure 2.8 b), demonstrating the quantitative synthesis of highly ordered sequence-controlled multi block copolymers. Additional chain extensions could also be achieved, although the

dispersities increased further. Nevertheless, a tetracosia (24) multi block copolymer could be attained. The final product contained no contaminating halide or sulphur moieties, in contrast with both classical ATRP and RAFT polymerisation where typical purification methods such as precipitation or dialysis cannot remove the covalently attached halogen or RAFT agent.⁴⁷⁻⁴⁹

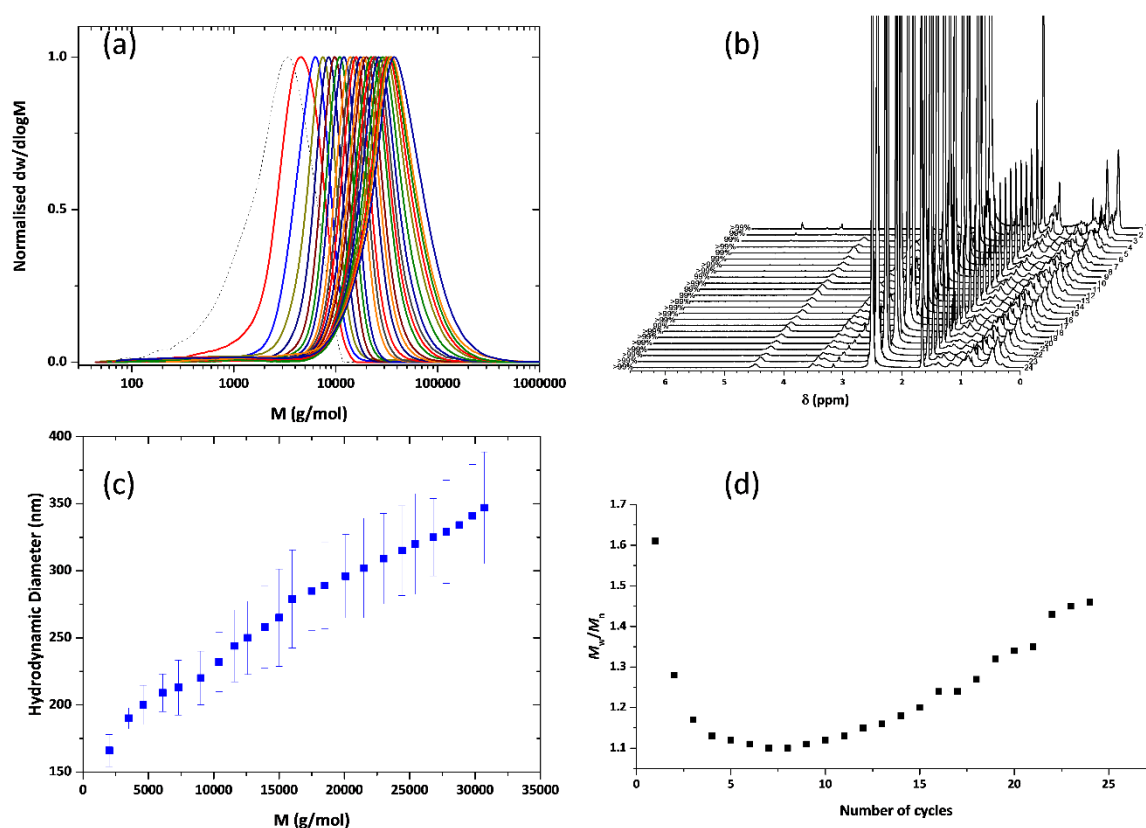


Figure 2.6: Synthesis and characterisation of model heneicasoblock BMA homopolymer. (a) SEC traces of molecular weight distributions for consecutive cycles during the synthesis of the heneicasoblock copolymer, (b) ^1H NMR spectra for consecutive cycles, (c) hydrodynamic diameter evolution of the heneicasoblock copolymer, as obtained by Z-average measurements versus the number average molecular weight (M_n) as measured by DLS and (d) evolution of dispersity (\mathcal{D}) values for consecutive cycles.

Table 2.3: Characterisation data for the synthesis of the tetracosablock copolymer in emulsion at 85 °C with potassium persulfate as initiator.

Entry	Cycle	Conv. (%)	$M_{n,th}$ (g.mol ⁻¹)	$M_{n,SEC}$ (g.mol ⁻¹)	\bar{D}	Particle Diameter (nm)	\bar{D}_{DLS}
1	CTA	>99	2000	2000	1.61	165	0.049
2	1	98	3400	3700	1.28	188	0.034
3	2	99	5200	5300	1.17	198	0.074
4	3	>99	7200	6600	1.13	204	0.060
5	4	99	8600	7700	1.12	210	0.030
6	5	99	10400	9000	1.11	214	0.066
7	6	>99	12400	10100	1.10	223	0.089
8	7	>99	13800	11100	1.10	234	0.102
9	8	98	15600	12700	1.11	243	0.076
10	9	>99	17600	13800	1.12	263	0.137
11	10	98	19000	14700	1.13	271	0.136
12	11	99	20800	16100	1.15	280	0.099
13	12	>99	22800	17400	1.16	286	0.093
14	13	>99	24200	18400	1.18	292	0.135
15	14	>99	26000	20500	1.20	300	0.127
16	15	>99	28000	21200	1.24	304	0.099
17	16	98	29400	22700	1.24	313	0.126
18	17	>99	31200	24100	1.27	331	0.130
19	18	>99	33200	25800	1.32	341	0.116
20	19	>99	34600	28100	1.34	353	0.139
21	20	>99	36400	29500	1.35	360	0.112
22	21	>99	38400	30500	1.43	365	0.064
23	22	>99	39800	31800	1.45	373	0.135
24	23	>99	41600	33700	1.46	380	0.140

As high molecular weight block copolymers are of interest because of their ability to self-assemble and/or phase separate to form higher ordered structures in both solution and solid state, it was decided to probe the potential of the technique for the synthesis of higher molecular weight multi block copolymers. Under the previously described conditions, each block was designed to have $DP_n = 45$, resulting in a well-defined heptablock multi block copolymer consisting of MMA, BMA, BzMA and EHMA (Figure 2.1 c). Other important considerations when synthesising complex materials such as sequence-controlled multi block copolymers, are potential issues associated with scaling up of the polymerisation process. In order to bridge the gap between small scale synthesis in research laboratories and

commercialisation, and explore the robustness of this technique, the synthesis of the high molecular weight multi block copolymers was performed on a high multigram scale (~ 80 g) in a 0.5 L double jacketed reactor (Figure 2.9 a). This is in contrast with the solid peptide syntheses or even with iterative exponential growth approaches, which are typically limited to milligrams of product.²¹ Despite this process scale up, quantitative or near quantitative conversions ($> 99\%$) were achieved throughout the monomer addition cycles (Figure 2.10 b). DLS showed a gradual evolution of the hydrodynamic diameter (Figure 2.10 a) and the final polymer possesses a dispersity value of 1.24 ($M_n \sim 41300$ g mol⁻¹, Table 2.1, entry 3). The ease of scale up and maintenance of polymer architectural control highlights the versatility and robustness of the system in facilitating the synthesis of higher molecular weight materials (Figures 2.10 c & d and Tables 2.4 and Section Z.4.4, Table 2.8 for further synthetic details). As such, the diblock and triblock copolymers that are typically employed at this molecular weight ($M_n \sim 10000$ - 40000 g mol⁻¹) can be easily prepared quantitatively within a few hours. Post-synthesis, the multi block was isolated *via* dialysis, yielding 80 g of a white solid material (Figure 2.9 b). It should be highlighted that because the macromonomer possesses a dual role by simultaneously being the CTA and the last (or first) building block, the final material is a clear white solid, in contrast to copper or sulphur catalysed polymerisations, where brown/green and pink/yellow products are typically obtained at the end of the polymerisations and even after several purification processes (*e.g.* dialysis, precipitation etc.) the RAFT agent and the halogen will still be present at the termini of the macromolecules.

Table 2.4: Characterisation data for the synthesis of the heptablock copolymer in emulsion at 85 °C with potassium persulfate as initiator.

Entry	Cycle	Conv. (%)	$M_{n,th}$ (g.mol ⁻¹)	$M_{n,SEC}$ (g.mol ⁻¹)	\bar{D}	Particle Diameter (nm)	\bar{D}_{DLS}
1	CTA	100	1800	2400	1.52	169	0.042
2	1	100	8200	7600	1.08	218	0.086
3	2	99	16100	16100	1.10	270	0.124
4	3	100	25000	22200	1.13	324	0.112
5	4	99	31400	27600	1.15	340	0.133
6	5	>99	39300	33900	1.21	365	0.136
7	6	98	48200	41300	1.24	399	0.125

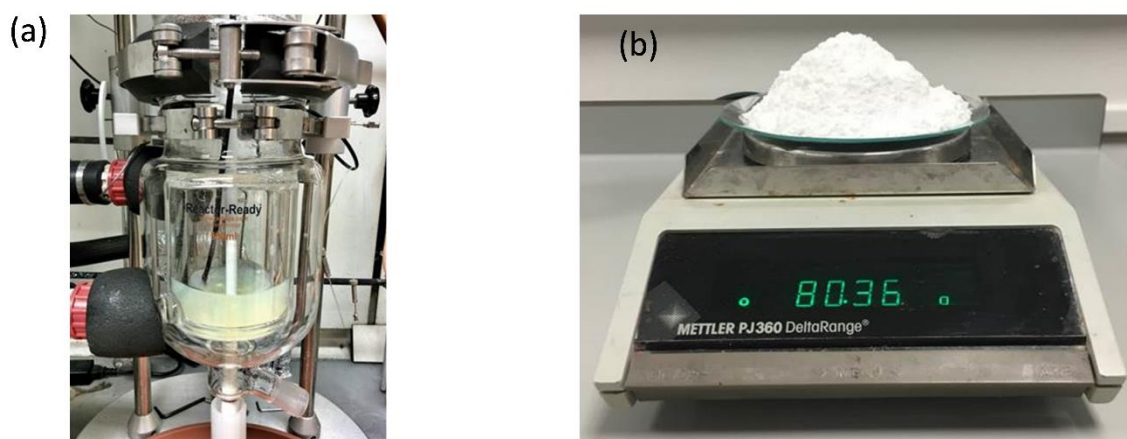


Figure 2.7: Scalable synthesis of the high molecular weight hexablock copolymer. (a) Image of the double jacketed 0.5 L reactor utilised for the high scale synthesis and (b) total amount of material/product obtained after 6 successive additions.

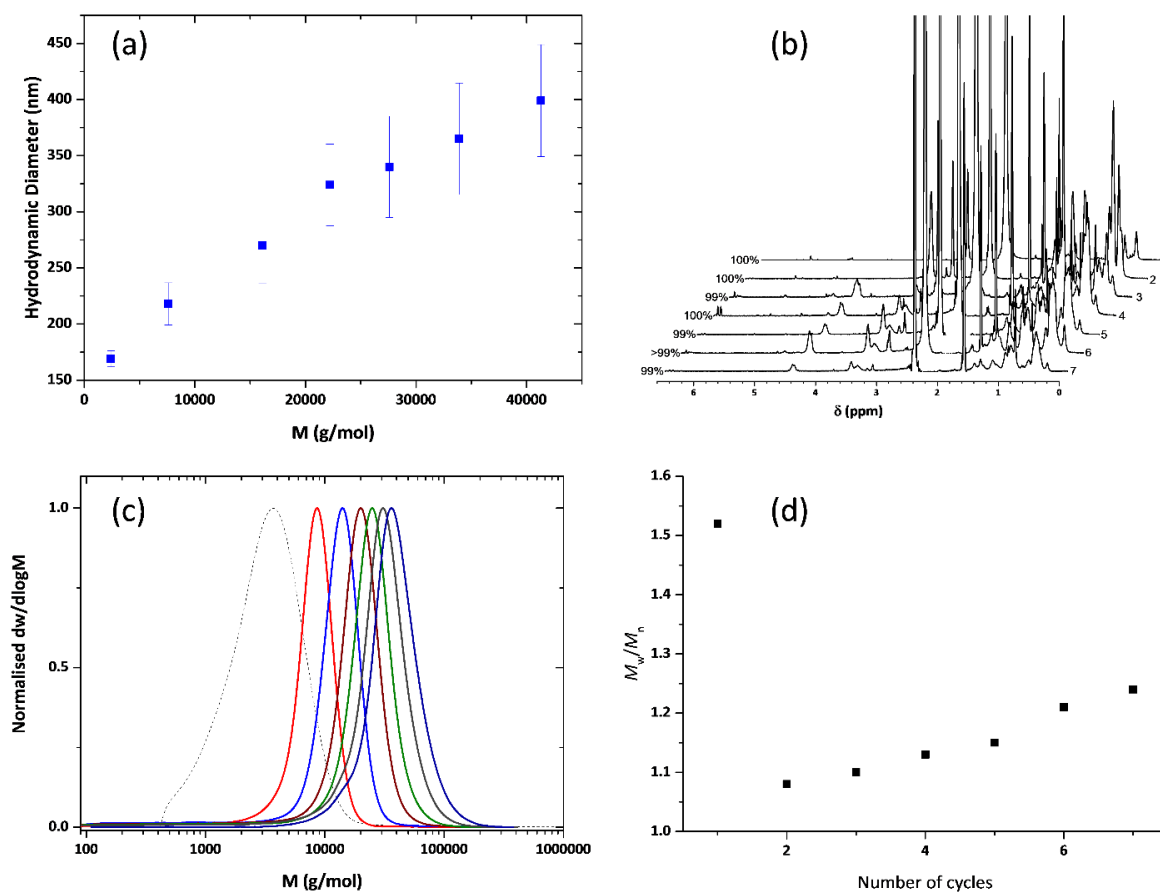


Figure 2.8: (a) hydrodynamic diameter evolution of the heptablock homopolymer, as obtained by Z-average measurements versus the number average molecular weight (M_n) as measured by DLS, (b) ^1H NMR traces for the synthesis of the heptablock copolymer following various patterns, (c) SEC and (d) dispersity (\mathcal{D}) as a function of the number of cycles for the heptablock copolymer. The copolymer consists of BMA, BzMA, EHMA and MMA at 85°C (in a 0.5 L reactor applying monomer starved conditions) *via* a segregation approach of emulsion polymerisation utilizing KPS as initiator and $\text{PMMA} \sim 2000 \text{ g mol}^{-1}$ as the initial chain transfer agent.

The vast majority of the studies associated with multi block copolymers maintain the same DP_n (or chain length) for each block. For example, the synthesis of a decablock with $DP_n \sim 10$ per block or a hexablock with $DP_n \sim 45$ per block does not necessarily mean that any combination of chain length can be incorporated in the same multi block copolymer. At the same time, the multi blocks reported typically follow a specific pattern (*e.g.* ABCDABCD) and thus a question arises about whether each monomer can equally support the propagation

(*e.g.* will ABCD work as well as ACBD and so on). To explore this, a gradually increasing *DP* undecablock gradient multi block copolymer was targeted, poly(BMA₅-*b*-BzMA₁₀-*b*-EHMA₁₅-*b*-BMA₂₀-*b*-EHMA₂₅-*b*-EHMA₃₀-*b*-BzMA₃₅-*b*-BzMA₄₀-*b*-BMA₄₅-*b*-BMA₅₀-*b*-MMA₁₀), where the propagation of each monomer was investigated (Figure 2.1 d, Tables 2.5 and Section 2.4.4, Table 2.9). Indeed, all of the methacrylate monomers examined here were found to efficiently support the propagation, enabling the desired manipulation of the monomer sequence to yield a well-defined undecablock multi block copolymer of $M_n \sim 42000 \text{ g mol}^{-1}$, with good agreement between theoretical and experimental molecular weights and narrow MWDs ($\mathcal{D} \sim 1.25$, Figures 2.11 a & d). Notably, relatively hydrophobic monomers have been employed in these studies as a certain degree of hydrophobicity is required in order to perform a successful emulsion polymerisation; that is, an appropriate equilibrium of monomer is required in both the oil and water phases. However, for applications where hydrophilic monomers are required it is envisaged that an inverse emulsion polymerisation might alternatively be utilised as well as a combination of protected and unprotected monomers for amphiphilic structures. Finally, it should also be noted that a true proof of the exact structure of the final materials is challenging, if not impossible to obtain. Thus, the structure of these complex architectures can be inferred from the history of the preparation and the performance of DLS, GPC and NMR analysis. As such, it would be very interesting in the future if the information stored in such complex macromolecules could be decoded.

Table 2.5: Characterisation data for the synthesis of the undecablock copolymer in emulsion at 85 °C with potassium persulfate as initiator.

Entry	Cycle	Conv. (%)	$M_{n,th}$ (g.mol ⁻¹)	$M_{n,SEC}$ (g.mol ⁻¹)	\bar{D}	Particle Diameter (nm)	\bar{D}_{DLS}
1	CTA	>99	2000	2300	1.65	174	0.128
2	1	98	2700	3500	1.27	189	0.051
3	2	99	4500	5900	1.13	204	0.072
4	3	99	7500	8500	1.09	221	0.070
5	4	>99	10800	11000	1.08	248	0.135
6	5	>99	15800	14800	1.07	276	0.095
7	6	>99	21700	18500	1.09	315	0.148
8	7	100	27900	23200	1.12	327	0.144
9	8	100	30600	29300	1.17	362	0.096
10	9	>99	37000	34700	1.18	436	0.296
11	10	>99	44100	42000	1.25	453	0.250

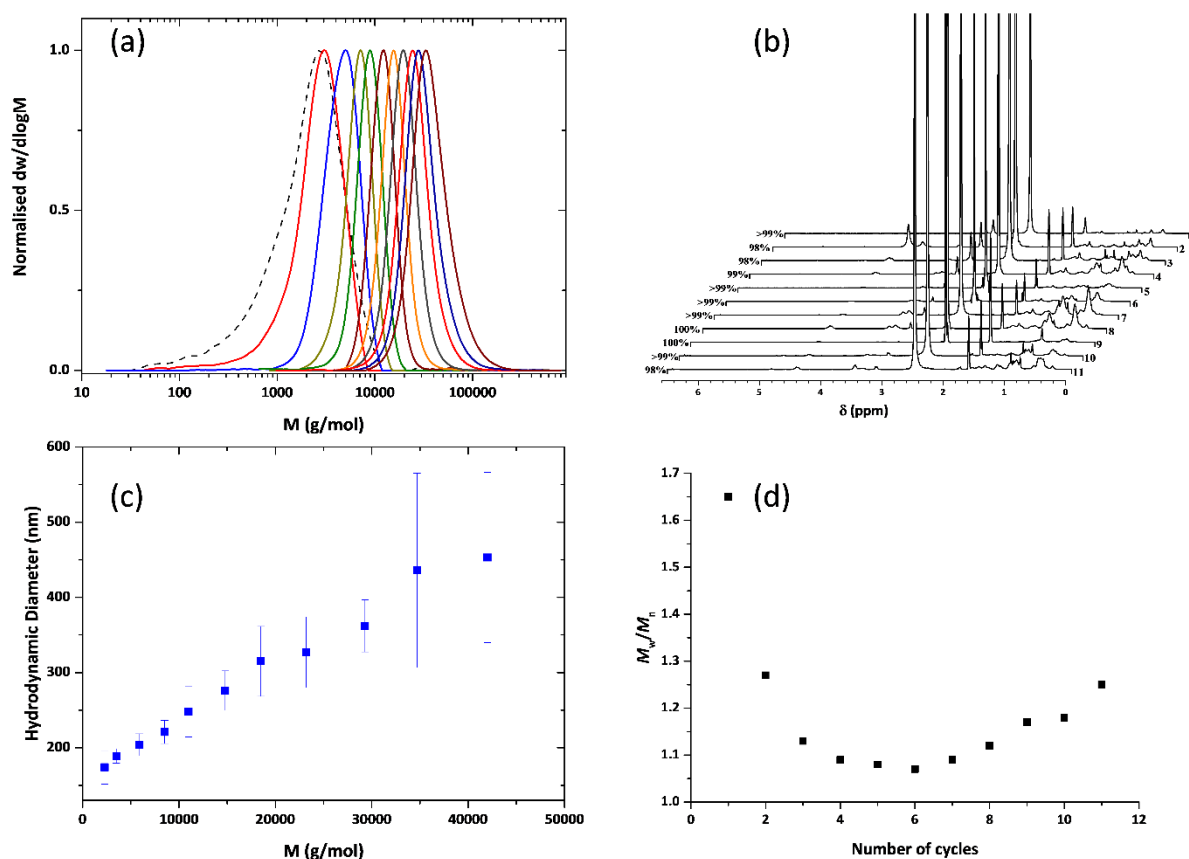


Figure 2.9: (a) SEC, (b) ¹H NMR traces for the synthesis of the undecablock copolymer following various patterns, (c) hydrodynamic diameter evolution of the undecablock homopolymer, as obtained by Z-average measurements versus the number average molecular weight (M_n) as measured by DLS and (d) dispersity (\mathcal{D}) as a function of the number of cycles for the undecablock copolymer. The copolymer consists of BMA, BzMA, EHMA and MMA at 85 °C (in a 0.5 L reactor applying monomer starved conditions) *via* a segregation approach of emulsion polymerisation utilizing KPS as initiator and PMMA $\sim 2000 \text{ g mol}^{-1}$ as the initial chain transfer agent.

2.3 Conclusions

In summary, it was demonstrated that a segregation approach of emulsion polymerisation is able to produce well-defined sequence-controlled macromolecules. Despite altering the sequence of the monomer composition, narrow molecular weight distributions were obtained achieving a heneicosablock copolymer, with quantitative conversions attained throughout all the iterative monomer additions. Higher molecular weight multi block

copolymers could also be synthesised in a quantitative manner, which were subsequently scaled up to ~ 80 g, further highlighting the robustness of the technique. The absence of any transition metal or sulphur catalysts, the scalability of the process, the quantitative yields (> 99 %) and the high polymerisation rates despite such low activated monomer pave the way for the synthesis of a new class of macromolecular sequence controlled materials for a wide range of applications including nanostructured materials, polymeric phase separation, single chain folding and drug delivery, among others.

2.4 Experimental

2.4.1 Materials and Methods

All materials were purchased from Sigma or Fischer Scientific and used as received unless otherwise stated. CoBF was previously synthesised in the Haddleton Group.

2.4.2 Instrumentation

^1H NMR spectra were recorded on Bruker DPX-300 and HD-400 spectrometers using a mixture of deuterated chloroform and deuterated acetone (v/v=3/2), both obtained from Aldrich. Chemical shifts are given in ppm downfield from the internal standard tetramethylsilane. SEC analyses were performed on an Agilent 1260 SEC-MDS fitted with differential refractive index (DRI), light scattering (LS) and viscometry (VS) detectors equipped with 2 x PLgel 5 mm mixed-D columns (300 x 7.5 mm), 1 x PLgel 5 mm guard column (50 x 7.5 mm) and autosampler. Narrow linear poly(methyl methacrylate) standards in range of 200- 1.0×10^6 g mol $^{-1}$ were used to calibrate the system. All samples were passed through 0.45 μm PTFE filter prior to analysis. The mobile phase was chloroform with 2 % triethylamine at a flow

rate of 1.0 mL min^{-1} . SEC data were analysed using Cirrus v3.3. Matrix assisted laser desorption ionization mass spectrometry (MALDI-ToF-MS) was conducted using a Bruker Daltonics Ultra flex II MALDI-ToF-MS mass spectrometer, equipped with a nitrogen laser delivering 2 ns laser pulses at 337 nm with positive ion ToF detection performed using an accelerating voltage of 25 kV. Solutions in tetrahydrofuran (50 μL) of 2,5-dihydroxybenzoic acid (DHB) as matrix (saturated solution), sodium iodide as cationization agent (1.0 mg mL^{-1}) and sample (1.0 mg mL^{-1}) were mixed, and 0.7 μL of the mixture was applied to the target plate. Spectra were recorded in reflector mode calibrating PEG-Me 1100 kDa. DLS measurements were performed on a Malvern Instruments Zetasizer Nano Series instrument with a detection angle of 173° , where the Z-average mean hydrodynamic diameter and the width of the particle size distribution (\mathcal{D}_{DLS}) were obtained from analysis of the autocorrelation function. 1 μL of latex was diluted with 1 mL of deionized water previously filtered with 0.20 μm membrane to ensure the minimisation of dust and other particulates. At least 3 measurements at 25°C were made for each sample with an equilibrium time of 2 min before starting measurement.

2.4.3 General procedures

(a) Process for the synthesis of PMMA macromonomer by CCTP in emulsion. In a typical CCTP in emulsion, CoBF (7.5 mg) was placed in a 100 mL round bottom flask together with a stirring bar. Nitrogen was purged in the flask for at least 1 h. Subsequently, MMA (20 mL, 18.72 g, 186.98 mmol) previously degassed for 30 min was added to the flask *via* a degassed syringe. The mixture was vigorously stirred under inert atmosphere until total dissolution of the catalyst. Meanwhile, 4,4'-azobis(4-cyanovaleric acid) (CVA) (0.5 g, 1.78 mmol), sodium dodecyl sulphate (SDS) (0.3 g, 1.04 mmol) and 130 mL of water were charged into a three-neck, 500 mL double jacketed reactor, equipped with a RTD temperature probe and an

overhead stirrer. The mixture was purged with nitrogen and stirred at 325 rpm for at least 30 min. Subsequently, the mixture was heated under inert atmosphere. When the temperature in the reactor reached 70 °C, the addition of the MMA-CoBF solution started using a degassed syringe and a syringe pump (feeding rate = 0.666 mL/min, feeding time = 30 min). When the addition was over, stirring continued for another 30 min under the same conditions. Subsequently, the heat pump settings were adjusted accordingly in order to reach a temperature of at least 80 °C in the reactor vessel and stirring continued for 60 min. The number average molecular weight of the macromonomer was calculated from the ^1H NMR spectra.

(b) General process for the synthesis of multi block copolymers by Free-Radical polymerisation in emulsion. The amount of monomer to be subsequently added to the PMMA macromonomer latex was calculated according to the desired DP_n . For each addition, the volume of aqueous KPS solution added was equal to the monomer volume. The additions were stopped and dilutions with water were made, when solid content reached values above which coagulation was very likely to occur. After every dilution, the solid content of the latex was measured (in g mL^{-1}) and the value was taken into account for calculating the amounts of reagents of the next addition cycle.

(c) Typical process for the chain extension of PMMA macromonomer with BMA ($DP_n=10$) by Free-Radical polymerisation in emulsion. 125 mL of PMMA macromonomer latex (0.129 g mL^{-1}) were diluted by adding 37 mL of water to achieve a 10 % solid content. The resulting latex was charged in the reactor and purged with nitrogen for 30 min under stirring. Subsequently, the emulsion was heated. When the temperature in the reactor reached 85-86 °C and was stabilised, the simultaneous addition of BMA (15.9 mL, 14.22 g, 0.1 mol) and

potassium persulfate aqueous solution (79.5 mg potassium persulfate in 15.9 mL of water), both previously degassed for 30 min started by the use of degassed syringes and a syringe pump (feeding rate = 0.16 mL min⁻¹, feeding time = 100 min). When the addition was over, stirring continued for another 60 min under the same conditions.

2.4.4 Numerical data

Table 2.6: Experimental conditions used for the preparation of the tetracosablock PBMA homopolymer in emulsion at 85 °C with potassium persulfate as initiator.

Cycle	M	DP _n targeted	m _{monomer} added (g)	M _{CTA} added (g)	m _{KPS} added (mg)	V _{H2O} added (mL)	V _{total} (mL) ^[a]	S.C. (g.mL ⁻¹)	% wt solids
2	BMA	10	14.220	18	79.53	15.906	177.906	0.181	15.33
3	BMA	10	13.915	31.315	77.82	15.565	188.471	0.240	19.35
4	BMA	10	13.611	44.03	76.13	15.225	198.696	0.290	22.48
5	BMA	10	13.317	56.191	74.48	14.896	208.592	0.333	24.99
6	BMA	10	13.036	67.843	72.91	14.582	218.174	0.371	27.04
7 ^b	BMA	10	4.117	25.48	23.03	4.605	233.925	0.126	11.23
8	BMA	10	4.038	28.967	22.58	4.517	233.442	0.141	12.39
9	BMA	10	3.959	32.3	22.14	4.428	232.87	0.156	13.47
10	BMA	10	3.881	35.479	21.71	4.341	232.211	0.169	14.49
11	BMA	10	3.803	38.515	21.27	4.254	231.465	0.183	15.46
12	BMA	10	3.726	41.403	20.84	4.168	230.633	0.196	16.36
13 ^c	BMA	10	2.827	34.2	15.81	3.162	310.962	0.119	10.64
14	BMA	10	2.785	36.432	15.57	3.115	309.077	0.127	11.26
15	BMA	10	2.743	38.582	15.34	3.068	307.145	0.134	11.86
16	BMA	10	2.701	40.655	15.11	3.021	305.166	0.142	12.44
17	BMA	10	2.659	42.646	14.87	2.974	303.140	0.149	12.99
18	BMA	10	2.618	44.560	14.64	2.928	301.068	0.157	13.55
19 ^d	BMA	10	1.688	30.400	9.44	1.888	275.488	0.116	10.43
20	BMA	10	1.659	31.508	9.28	1.856	272.344	0.122	10.86
21	BMA	10	1.630	32.557	9.12	1.823	269.167	0.127	11.27
22	BMA	10	1.601	33.552	8.95	1.791	265.958	0.132	11.67
23	BMA	10	1.572	34.493	8.79	1.758	262.716	0.137	12.07
24	BMA	10	1.543	35.380	8.63	1.726	259.442	0.142	12.46

^a after the end of each cycle, a sample of 5 mL was taken. The amount of CTA removed from the system was taken into account for the calculations of the next cycle

^b 70 mL of the latex of cycle 6 were diluted to 10 % wt of solids by adding 159.32 mL of H₂O

^c 180 mL of the latex of cycle 12 were diluted to 10 % wt of solids by adding 127.8 mL of H₂O

^d 200 mL of the latex of cycle 18 were diluted to 10 % wt of solids by adding 73.6 mL of H₂O

Table 2.7: Experimental conditions used for the preparation of the tetracosablock copolymer in emulsion at 85 °C with potassium persulfate as initiator.

Cycle	M	DP_n targeted	M_{monomer} added (g)	M_{CTA} added (g)	m_{KPS} added (mg)	$V_{\text{H}_2\text{O}}$ added (mL)	V_{total} (mL) ^[a]	S.C. (g.mL ⁻¹)	% wt solids
2	BMA	10	12.798	18	71.57	14.315	176.315	0.175	14.87
3	BzMA	10	15.978	29.923	76.82	15.364	186.679	0.246	19.74
4 ^b	EHMA	10	5.548	14.4	31.34	6.269	135.869	0.147	12.80
5	BMA	10	3.795	19.213	21.22	4.245	135.114	0.170	14.55
6	BzMA	10	4.678	22.158	22.48	4.497	134.611	0.199	16.62
7 ^c	EHMA	10	2.066	10.725	11.67	2.335	98.86	0.129	11.46
8	BMA	10	1.393	12.146	7.79	1.558	95.418	0.142	12.43
9	BzMA	10	1.689	12.829	8.12	1.624	92.042	0.158	13.62
10 ^d	EHMA	10	1.393	10.85	7.87	1.574	99.224	0.123	10.98
11	BMA	10	0.939	11.628	5.25	1.050	95.274	0.132	11.65
12	BzMA	10	1.137	11.907	5.47	1.094	91.368	0.143	12.49
13	EHMA	10	1.187	12.329	6.71	1.342	87.71	0.154	13.35
14	BMA	10	0.795	12.746	4.44	0.889	83.599	0.162	13.94
15	BzMA	10	0.955	12.731	4.59	0.918	79.517	0.172	14.68
16 ^e	EHMA	10	0.901	11.69	5.09	1.018	106.228	0.119	10.59
17	BMA	10	0.609	11.996	3.41	0.681	101.909	0.124	11.01
18	BzMA	10	0.739	11.985	3.55	0.711	97.620	0.130	11.53
19	EHMA	10	0.775	12.074	4.38	0.876	93.496	0.137	12.08
20	BMA	10	0.521	12.164	2.92	0.583	89.079	0.142	12.47
21	BzMA	10	0.628	11.975	3.03	0.605	84.684	0.149	12.95
22 ^f	EHMA	10	0.563	10.22	3.18	0.635	92.615	0.116	10.43
23	BMA	10	0.378	10.203	2.12	0.423	88.038	0.120	10.73
24	BzMA	10	0.472	10.341	2.27	0.453	86.491	0.125	11.11

^a after the end of each cycle, a sample of 5 mL was taken. The amount of CTA removed from the system was taken into account for the calculations of the next cycle

^b 60 mL of the latex of cycle 3 were diluted to 10 % wt of solids by adding 69.6 mL of H₂O

^c 55 mL of the latex of cycle 6 were diluted to 10 % wt of solids by adding 41.52 mL of H₂O

^d 70 mL of the latex of cycle 9 were diluted to 10 % wt of solids by adding 27.65 mL of H₂O

^e 70 mL of the latex of cycle 15 were diluted to 10 % wt of solids by adding 35.21 mL of H₂O

^f 70 mL of the latex of cycle 21 were diluted to 10 % wt of solids by adding 21.98 mL of H₂O

Table 2.8: Experimental conditions used for the preparation of the heptablock copolymer in emulsion at 85 °C with potassium persulfate as initiator.

Cycle	M	DP_n targeted	m_{monomer} added (g)	M_{CTA} added (g)	m_{KPS} added (mg)	$V_{\text{H}_2\text{O}}$ added (mL)	V_{total} (mL) ^[a]	S.C. (g.mL ⁻¹)	% wt solids
2 ^b	BMA	45	50.122	14.1	280.32	56.065	226.065	0.284	22.12
3 ^c	BzMA	45	27.295	27.4	131.22	26.245	272.845	0.200	16.69
4 ^d	EHMA	45	16.038	28.65	90.61	18.123	275.973	0.162	13.94
5	BMA	45	11.230	43.878	62.81	12.562	283.535	0.194	16.27
6	BzMA	45	14.084	54.138	67.71	13.542	292.077	0.234	18.93
7	EHMA	45	15.379	67.052	86.89	17.378	304.455	0.271	21.31

^a after the end of each cycle, a sample of 5 mL was taken. The amount of CTA removed from the system was taken into account for the calculations of the next cycle

^b 100 mL of the latex of cycle 1 were diluted by adding 70 mL of H₂O

^c 100 mL of the latex of cycle 2 were diluted by adding 146.6 mL of H₂O

^d 150 mL of the latex of cycle 3 were diluted to 10 % wt of solids by adding 107.85 mL of H₂O

Table 2.9: Experimental conditions used for the preparation of the undecablock copolymer in emulsion at 85 °C with potassium persulfate as initiator.

Cycle	M	DP _n targeted	m _{monomer} added (g)	M _{CTA} added (g)	m _{KPS} added (mg)	V _{H2O} added (mL)	V _{total} (mL) ^[a]	S.C. (g.mL ⁻¹)	% wt solids
2	BMA	5	6.399	18	35.79	7.158	169.158	0.144	12.61
3	BzMA	10	15.937	23.679	76.62	15.324	179.482	0.221	18.08
4	EHMA	15	25.718	38.511	145.3	29.060	203.542	0.316	23.99
5 ^b	BMA	20	6.962	18.36	38.93	7.787	173.027	0.146	12.77
6	EHMA	25	11.959	24.592	67.56	13.513	181.54	0.201	16.76
7	EHMA	30	13.963	35.546	78.89	15.778	192.318	0.257	20.47
8	BzMA	35	14.468	48.224	69.55	13.911	201.229	0.312	23.75
9 ^c	BzMA	40	4.073	15.35	19.58	3.916	142.066	0.137	12.03
10	BMA	45	3.486	18.738	19.49	3.899	140.965	0.158	13.62
11	BMA	50	3.735	21.434	20.89	4.178	140.143	0.179	15.23

^a after the end of each cycle, a sample of 5 mL was taken. The amount of CTA removed from the system was taken into account for the calculations of the next cycle

^b 60 mL of the latex of cycle 4 were diluted to 10 % wt of solids by adding 105.24 mL of H₂O

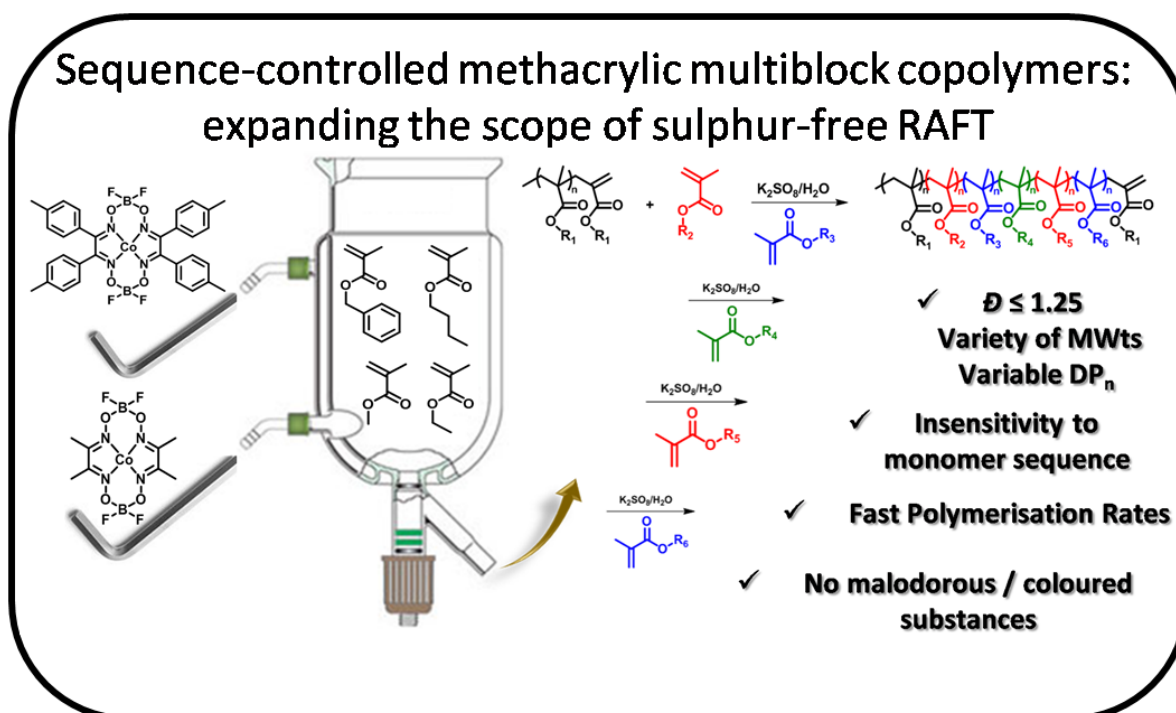
^c 50 mL of the latex of cycle 8 were diluted to 10 % wt of solids by adding 88.15 mL of H₂O

2.5 References

- 1 R. B. Merrifield, *J. Am. Chem. Soc.*, 1963, **85**, 2149-2154.
- 2 J.-F. Lutz, M. Ouchi, D. R. Liu, and M. Sawamoto, *Science*, 2013, **341**.
- 3 M. Ouchi, N. Badi, J.-F. Lutz, and M. Sawamoto, *Nat. Chem.*, 2011, **3**, 917-924.
- 4 N. Badi and J.-F. Lutz, *Chem. Soc. Rev.*, 2009, **38**, 3383-3390.
- 5 J.-F. Lutz, *Polym. Chem.*, 2010, **1**, 55-62.
- 6 M. Zamfir and J.-F. Lutz, *Nat. Commun.*, 2012, **1138**.
- 7 J. Vandenberg, G. Reekmans, P. Adriaensens and T. Junkers, *Chem. Sci.*, 2015, **6**, 5753-5761.
- 8 J. Vandenberg, G. Reekmans, P. Adriaensens and T. Junkers, *Chem. Commun.*, 2013, **49**, 10358-10360.
- 9 K. Nakatani, Y. Ogura, Y. Koda, T. Terashima and M. Sawamoto, *J. Am. Chem. Soc.*, 2012, **134**, 4373-4383.

- 10 Y. Ogura, T. Terashima and M. Sawamoto, *ACS Macro Lett.*, 2013, **2**, 985-989.
- 11 S. Ida, M. Ouchi and M. Sawamoto, *J. Am. Chem. Soc.*, 2010, **132**, 14748-14750.
- 12 S. Pfeifer and J.-F. Lutz, *J. Am. Chem. Soc.*, 2007, **129**, 9542-9543.
- 13 M.-A. Berthet, Z. Zarafshani, S. Pfeifer and J.-F. Lutz, *Macromolecules*, 2010, **43**, 44-50.
- 14 Y. Guo, J. Zhang, P. Xie, X. Gao and Y. Luo, *Polym. Chem.*, 2014, **5**, 3363-3371.
- 15 S. Pfeifer, Z. Zarafshani, N. Badi and J.-F. Lutz, *J. Am. Chem. Soc.*, 2009, **131**, 9195-9197.
- 16 L. Hartmann and H.-G. Börner, *Adv. Mater.*, 2009, **21**, 3425-3431.
- 17 R. N. Zuckermann, J. M. Kerr, S. B. H. Kent and W. H. Moos, *J. Am. Chem. Soc.*, 1992, **114**, 10646-10647.
- 18 R. McHale, J. P. Patterson, P. B. Zetterlund and R. K. O'Reilly, *Nat. Chem.*, 2012, **4**, 491-497.
- 19 M. Ueda, *Prog. Polym. Sci.*, 1999, **24**, 699-730.
- 20 E. Bayer and M. Mutter, *Nature*, 1972, **237**, 512-513.
- 21 J. C. Barnes, D. J. C. Ehrlich, A. X. Gao, F. A. Leibfarth, Y. Jiang, E. Zhou, T. F. Jamison and J. A. Johnson, *Nat. Chem.*, 2015, **7**, 810-815.
- 22 A. H. Soeriyadi, C. Boyer, F. Nyström, P. B. Zetterlund and M. R. Whittaker, *J. Am. Chem. Soc.*, 2011, **133**, 11128-11131.
- 23 A. Anastasaki, C. Waldron, P. Wilson, C. Boyer, P. B. Zetterlund, M. R. Whittaker and D. M. Haddleton, *Acs Macro Lett.*, 2013, **2**, 896-900.
- 24 A. Anastasaki, V. Nikolaou, G. S. Pappas, Q. Zhang, C. Wan, P. Wilson, T. P. Davis, M. R. Whittaker and D. M. Haddleton, *Chem. Sci.*, 2014, **5**, 3536-3542.
- 25 A. Anastasaki, V. Nikolaou, N. W. McCaul, A. Simula, J. Godfrey, C. Waldron, P. Wilson, K. Kempe and D. M. Haddleton, *Macromolecules*, 2015, **48**, 1404-1411.
- 26 F. Alsubaie, A. Anastasaki, P. Wilson and D. M. Haddleton, *Polym. Chem.*, 2015, **4**, 106-112.
- 27 Q. Zhang, J. Collins, A. Anastasaki, R. Wallis, D. A. Mitchell, C. R. Becer and D. M. Haddleton, *Angew. Chem. Int. Ed.*, 2013, **52**, 4435-4439.
- 28 J. Vandenberg and T. Junkers, *Macromolecules*, 2014, **47**, 5051-5059.
- 29 Y.-M. Chuang, A. Ethirajan and T. Junkers, *ACS Macro Lett.*, 2014, **3**, 732-737.
- 30 G. Gody, T. Maschmeyer, P. B. Zetterlund and S. Perrier, *Nat. Commun.*, 2013, **4**.
- 31 L. Martin, G. Gody and S. Perrier, *Polym. Chem.*, 2015, **6**, 4875-4886.
- 32 T. Junkers and B. Wenn, *React. Chem. Eng.*, 2016, **1**, 60-64.
- 33 B. Wenn, A. C. Martens, Y. M. Chuang, J. Gruber and T. Junkers, *Polym. Chem.*, 2016, **7**, 2720-2727.
- 34 C. Boyer, A. H. Soeriyadi, P. B. Zetterlund and R. M. Whittaker, *Macromolecules*, 2011, **44**, 8028-8033.
- 35 P. B. Zetterlund, S. C., Thickett, S. Perrier, E. Bourgeat-Lami and M. Lansalot, *Chem. Rev.*, 2015, **115**, 9745-9800.
- 36 N. P. Truong, M. R. Whittaker, A. Anastasaki, D. M. Haddleton, J. F. Quinn and T. P. Davis, *Polym. Chem.*, 2016, **7**, 430-440.
- 37 C. L. Moad, G. Moad, E. Rizzardo and S. H. Thang, *Macromolecules*, 1996, **29**, 7717-7726.
- 38 L. Hutson, J. Krstina, C. L. Moad, G. Moad, G. R. Morrow, A. Postma, E. Rizzardo and S. H. Thang, *Macromolecules*, 2004, **37**, 4441-4452.
- 39 J. Krstina, G. Moad, E. Rizzardo, C. L. Winzor, C. T. Berge and M. Fryd, *Macromolecules*, 1995, **28**, 5381-5385.
- 40 G. Gody, P. B. Zetterlund, S. Perrier and S. Harrisson, *Nat. Commun.*, 2016, **7**.

- 41 J. P. A. Heuts and N. M. B. Smeets, *Polym. Chem.*, 2011, **2**, 2407-2423.
- 42 M. Buback, C. H. Kurz and C. Schmaltz, *Macromol. Chem. Phys.*, 1998, **199**, 1721-1727.
- 43 S. Beuermann, M. Buback, T. P. Davis, R. G. Gilbert, R. A. Hutchinson, O. F. Olaj, G. T. Russell, J. Schweer and A. M. van Herk, *Macromol. Chem. Phys.*, 1997, **198**, 1545-1560.
- 44 M. D. Zammit, M. L. Coote, T. P. Davis and G. D. Willett, *Macromolecules*, 1998, **31**, 955-963.
- 45 N. P. Truong, M. V. Dussert, M. R. Whittaker, J. F. Quinn and T. P. Davis, *Polym. Chem.*, 2015, **6**, 3865-3874.
- 46 R. G. Gilbert, *Emulsion polymerization: A mechanistic approach*, Academic Press, 1995.
- 47 H. Willcock and R. O'Reilly, *Polym. Chem.*, 2010, **1**, 149-157.
- 48 C.-W. Chang, E. Bays, L. Tao, S. N. S. Alconcel and H. D. Maynard, *Chem. Commun.*, 2009, 3580-3582.
- 49 D. Pissuwan, C. Boyer, K. Gunasekaran, T. P. Davis and V. Bulmus, *Biomacromolecules*, 2010, **11**, 412-420.



Sulphur-free reversible addition fragmentation transfer polymerisation (SF-RAFT) in emulsion allows access to the synthesis of sequence-controlled methacrylic multi block copolymers. Herein, the scope of SF-RAFT emulsion polymerisation is expanded by utilising four different macrochain transfer agents (mCTA) to mediate the synthesis of diblocks and sequence-controlled methacrylic multi block copolymers. Poly(methyl methacrylate) (PMMA), poly(butyl methacrylate) (PBMA), poly(ethyl methacrylate) (PEMA) and poly(benzyl methacrylate) (PBzMA) of a similar M_n ($\sim 4300 \text{ g mol}^{-1}$) were successfully synthesised via catalytic chain transfer polymerisation (CCTP) in emulsion. The capability of these mCTAs to act as macroinitiators was investigated through the synthesis of “in situ” diblock copolymers and was then expanded to the synthesis of deca and hexablock multi block copolymers with varying degrees of polymerisation ($DP_n = 10\text{-}50$ per block, $M_{n, total} = 7000\text{-}55000 \text{ g mol}^{-1}$) yielding well-defined copolymers with controlled molecular weights, quantitative conversions ($> 99\%$) and low dispersities ($\bar{D} \sim 1.2$) without employing sulphur or transition metal reagents.

3.1 Introduction

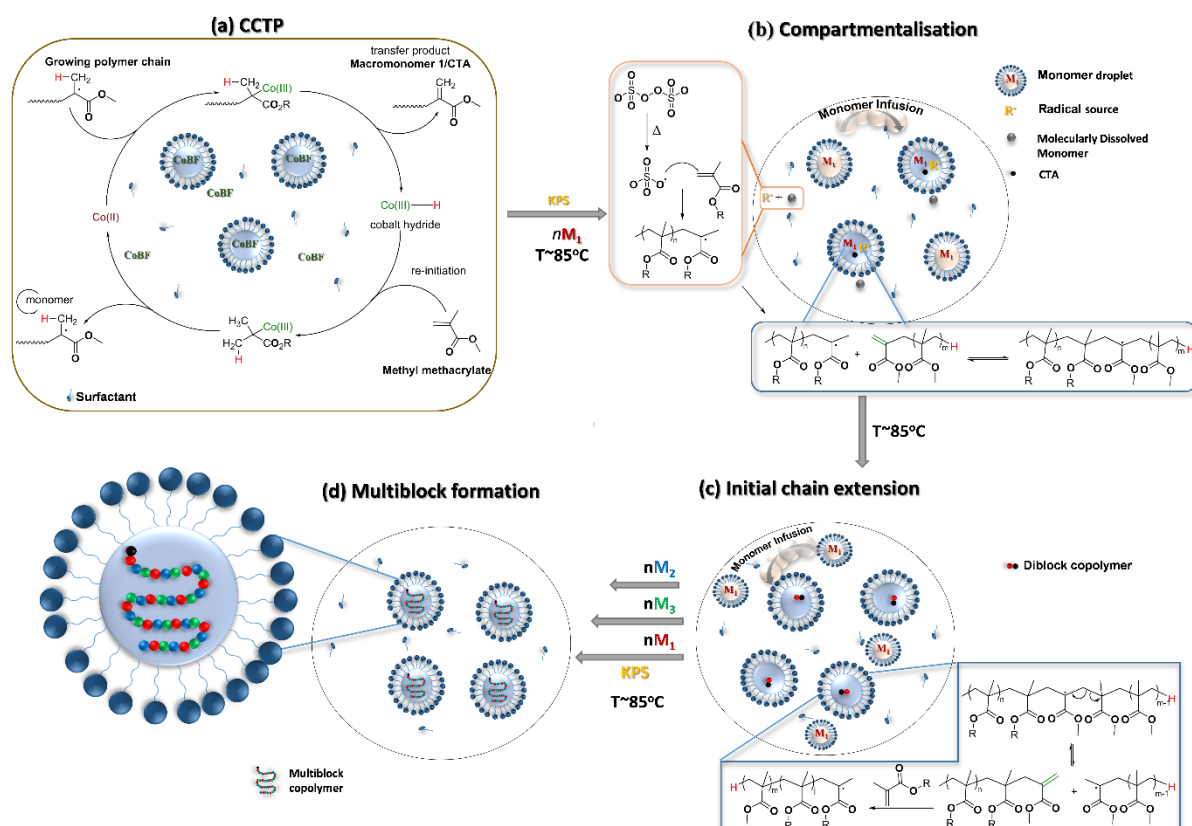
Nature is capable of achieving a high level of sequence control in the synthesis of natural polymers such as DNA and proteins. In contrast, synthetic chemists are currently far away from replicating this precision.¹ Solid-state peptide synthesis (Merrifield synthesis) remains a benchmark towards this target providing a reliable method for the synthesis of precisely controlled macromolecules.² However, this strategy is time consuming, challenging to scale up and is also limited to lower molar masses and as such alternative strategies have also been explored. It is also noted that a distribution of masses within a polymeric material is often a desirable property. Single monomer insertion,³⁻⁶ tandem monomer addition and modification,^{7, 8} kinetic control,^{9, 10} segregating templating,^{11, 12} selected reactivities,¹³ sequential growth on soluble polymer supports and discrete oligomers strategies have successfully been developed although also suffer from related issues (*e.g.* limited to low molecular weight oligomers).¹⁴⁻¹⁸

In contrast, sequence-controlled multi block copolymers obtained through controlled polymerisation strategies offer a scalable and faster alternative allowing access to higher molecular weight materials with a wide range of functionalities.^{1, 11, 19, 20} Whittaker and co-workers reported the first example of one pot sequence-controlled acrylic multi blocks *via* Cu(0)-wire reversible deactivation radical polymerisation (RDRP).²¹ The same group subsequently expanded the scope to include the synthesis of higher molecular weight and star sequence-controlled multi block copolymers.^{22, 23} Subsequently, Haddleton, Junkers and co-workers introduced sequence-controlled multi blocks mediated by a light-mediated copper polymerisation.²⁴⁻²⁶ Finally, a novel approach exploiting the disproportionation of CuBr/Me₆-Tren in water was employed to confer control over the synthesis of acrylamide

based multi block copolymers.²⁷ Aside from copper, traditional reversible addition-fragmentation transfer (RAFT) polymerisation has been employed by Perrier and co-workers yielding an impressive icosablock copolymer consisting of various acrylamides.²⁸⁻³¹ Very fast reaction rates could be maintained throughout the sequential monomer additions helped by the high propagation rate constant of acrylamides. However, all these approaches suffer from two main limitations. The first one is their incapability to efficiently polymerise low k_p monomer families such as methacrylates; this monomer category exhibits much slower polymerisation rates than acrylamides or acrylics, and is susceptible to more side reactions.³²⁻
³⁶ The second drawback is that the final multi block copolymers are often contaminated by either copper or sulphur residues which can induce undesired odour and potential toxicity in the final materials and thus require time-consuming and relatively expensive purification methods or post-polymerisation modification strategies. Other limitations of these techniques include somewhat high dispersity values, significant side reactions when water is employed as the reaction medium, slow polymerisation rates and non-quantitative conversions throughout the sequential monomer additions.^{37-39, 22}

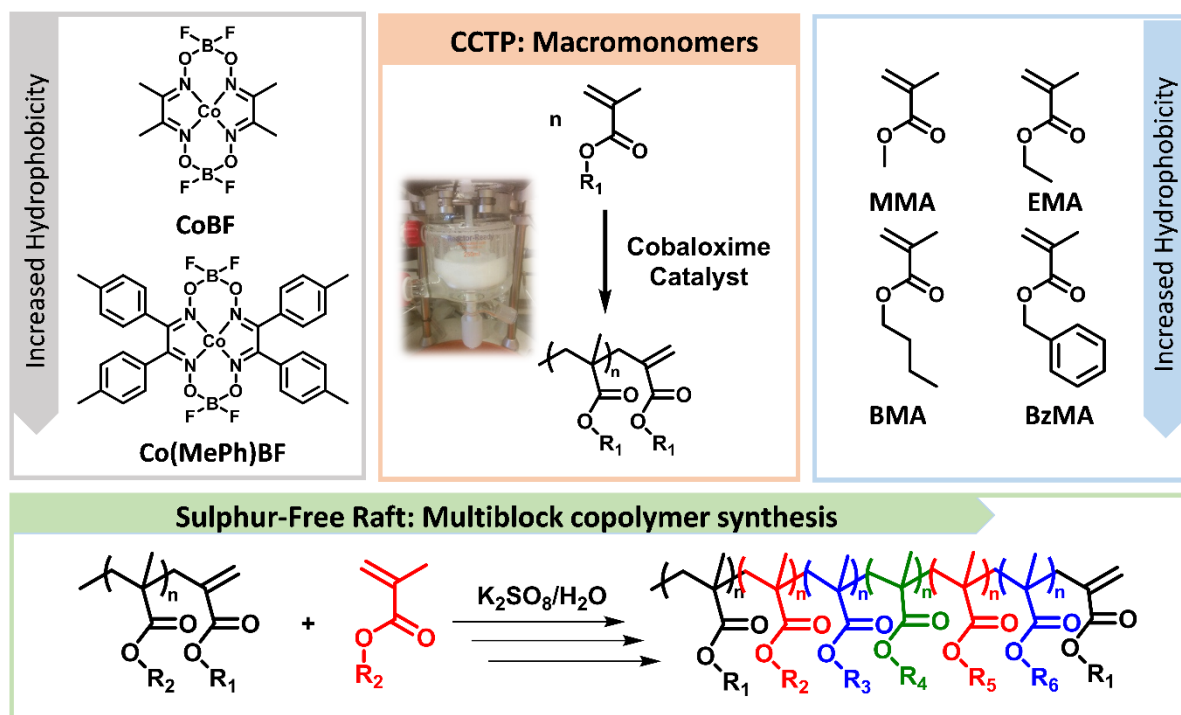
Our group has reported the sequence-controlled methacrylic multi block copolymers *via* a SF-RAFT emulsion polymerisation strategy, as presented in the previous chapter.⁴⁰ CCTP in emulsion was initially employed to synthesise poly(methyl methacrylate) (PMMA) macromonomers/mCTAs bearing a vinyl group at the ω -terminus. This macromonomer was subsequently used as a mCTA to mediate the controlled polymerisation of methacrylates thanks to the susceptibility of the vinyl ω -end group to undergo radical addition resulting in the formation of a macromonomer-ended polymer radical which can undergo β -scission (addition/fragmentation).⁴¹ The latter reaction leads to a tertiary radical generated *via*

fragmentation of the adduct product.⁴² Subsequently, a new macromonomer/mCTA is formed through combination of the initial growing radical with the vinyl end group of the initial macromonomer. Importantly, the newly formed vinyl terminated polymer can act as a CTA following the same reaction mechanism (Scheme 3.1). Thus, the combination of CCTP and sulphur-free RAFT allowed access to the scalable synthesis of sequence-controlled methacrylic multi block copolymers while maintaining fast polymerisation rates ($\sim 2\text{-}3$ h per block), quantitative conversions ($> 99\%$) and low dispersity values (typically $\mathcal{D} < 1.3$) for the entire process. However, only PMMA of $M_n \sim 2000 \text{ g mol}^{-1}$ was used as the macromonomer/mCTA in this work.



Scheme 3.1: Complete mechanism of SF-RAFT in emulsion. (a) Initial macromonomer formation *via* CCTP in emulsion (b) Compartmentalisation effect during the formation of primary radicals (c) Controlled chain extension in the polymer particles and (d) Sequential chain extensions *via* SF-RAFT.

Herein, the scope of SF-RAFT emulsion polymerisation is expanded by synthesising four different macromonomers with a terminal vinyl group, PMMA, PEMA, PBMA and PBzMA of comparable M_n ($\sim 4000 \text{ g mol}^{-1}$) *via* CCTP. Their capability to act as efficient chain transfer agents is investigated through the synthesis of diblocks and sequence-controlled multi block copolymers (Figure 3.2). Macromonomers of higher M_n are also be reported and compared with lower M_n analogues with the goal of revealing the potential and the limitations of this system.



Scheme 3.2: Schematic diagram showing the concept of the synthesis of sequence-controlled multi block copolymers by the use of macromonomers as macro chain transfer agents (CTA). Catalyst type and concentration are optimised as to provide macromonomers of the desired M_n which subsequently serve as CTA in the free radical polymerisation of methacrylic monomers.

3.2 Results and Discussion

3.2.1 Synthesis of macromonomers/macro chain transfer agents

The initial target was to obtain various macromonomers of comparable M_n in order to assess their capability to act as successful chain transfer agents. As previous studies focused on $M_n \sim 2000 \text{ g mol}^{-1}$ or even lower (*e.g.* dimers/trimers),⁴³ it was considered to target a constant M_n of $\sim 4000 \text{ g mol}^{-1}$ for all macromonomers, namely PMMA, PEMA, PBMA and PBzMA. In the previous chapter, sequence-controlled methacrylic multi block copolymers using PMMA macromonomer ($M_n \sim 2000 \text{ g mol}^{-1}$) were successfully demonstrated. In order to achieve such low molecular weight PMMA, high concentrations of bis[(difluoroboryl)]

dimethylglyoximate]cobalt(II) (CoBF) (104 ppm) were required.⁴⁰ In agreement with the previous experiments, all macromonomers were synthesised in a double-jacketed reactor (supplied with a temperature detector and overhead stirrer) *via* CCTP emulsion polymerisation. For the case of PMMA, lower concentration of CoBF was essential (42 ppm, Table 3.1, entry 5, Figure 3.1) in order to achieve $M_n \sim 4300 \text{ g mol}^{-1}$. The presence of the ω -end group vinyl protons was confirmed by both ^1H NMR and MALDI-ToF-MS (Figures 3.2 & 3), the latter showing a major polymer peak distribution identified as PMMA chains with a proton α -chain end, thus confirming that initiation *via* H-transfer from Co^{III} complex is the dominant mode of initiation, as suggested by the mechanism of CCTP (Scheme 3.3).

Table 3.1: Synthesis and characterisation data for the PMMA macromonomers synthesised in this study.

Entry	Mass of catalyst (mg)	[catalyst] (ppm)	Conv. (%)	M_n, NMR ($\text{g}\cdot\text{mol}^{-1}$)	M_n, SEC ($\text{g}\cdot\text{mol}^{-1}$)	\mathcal{D}	S.C. ($\text{g}\cdot\text{mL}^{-1}$)	% wt solids	Particle Diameter (nm)	\mathcal{D}_{DLS}
1	14.2	197	100	900	1100	1.44	0.102	8.91	-	-
2	7.2	100	>99	1700	1900	1.53	0.126	11.01	148	0.065
3	4.7	65	>99	2900	3600	1.48	0.156	13.08	177	0.048
4	2.7	38	>99	4500	5500	1.54	0.152	13.27	135	0.055
5	3	42	>99	4300	5200	1.52	0.131	11.44	108	0.050

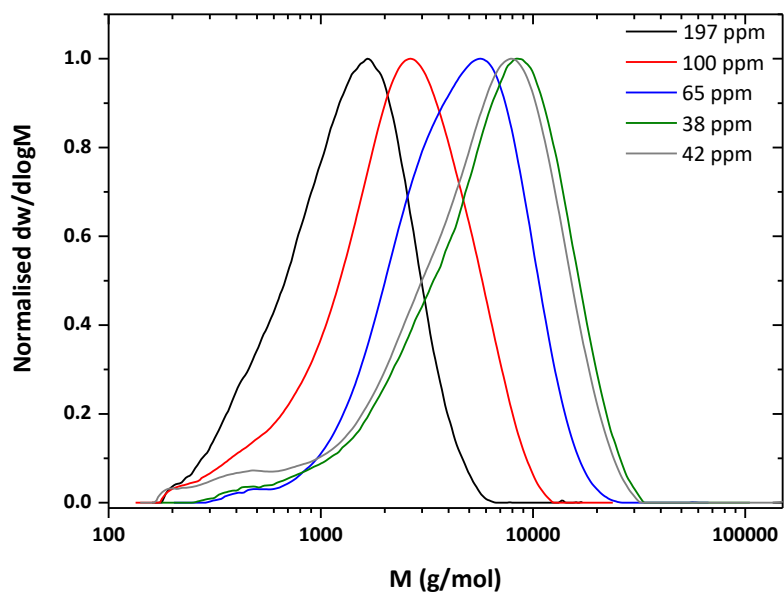


Figure 3.1: SEC chromatograms of the PMMA macromonomers synthesised by various amounts of CoBF₄.

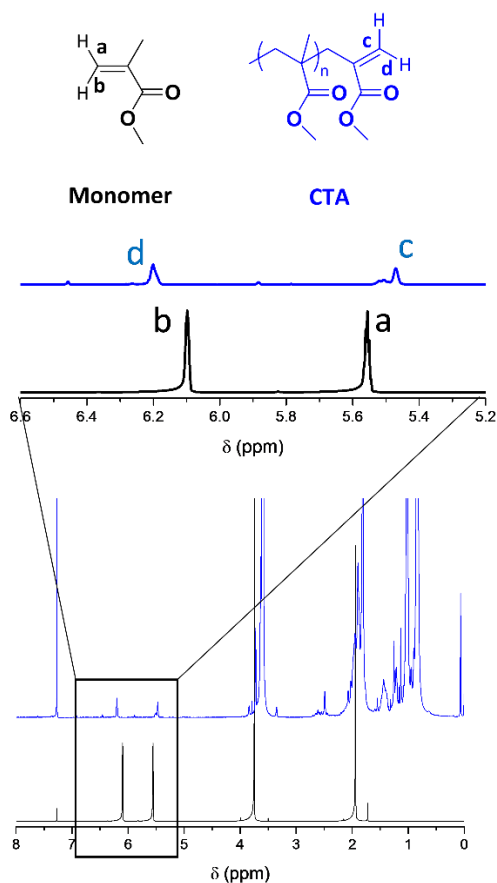


Figure 3.2: ¹H NMR spectrum of the PMMA macromonomer synthesised *via* CCTP in emulsion and the MMA monomer.

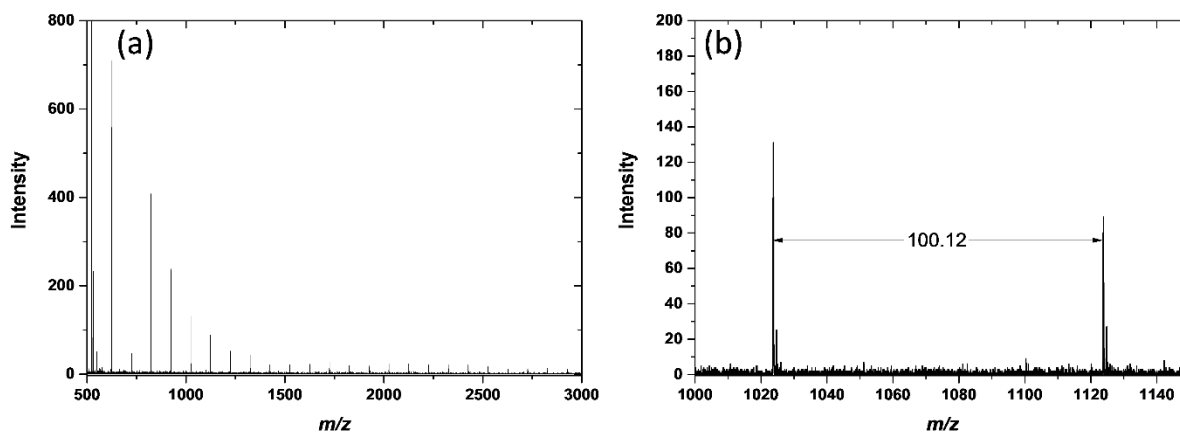
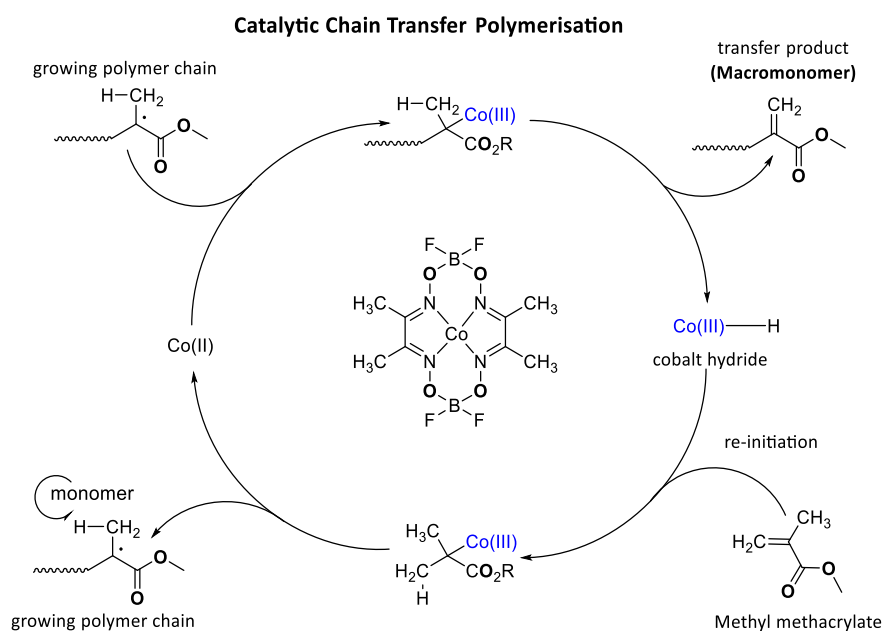


Figure 3.3: (a) MALDI-ToF MS spectrum of the PMMA macromonomer synthesised *via* CCTP in emulsion and (b) Expanded MALDI-ToF MS spectrum of the PMMA macromonomer.



Scheme 3.3: Proposed mechanism for CCTP.⁴⁴

Under otherwise identical conditions (42 ppm of CoBF) the polymerisation of EMA was then attempted. However, a rather higher M_n was obtained ($M_n \sim 7000 \text{ g mol}^{-1}$, Table 3.2, entry 1). In order to address this, higher concentrations of catalyst were investigated. It was found that 65 ppm of CoBF allowed access to PEMA of $M_n \sim 4300 \text{ g mol}^{-1}$ (Table 3.2, entry 2, Figures 3.4 & 5).

Table 3.2: Synthesis and characterisation data for the PEMA macromonomers synthesised in this study.

Entry	Mass of catalyst (mg)	[catalyst] (ppm)	Conv. (%)	M_n , NMR (g.mol ⁻¹)	M_n , SEC (g.mol ⁻¹)	\bar{D}	S.C. (g.mL ⁻¹)	% wt solids	Particle Diameter (nm)	\bar{D}_{DLS}
1	2.6	42	99	7000	12200	1.92	0.135	11.85	125	0.064
2	4.0	65	99	4300	5000	1.57	0.119	10.45	111	0.086
3	4.4	71	>99	4200	4300	1.63	0.128	11.25	141	0.068
4	4.5	73	>99	3800	2900	1.97	0.130	11.40	126	0.071

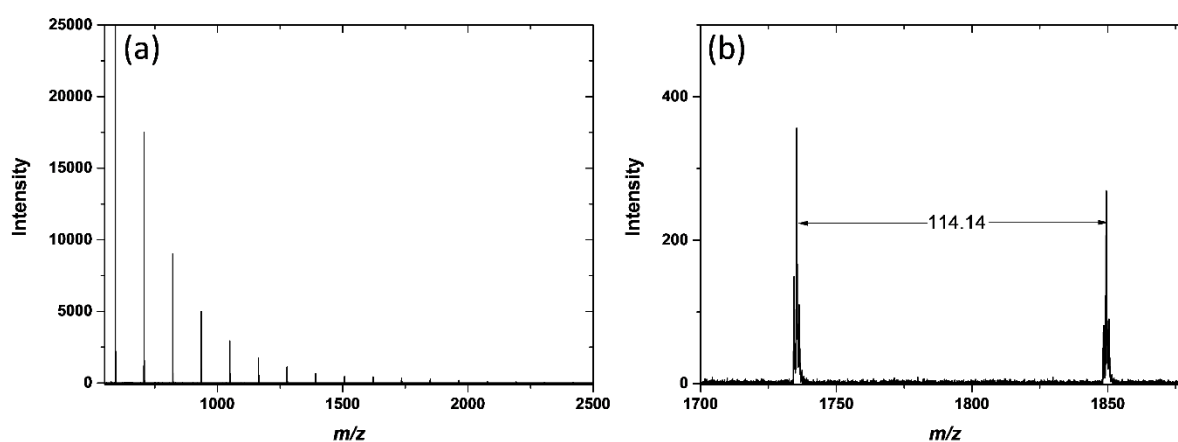


Figure 3.4: (a) MALDI-ToF MS spectrum of the PEMA macromonomer synthesised *via* CCTP in emulsion and (b) Expanded MALDI-ToF MS spectrum of the PEMA macromonomer.

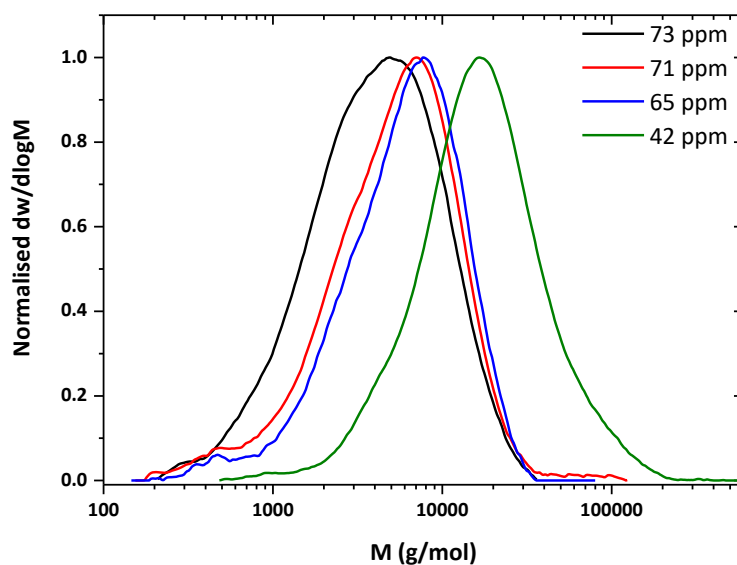


Figure 3.5: SEC chromatograms of the PEMA macromonomers synthesised by various amounts of CoBF.

The differences in catalyst concentration required to achieve comparable molecular weights can be attributed to the partition coefficient (m_{Co}), which is equal to the ratio of the catalyst concentration in the dispersed phase (monomer) to that in the aqueous phase ($m_{Co} = [Co]_{disp}/[Co]_{aq}$) and differs for each monomer.⁴⁴ The catalyst needs to be present at the loci of polymerisation and thus mass transport of the catalyst between continuous and dispersed phase is required.⁴⁵ Although CoBF proved to be a very efficient catalyst for the polymerisation of MMA and EMA, it is insoluble in BMA and BzMA (in concentrations higher than 60 ppm). In order to circumvent this, the more hydrophobic catalyst bis[(difluoroboryl)dimethylphenylglyoximato]cobalt(II) (Co(MePh)BF) was used in place of CoBF (Scheme 3.2). Under optimised conditions, PBMA and PBzMA macromonomers (Tables 3.3 & 4, Figures 3.6 & 7) of $M_n \sim 4200 \text{ g mol}^{-1}$ and 4400 g mol^{-1} were synthesised.

Table 3.3: Synthesis and characterisation data for the PBMA macromonomers synthesised in this study.

Entry	Mass of catalyst (mg)	[catalyst] (ppm)	Conv. (%)	$M_{n, NMR}$ (g.mol ⁻¹)	$M_{n, SEC}$ (g.mol ⁻¹)	\bar{D}	S.C. (g.mL ⁻¹)	% wt solids	Particle Diameter (nm)	\bar{D}_{DLS}
1	2.9	60	98	12400	12300	1.79	0.126	11.95	159	0.037
2	5.2	60	>99	27500	27100	1.76	0.132	12.03	58	0.075
3	8.7	100	>99	15900	18500	1.68	0.129	11.98	56	0.027
4	12.1	140	99	10600	13300	1.68	0.136	12.07	53	0.061
5	15.6	180	>99	9400	11600	1.65	0.129	11.96	54	0.078
6	20.8	240	99	7600	9700	1.68	0.133	12.01	54	0.046
7	22.5	260	99	7200	8500	1.81	0.138	12.10	52	0.070
8	27.7	320	>99	5100	7100	1.64	0.135	11.82	50	0.042
9	29.5	340	>99	4200	8500	1.42	0.122	12.23	52	0.040

Table 3.4: Synthesis and characterisation data for the PBzMA macromonomer synthesised in this study.

Entry	Mass of catalyst (mg)	[catalyst] (ppm)	Conv. (%)	$M_{n, NMR}$ (g.mol ⁻¹)	$M_{n, SEC}$ (g.mol ⁻¹)	\bar{D}	S.C. (g.mL ⁻¹)	% wt solids	Particle Diameter (nm)	\bar{D}_{DLS}
1	5.3	65	99	98300	131600	4.4	0.158	13.63	209	0.018
2	15.8	195	>99	96400	94200	3.7	0.154	13.26	199	0.011
3	19.5	240	>99	26300	22200	1.91	0.157	13.44	190	0.014
4	24.4	300	>99	10900	8000	1.85	0.153	13.19	162	0.015
5	32.5	400	>99	4400	3400	1.78	0.163	14.04	161	0.025

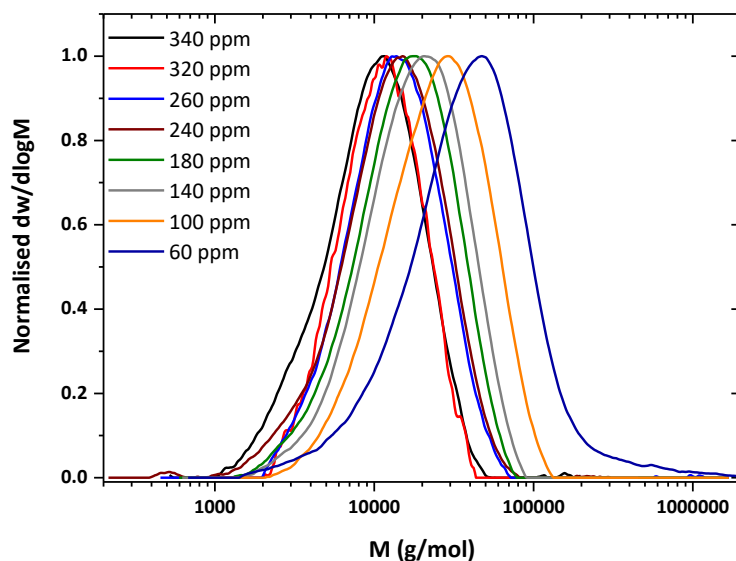


Figure 3.6: SEC chromatograms of the PBMA macromonomers synthesised by various amounts of Co(MePh)BF.

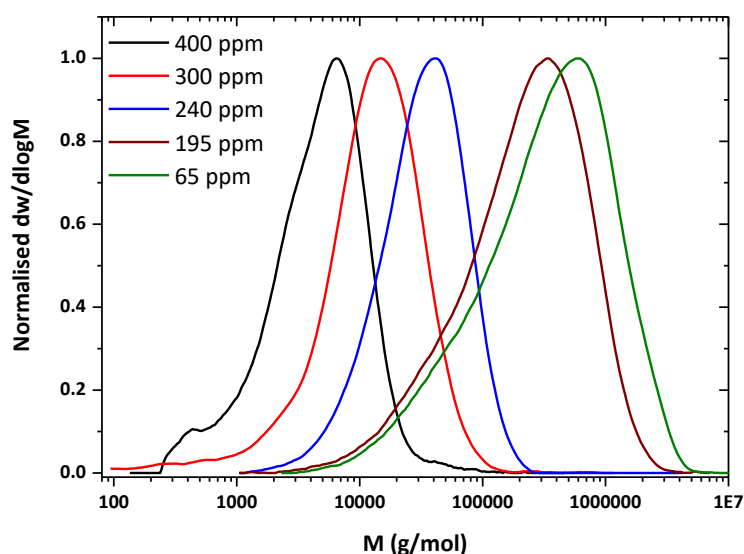


Figure 3.7: SEC chromatogram of the PBzMA macromonomers synthesised by various amounts of Co(MePh)BF.

For all macromonomers synthesised, ^1H NMR analysis confirmed full monomer conversion (> 99%) and the existence of the vinyl group at the ω -chain end. MALDI-ToF-MS also showed very high end group fidelity for all macromonomers confirming the successful synthesis (Figures 3.8 & 9). Finally, dynamic light scattering (DLS) was additionally employed

showing that the particle size mainly depends on the nature of the polymer targeted rather than the final M_n . It is noted, that latexes generated upon the polymerisation of BMA consisted of considerably smaller particles as opposed to the other three monomers studied.

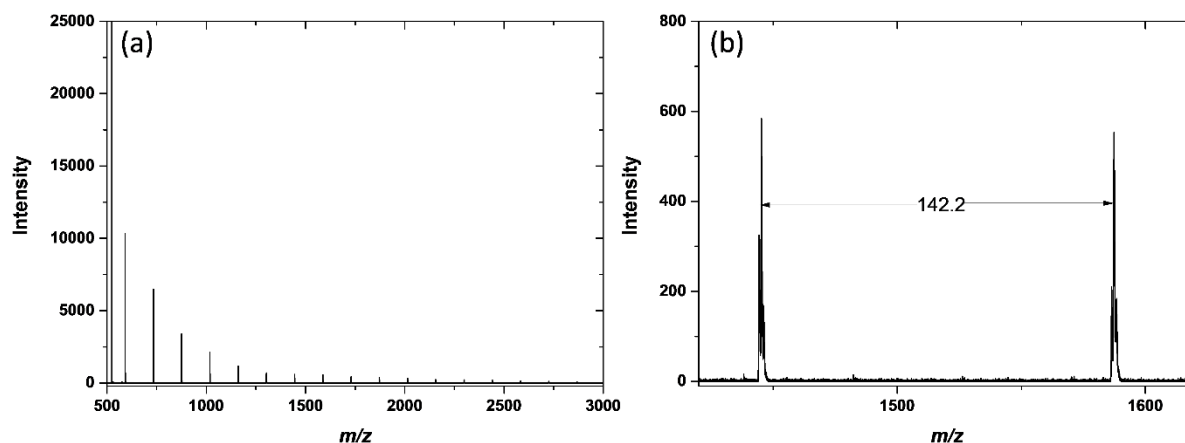


Figure 3.8: (a) MALDI-ToF MS spectrum of the PBMA macromonomer synthesised *via* CCTP in emulsion and (b) Expanded MALDI-ToF MS spectrum of the PBMA macromonomer.

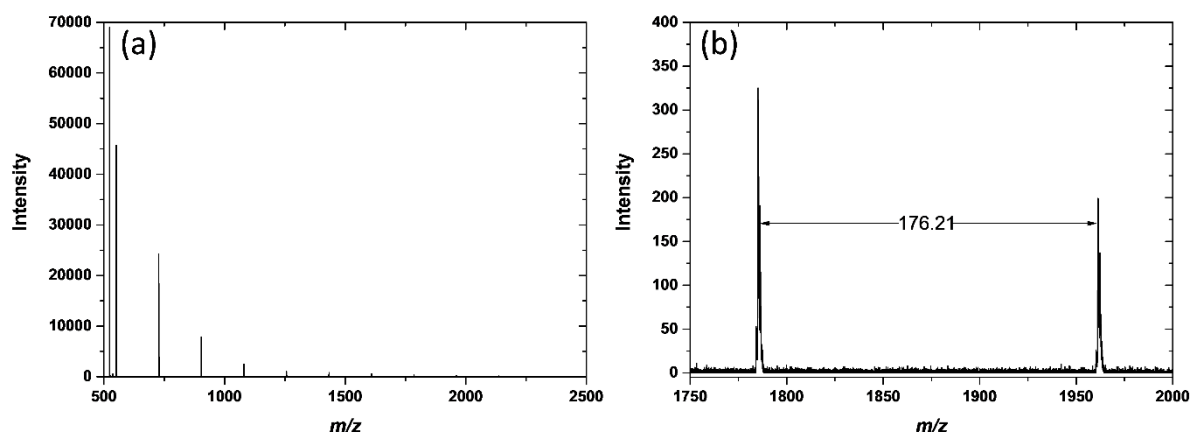


Figure 3.9: (a) MALDI-ToF MS spectrum of the PBzMA macromonomer synthesised *via* CCTP in emulsion and (b) Expanded MALDI-ToF MS spectrum of the PBzMA macromonomer.

3.2.2 Synthesis of methacrylic diblock copolymers using PMMA, PEMA, PBMA and PBzMA as macromonomers/macro chain transfer agents

After obtaining different macromonomers of comparable M_n the next step was to assess their capability to mediate the polymerisation of methacrylates. BMA was selected and kinetics in the presence of PMMA were initially conducted targeting $DP_n = 80$ ($[\text{monomer}] : [\text{CTA}] = 1 : 80$). Samples were periodically taken from the reaction mixture and SEC showed a gradual decrease of the dispersity from 1.55 (dispersity of PMMA macromonomer prior to BMA addition) to $\mathcal{D} \sim 1.17$ for the final diblock copolymer (Table 3.5, Figure 3.10).

Table 3.5: Data for the free radical polymerisation of BMA in emulsion in the presence of PMMA macromonomer.

BMA added (eq)	$M_{n, \text{Th}}$	$M_{n, \text{NMR}}$ (g.mol ⁻¹)	DP_n NMR	$M_{n, \text{SEC}}$ (g.mol ⁻¹)	\mathcal{D}	Particle Diameter (nm)	\mathcal{D}_{DLS}
-	3800	3800	-	4,500	1.55	113	0.063
16	6100	4800	7	5,200	1.49	124	0.050
32	8400	7000	22	7,600	1.30	136	0.044
48	10600	9400	39	9,100	1.23	146	0.018
64	12900	11200	52	11,000	1.20	154	0.020
80	15200	15100	80	13,000	1.17	163	0.043

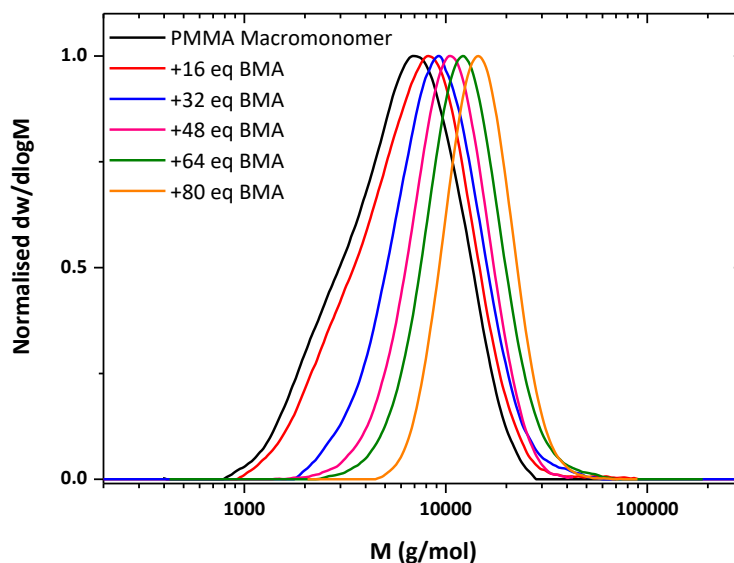


Figure 3.10: SEC chromatograms of the samples taken during the free radical polymerisation of BMA in the presence of PMMA macromonomer.

In a similar vein, PBMA macromonomer was also employed to polymerise BMA with the kinetics exhibiting virtually identical behaviour and SEC showing a clear shift to higher molecular weights and constantly decreasing dispersities (Table 3.6, Figure 3.11). It is noted that although macromonomers of higher M_n than in previous reports were used, the “living” characteristics of the system could be maintained and low dispersity diblock copolymers were achieved.

Table 3.6: Data for the free radical polymerisation of BMA in emulsion in the presence of PBMA macromonomer.

BMA added (eq)	$M_{n,Th}$	$M_{n,NMR}$ (g.mol ⁻¹)	DP_n NMR	$M_{n,SEC}$ (g.mol ⁻¹)	\bar{D}	Particle Diameter (nm)	\bar{D}_{DLS}
-	5100	5100	36	6400	1.65	52	0.040
16	7400	5800	41	7000	1.61	53	0.035
32	9700	7200	51	8500	1.44	59	0.130
48	11900	9200	65	10100	1.30	62	0.051
64	14200	11400	80	11500	1.29	66	0.040
80	16500	17400	122	14600	1.25	74	0.055

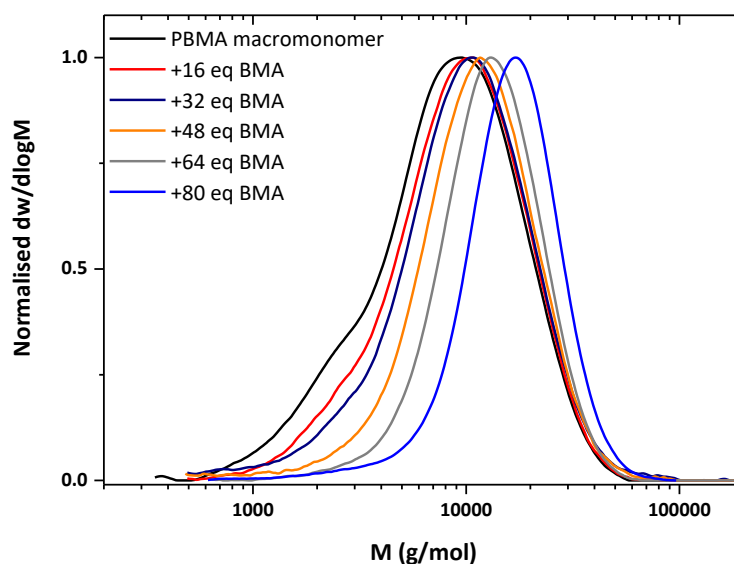


Figure 3.11: SEC chromatograms of the samples taken during the free radical polymerisation of BMA in the presence of PBMA macromonomer.

Having demonstrated a similar kinetic behaviour for two different macromonomers, PEMA and PBzMA were also employed targeting $DP_n = 80$. All tested macromonomers (Section P.4.4, Table 3.17) were capable of successfully mediating the polymerisation of BMA yielding nearly identical diblock copolymers (Figure 3.12 a) with low dispersity values (< 1.28) and reasonable agreement between theoretical and experimental molar masses (Table 3.7). In

particular, when PMMA and PEMA macromonomers were employed, diblock copolymers with a final dispersity of 1.23 and 1.20 respectively were obtained. For the case of PBMA and PBzMA slightly higher dispersities were achieved ($\mathcal{D} \sim 1.27$) (Table 3.7). To further probe the potential of the macromonomers in maintaining control for higher molecular weights a more challenging diblock was targeted, aiming for $DP_n = 400$ of BMA. Despite the higher targeted molecular weight, all macromonomers yielded well-controlled polymers with dispersities as low as 1.17 and $M_n \sim 60000 \text{ g mol}^{-1}$ (Figure 3.12 b, Table 3.8). Thus, it was concluded that regardless the type of the macromonomer used, SF-RAFT emulsion polymerisation was unaffected allowing access to well-defined diblock copolymers. Importantly, in all cases, full monomer conversion could be achieved (> 99%) suggesting that these macromonomers could be potentially used for more complex targets such as sequence-controlled multi block copolymers.

Table 3.7: Synthesis and characterisation data for the diblock copolymers ($DP_n=80$) synthesised by the use of different CTAs.

Entry	Employed CTA	Conv. (%)	DP_n NMR	M_n , NMR ($\text{g}\cdot\text{mol}^{-1}$)	M_n , SEC ($\text{g}\cdot\text{mol}^{-1}$)	\mathcal{D}	Particle Diameter (nm)	\mathcal{D}_{DLS}
1	PMMA	>99	84	16200	12800	1.23	148	0.041
2	PEMA	>99	82	16000	12300	1.20	157	0.044
3	PBzMA	>99	71	14500	11600	1.28	489	0.078
4	PBMA	>99	82	15900	13500	1.27	77	0.026

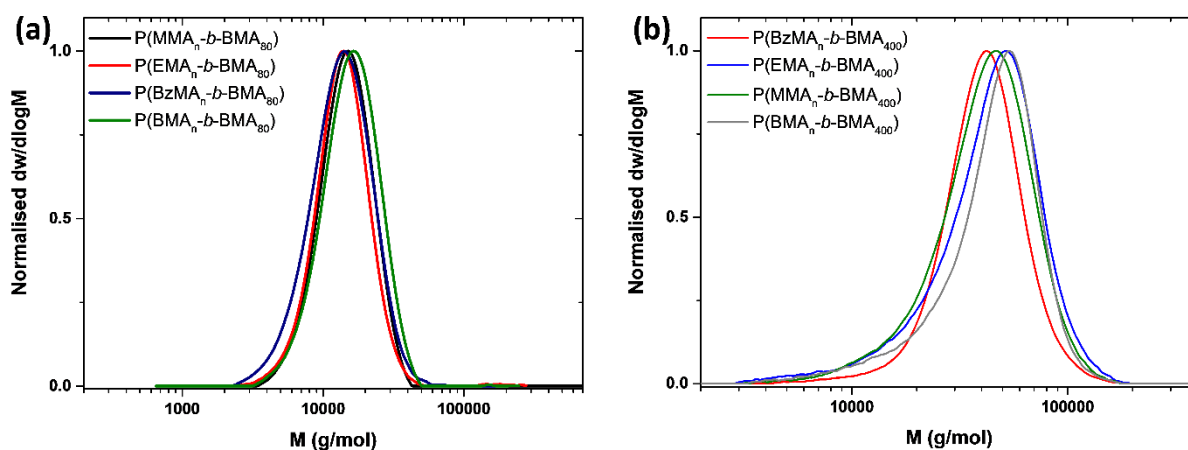


Figure 3.12: (a) SEC traces of molecular weight distributions for the diblock macromonomers formed by different CTAs ($DP_n=80$ BMA) and (b) SEC traces of molecular weight distributions for the diblock macromonomers formed by different CTAs ($DP_n=400$ BMA).

Table 3.8: Data for the free radical polymerisation of BMA in emulsion in the presence of PMMA, PEMA, PBzMA and PBMA macromonomer ($DP_n=400$).

Entry	Employed CTA	Conv. (%)	DP_n NMR	$M_{n,NMR}$ ($g \cdot mol^{-1}$)	$M_{n,SEC}$ ($g \cdot mol^{-1}$)	\bar{D}	S.C. ($g \cdot mL^{-1}$)	% wt solids	Particle Diameter (nm)	\bar{D}_{DLS}
1	PMMA	99	428	65200	37100	1.26	0.223	18.24	197	0.044
2	PEMA	>99	394	60300	39900	1.27	0.227	18.48	221	0.083
3	PBzMA	>99	424	64700	38100	1.17	0.219	17.99	856	0.109
4	PBMA	99	384	58800	42800	1.2	0.227	18.48	144	0.157

It is also worth mentioning that although deionised water was used for the aforementioned experiments, tap water appeared to be equally efficient and no compromise over the dispersity or the control over the polymerisation was observed further highlighting the robustness of this system (Table 3.9, Figure 3.13).

Table 3.9: Characterisation data for the free radical polymerisation of BMA in the presence of PMMA macromonomer ($DP_n=80$) in emulsion using tap water.

Entry	Employed CTA	Conv. (%)	M_n, NMR ($\text{g}\cdot\text{mol}^{-1}$)	M_n, SEC ($\text{g}\cdot\text{mol}^{-1}$)	\mathcal{D}	S.C. ($\text{g}\cdot\text{mL}^{-1}$)	% wt solids	Particle Diameter (nm)	\mathcal{D}_{DLS}
1	CoBF	>99	1400	1800	1.44	0.144	11.62	178	0.008
2	PMMA	>99	13800	12200	1.1	0.220	18.05	380	0.016

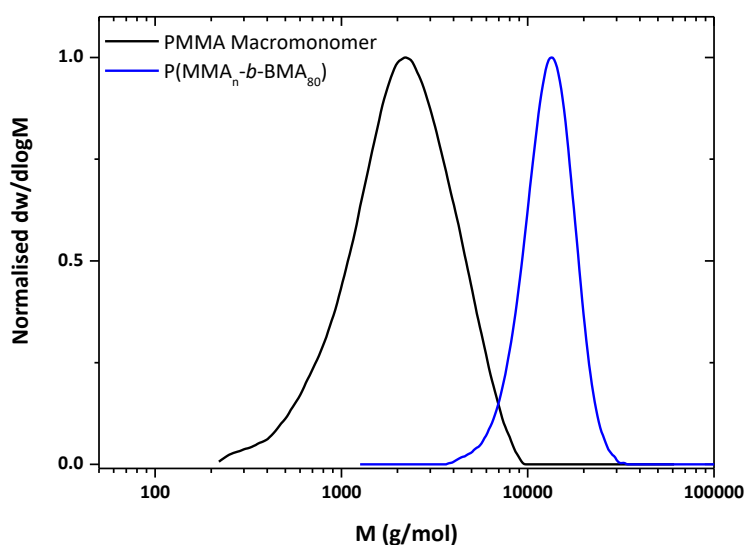


Figure 3.13: SEC chromatograms of the PMMA macromonomer and the corresponding $P(\text{MMA}_n\text{-}b\text{-BMA}_{80})$ diblock prepared in emulsion using tap water.

3.2.3 Synthesis of sequence-controlled methacrylic copolymers using PMMA, PEMA, PBMA and PBzMA as macromonomers/chain transfer agents

The PBMA macromonomer ($M_n=4300 \text{ g mol}^{-1}$, $\mathcal{D} \sim 1.91$) was subsequently used as a chain-transfer agent to facilitate the synthesis of multi block copolymers, employing an initial ratio of $[\text{CTA}]:[\text{monomer}]:[\text{initiator}] = 1:10:0.03$ and each block was designed to be $DP_n=10$. It is important to highlight that lower molecular weights were not targeted in order to limit the proportion of missing blocks (percentage of defective chains) in the final multi block copolymer, which should be as low as possible according to Harrison, Perrier and co-

workers.⁴⁶ Upon completion of the first monomer addition (BzMA) to the reaction mixture, the reaction was allowed to proceed for one hour to ensure quantitative or near-quantitative conversion. Indeed, ¹H NMR spectroscopy confirmed very high conversion (> 99%) while SEC showed a shift to higher molecular weights. BMA was subsequently added and when full conversion was reached, 2-ethylhexyl methacrylate (EHMA) was injected in the reaction mixture. This one pot sequential addition was repeated ten times resulting in an undecablock copolymer (including the CTA) with $M_n \sim 20200 \text{ g mol}^{-1}$ and a final dispersity of 1.29 (Table 3.10 Section 3.4.4, Table 3.18). Throughout all the monomer additions, the SEC distributions were monomodal (Figure 3.14), while ¹H NMR indicated full monomer conversion prior to the addition of the next block (Figure 3.15). Despite multiple chain extensions control over the molecular weight was maintained throughout, highlighting the capacity of PBMA to act as a very efficient chain transfer agent under SF-RAFT emulsion polymerisation.

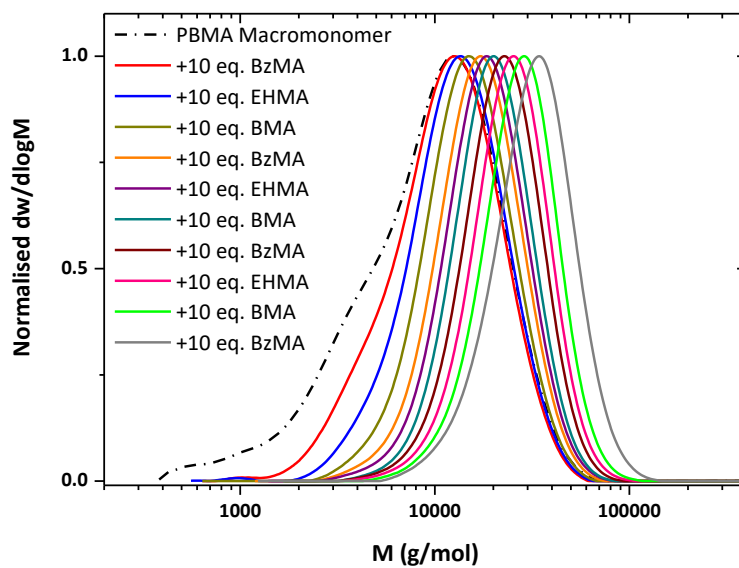


Figure 3.14: SEC traces of consecutive monomer additions for the preparation of the undecablock copolymer utilising PBMA macromonomer as CTA.

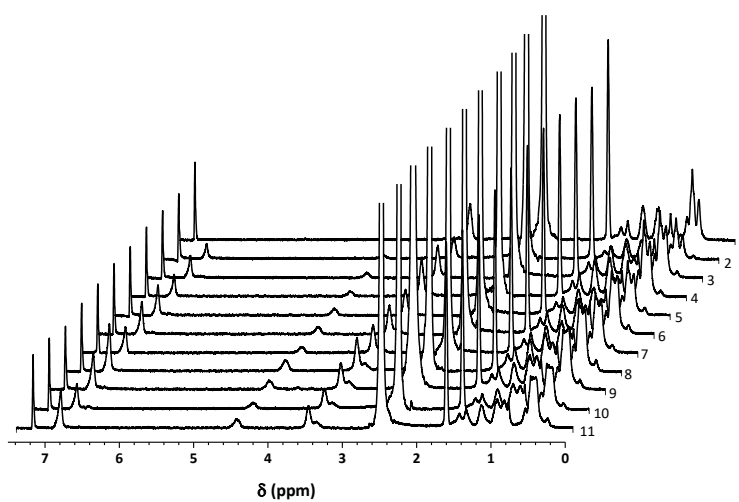


Figure 3.15: ^1H NMR spectra for consecutive cycles during synthesis of the undecablock copolymer utilising PBMA macromonomer as CTA.

Table 3.10: Characterisation data for the synthesis of the undecablock copolymer in emulsion at 85 °C with potassium persulfate as initiator, utilising PBMA macromonomer as CTA.

Entry	Cycle	Conv. (%)	$M_{n,th}$ (g.mol ⁻¹)	$M_{n,SEC}$ (g.mol ⁻¹)	\mathcal{D}	Particle Diameter (nm)	\mathcal{D}_{DLS}
1	CTA	99	4300	4300	1.91	55	0.046
2	1	>99	6100	5900	1.52	60	0.045
3	2	99	8100	7900	1.41	66	0.018
4	3	>99	9500	9100	1.33	71	0.025
5	4	>99	11300	11000	1.30	74	0.015
6	5	>99	13300	13000	1.27	77	0.033
7	6	99	14700	14100	1.24	81	0.004
8	7	>99	16500	16000	1.26	84	0.031
9	8	>99	18500	17600	1.25	92	0.082
10	9	99	19900	18900	1.25	96	0.024
11	10	99	21700	20500	1.29	99	0.023

Upon using PEMA ($M_n=4300 \text{ g mol}^{-1}$, $\mathcal{D} \sim 1.9$) as the macromonomer, a higher targeted DP_n was attempted ($DP_n = 25$ per block). Following addition of the first monomer, a significant decrease in the dispersity was observed ($\mathcal{D} \sim 1.24$) and the polymerisation reached very high monomer conversions (> 99%, Figure 3.16 b) in less than two hours. After this time period, a second monomer was added resulting in a further reduction on the dispersity ($\mathcal{D} \sim 1.20$). The sequential inclusion of various monomers finally yielded a nonablock copolymer (including the CTA) with a dispersity as low as 1.19 and a final $M_n \sim 28200 \text{ g mol}^{-1}$ (Figure 3.16 a, Table 3.11 Section 3.4.4, Table 3.19). SEC confirmed complete shifts to higher molecular weights throughout the monomer additions with the dispersity values being kept < 1.2 for the vast majority of the monomer additions which is a remarkable achievement for such a complex multi block structure.

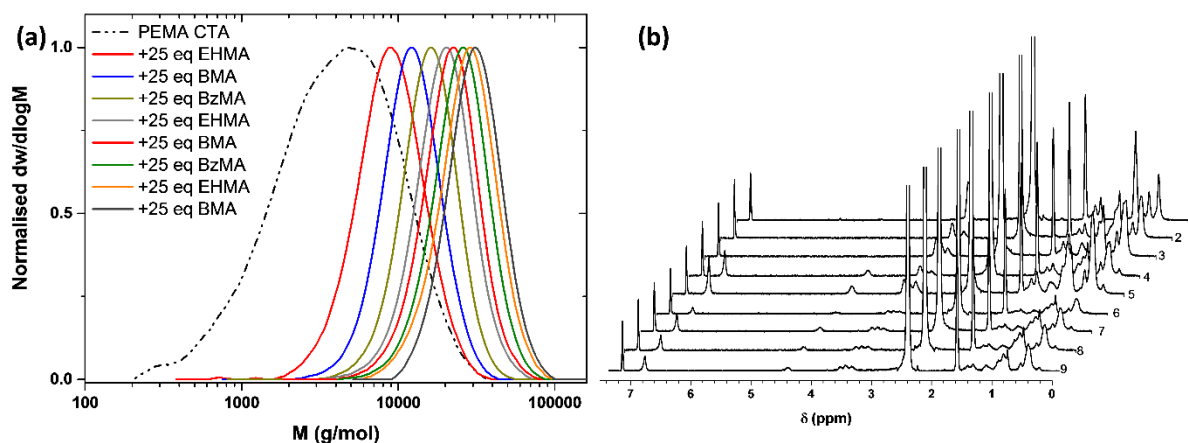


Figure 3.16: (a) SEC traces of consecutive monomer additions for the preparation of the nonablock copolymer ($DP_n = 25$ per block) utilising PEMA macromonomer as CTA and (b) ^1H NMR spectra for consecutive cycles during synthesis of the nonablock copolymer (values to the right indicate the number of sequential monomer additions carried out prior to collection of the spectrum).

Table 3.11: Characterisation data for the synthesis of the nonablock copolymer in emulsion at 85 °C with potassium persulfate as initiator, utilising PEMA macromonomer as CTA.

Entry	Cycle	Conv. (%)	$M_{n,th}$ (g.mol $^{-1}$)	$M_{n,SEC}$ (g.mol $^{-1}$)	\bar{D}	Particle Diameter (nm)	\bar{D}_{DLS}
1	CTA	>99	3800	2900	1.97	126	0.071
2	1	>99	8800	8000	1.24	165	0.074
3	2	99	12400	13100	1.20	174	0.062
4	3	>99	16800	14300	1.19	182	0.075
5	4	>99	22800	17800	1.18	188	0.068
6	5	99	25400	19700	1.17	193	0.068
7	6	>99	29800	22800	1.18	198	0.057
8	7	>99	34800	25400	1.18	202	0.089
9	8	>99	38400	28200	1.19	206	0.059

Finally, PBzMA was selected as the macromonomer ($M_n=4400$ g mol $^{-1}$, $\bar{D} \sim 1.78$). As high molecular weight multi block copolymers could be of a potential interest for a wide range of applications, including self-assembly in bulk and in solution, the technique was pushed to reach its limits by targeting $DP_n = 50$ per block. Remarkably, and despite the increased size of

block, a well-defined octablock copolymer (or nonablock including the CTA) could be obtained achieving $M_n \sim 30000 \text{ g mol}^{-1}$ and a dispersity of 1.28 for the final multi block copolymer (Figures 3.17 & 18, Table 3.12, Section 3.4.4, Table 3.20). From this data, it is apparent that PBzMA macromonomers are also capable of successfully mediating the synthesis of well-controlled multi block copolymers.

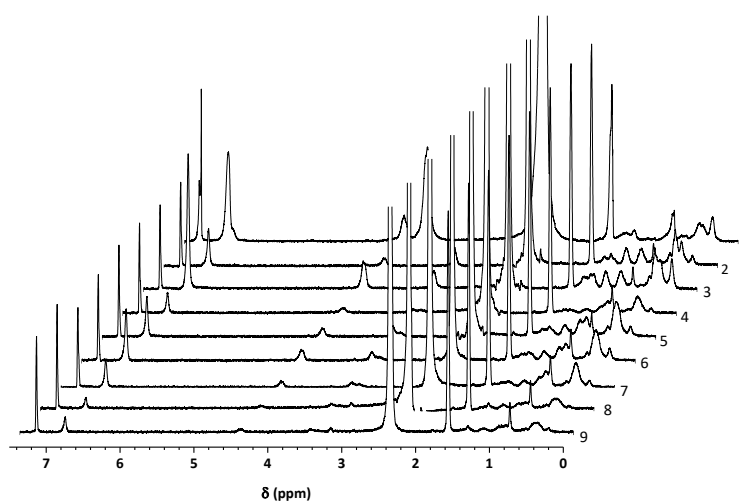


Figure 3.17: ^1H NMR spectra for consecutive cycles during synthesis of the nonablock copolymer utilising PBzMA macromonomer as CTA.

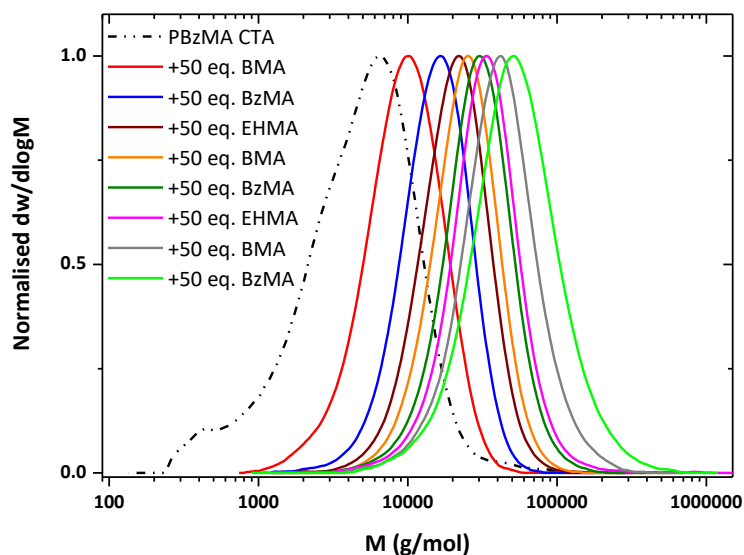


Figure 3.18: SEC traces of consecutive monomer additions for the preparation of the nonablock copolymer utilising PBzMA macromonomer as CTA.

Table 3.12: Characterisation data for the synthesis of the nonablock copolymer in emulsion at 85 °C with potassium persulfate as initiator, utilising PBzMA macromonomer as CTA.

Entry	Cycle	Conv. (%)	$M_{n,th}$ (g.mol ⁻¹)	$M_{n,SEC}$ (g.mol ⁻¹)	\bar{D}	Particle Diameter (nm)	\bar{D}_{DLS}
1	CTA	>99	4400	3400	1.78	161	0.025
2	1	>99	11500	8600	1.38	179	0.054
3	2	99	20300	14700	1.29	187	0.045
4	3	>99	30200	19400	1.26	197	0.057
5	4	99	37300	22300	1.27	204	0.044
6	5	99	46100	26900	1.29	206	0.063
7	6	99	56000	29800	1.28	214	0.051
8	7	>99	63100	35100	1.29	221	0.067
9	8	>99	71900	42100	1.34	229	0.045

3.2.4 Limitations of sulphur-free RAFT emulsion polymerisation towards narrow dispersity block copolymers

It was also considered interesting to explore the limitations of this system. In the previous chapter, PMMA of $M_n \sim 2000 \text{ g mol}^{-1}$ was employed and the dispersity was as low as ~ 1.12 after 4 monomer additions designed as $DP_n = 10$ per block. Herein, a PMMA of higher M_n was considered as CTA and as such a PMMA of M_n of 11700 g mol^{-1} was synthesised (Section P.4.4, Table 3.21). However, upon three monomer additions, a broad bimodal polymer peak distribution was observed by SEC with the final dispersity being ~ 2.4 , which is an indication of a normal free radical process (Table 3.13, Figure 3.19).

Table 3.13: Characterisation data for the synthesis of the tetrablock copolymer in emulsion at $85 \text{ }^\circ\text{C}$ with potassium persulfate as initiator, utilising high M_n PMMA macromonomer as CTA.

Entry	Cycle	$M_{n,\text{th}}$ ($\text{g}\cdot\text{mol}^{-1}$)	$M_{n,\text{SEC}}$ ($\text{g}\cdot\text{mol}^{-1}$)	\mathcal{D}
1	CTA	11700	12800	3.03
2	1	13100	12700	2.86
3	2	14900	12600	2.55
4	3	16900	13000	2.42

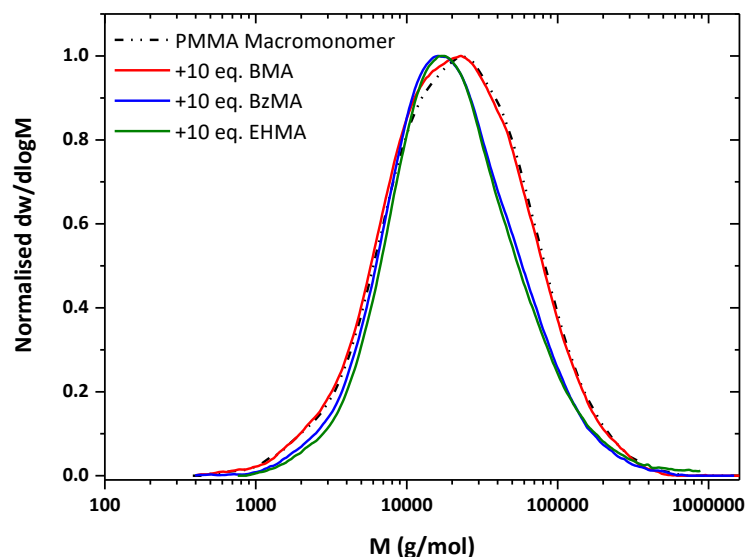


Figure 3.19: SEC traces of consecutive monomer additions for the preparation of the tetrablock copolymer utilising high M_n PMMA macromonomer as CTA.

Thus, PMMA of this M_n is not recommended to be used as a CTA to facilitate the synthesis of multi block copolymers. In order to further confirm this limitation, two PBMA macromonomers were also compared. In the previous section, PBMA of $M_n \sim 4300 \text{ g mol}^{-1}$ was successfully synthesised and subsequently used as CTA for the undecablock copolymer mentioned above. After four monomer additions the dispersity of the pentablock copolymer was ~ 1.30 (Table 3.14). However, when a PBMA of a higher M_n ($\sim 7200 \text{ g mol}^{-1}$) was employed instead, after the same number of additions a broader molecular weight distribution was observed ($\mathcal{D} \sim 1.45$, Figure 3.20, Table 3.14, Section 3.4.4, Table 3.22). Therefore, it is apparent that upon gradually increasing the molecular weight of the CTA, a compromise of control over the molecular distribution takes place as the number of chains with vinyl ω -end group is reduced as a result of conventional free radical termination events.

Table 3.14: Characterisation data for the synthesis of the pentablock copolymer in emulsion at 85 °C with potassium persulfate as initiator, utilising PBMA macromonomer as CTA.

Entry	Cycle	Conv. (%)	$M_{n,th}$ (g.mol ⁻¹)	$M_{n,SEC}$ (g.mol ⁻¹)	\bar{D}	Particle Diameter (nm)	\bar{D}_{DLS}
1	CTA	99	7200	8500	1.81	52	0.070
2	1	>99	9000	8000	1.73	56.2	0.039
3	2	99	11000	10100	1.63	60.3	0.067
4	3	>99	12400	10400	1.49	62.4	0.059
5	4	>99	14200	11500	1.45	64.6	0.051

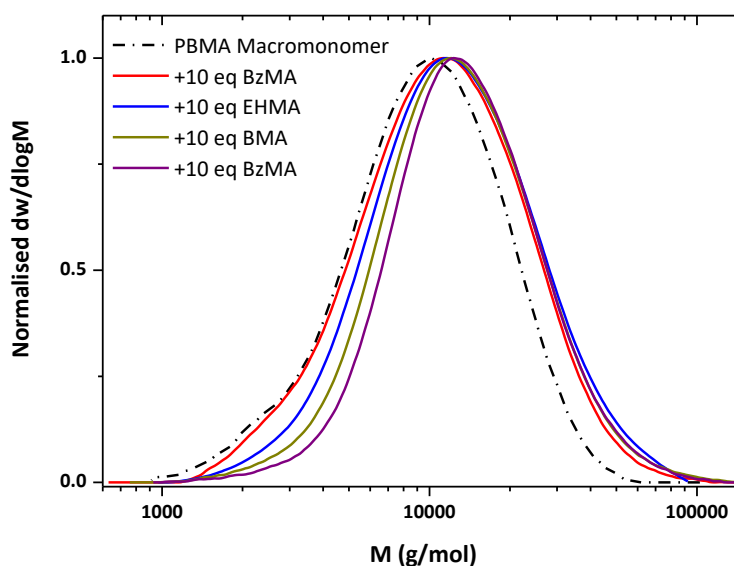


Figure 3.20: SEC traces of consecutive monomer additions for the preparation of the pentablock copolymer utilising high M_n PBMA macromonomer as CTA.

In addition to MMA, EMA, BzMA and BMA, different types of monomers were considered. Extremely hydrophobic monomers such as lauryl methacrylate (LMA) or isobornyl methacrylate are known for not being able to be successfully applied in emulsion polymerisation.⁴⁷ The polymerisation of isobutyl methacrylate (*i*BMA, $DP_n = 80$) in the presence of a PMMA CTA produced a diblock copolymer with a dispersity broader than that obtained when BMA was polymerised ($1.26 > 1.23$, Figure 3.21, Tables 3.15). However, by SEC

analysis, a shoulder towards lower molecular weight is evidenced. Thus, some monomers cannot provide equally narrow Mwt distributions when polymerised under the current conditions.

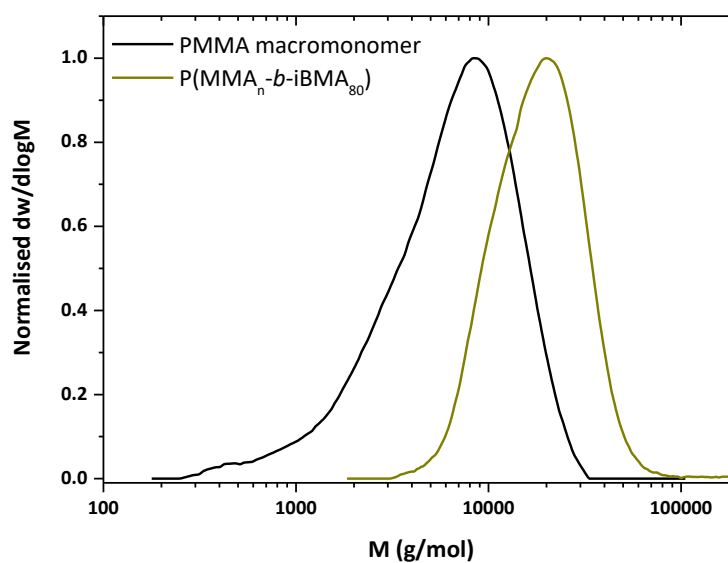


Figure 3.21: SEC traces of the PMMA macromonomer and the corresponding P(MMA_n-*b*-iBMA₈₀) diblock prepared in emulsion.

Table 3.15: Characterisation data for the free radical polymerisation of *i*BMA in the presence of PMMA macromonomer ($DP_n=80$) in emulsion.

Entry	Employed CTA	Conv. (%)	$M_{n, NMR}$ (g.mol ⁻¹)	$M_{n, SEC}$ (g.mol ⁻¹)	\bar{D}	S.C. (g.mL ⁻¹)	% wt solids	Particle Diameter (nm)	\bar{D}_{DLS}
1	CoBF	>99	4500	5800	1.54	0.144	12.85	138	0.041
2	PMMA	>99	16000	16000	1.26	0.191	16.0	182	0.040

Moreover, polymerisation of 2,2,2-trifluoroethyl methacrylate (TFEMA) was attempted. Similarly to *i*BMA, SEC analysis suggests that TFEMA did polymerise (Figure 3.22)

however, the obtained value for M_n was considerably lower than the theoretical (12300 g mol^{-1} compared to 17200 g mol^{-1}). Moreover, relatively high dispersity (1.37) indicates that such monomers represent the limits of hydrophobicity for the present conditions (Table 3.16). Notably, in this case, THF SEC had to be employed instead of CHCl_3 SEC as the similar refractive index (RI) of the formed polymer to the solvent did not allow reliable characterisation.

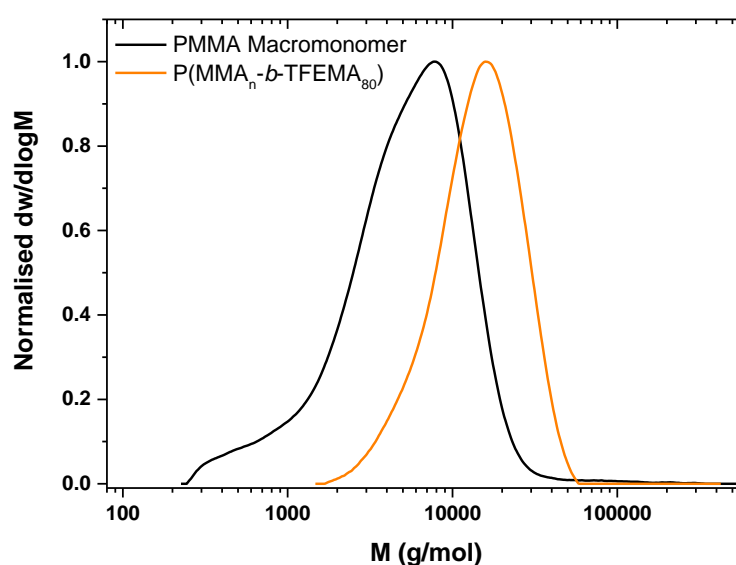


Figure 3.22: THF SEC traces of the pMMA macromonomer and the corresponding P(MMA_n-b-TFEMA₈₀) diblock prepared in emulsion.

Table 3.16: Data for the free radical polymerisation of TFEMA in the presence of PMMA macromonomer ($DP_n=80$) in emulsion.

Entry	Employed CTA	Conv. (%)	M_n , NMR ($\text{g}\cdot\text{mol}^{-1}$)	M_n , SEC ($\text{g}\cdot\text{mol}^{-1}$)	\bar{D}	S.C. ($\text{g}\cdot\text{mL}^{-1}$)	% wt solids	Particle Diameter (nm)	\bar{D}_{DLS}
1	CoBF	>99	3800	4600	1.53	0.115	11.12	107	0.049
2	PMMA	>99	19200	12300	1.37	0.194	18.06	149	0.078

3.3 Conclusions

In summary, the scope of sequence-controlled methacrylic multi block copolymers *via* SF-RAFT was expanded to include a broader range of chain transfer agents, namely PMMA, PEMA, PBMA and PBzMA. The synthesis of the macromonomers was successful by either changing the catalyst type and/or optimising the catalyst concentration. Subsequently all macromonomers were shown to efficiently catalyse the synthesis of sequence-controlled methacrylic multi block copolymers consisting of both lower and higher targeted degrees of polymerisation per block. Importantly, all multi blocks were synthesised in one pot *via* sequential monomer additions achieving very high monomer conversions and narrow molar mass distributions. In addition, both lower and higher M_n macromonomers were employed for the synthesis of complex multi blocks with the lower M_n ones achieving much higher efficiency thus highlighting the potential and the limitations of this system.

3.4 Experimental

3.4.1 Materials and Methods

Materials. Bis[(difluoroboryl) dimethylglyoximato]cobalt(II) (CoBF) was previously synthesised in the Haddleton Group as described in literature.⁴⁸ Methyl methacrylate (Aldrich, 99 %), ethyl methacrylate (Aldrich, 99 %), butyl methacrylate (Aldrich, 99 %), benzyl methacrylate (Aldrich, 96 %), 2-ethylhexyl methacrylate (Aldrich, 98 %), 4,4'-azobis(4-cyanovaleric acid) (Aldrich, ≥ 98 %) and potassium persulfate (Aldrich, 99.99 %) and sodium dodecyl sulfate (MP Biomedicals, LLC) were used as received.

3.4.2 Instrumentation

SEC analysis was performed on an Agilent 1260 SEC-MDS. The detectors included differential refractive index (DRI), light scattering (LS) and viscometry (VS). The columns were 2 x PLgel 5 mm mixed-D (300 x 7.5 mm), 1 x PLgel 5 mm guard column (50 x 7.5 mm). The instrument was equipped with an autosampler. Narrow linear poly(methyl methacrylate) standards of molecular weights between 200-1.0 x 10⁶ g mol⁻¹ were used to calibrate the system between 960 and 1,568,000 g mol⁻¹. All samples were passed through 0.45 µm PTFE filter in order to remove any residual catalyst. The mobile phase was chloroform with 2 % triethylamine at a flow rate of 1.0 mL min⁻¹. SEC data was analysed by the use of Cirrus v3.3 software. Matrix assisted laser desorption ionisation mass spectrometry (MALDI-ToF-MS) was conducted by the use of a Bruker Daltonics Ultra flex II MALDI-ToF-MS mass spectrometer, equipped with a nitrogen laser delivering 2 ns laser pulses at 337 nm with positive ion ToF detection performed using an accelerating voltage of 25 kV. Solutions were prepared as follows: *trans*-2-[3-(4-*tert*-Butylphenyl)-2-methyl-2-propenylidene]malononitrile (DCTB) as matrix (20 mg mL⁻¹), sodium iodide as cationisation agent (6 mg mL⁻¹) in tetrahydrofuran (20 µL) and sample (1, 5, 10 mg mL⁻¹) were mixed, and 0.5 µL of the mixture was applied on the target plate. Spectra recording was made in linear mode calibrating PEG-Me 1,900 Da. ¹H NMR spectra were recorded on Bruker DPX-300 spectrometer using a mixture of deuterated solvents (chloroform/acetone=3/2) for the latex samples and deuterated chloroform for the dry samples. Deuterated solvents were obtained from Aldrich. Chemical shifts are given in ppm downfield from the internal standard tetramethylsilane. DLS measurements were performed on a Malvern instrument Zetasizer Nano Series instrument. The detection angle was 173°. The intensity weighted mean hydrodynamic size (Z-average) and the width of particle size distribution (\mathcal{D}_{DLS}) were obtained by analysing the autocorrelation function. 1 µL

of latex was diluted with 1 mL of deionised water previously filtered with 0.20 μm membrane to remove any dust or other particulates. A minimum of 3 measurements were performed for each sample at 25 °C with an equilibrating time of 2 min before starting measurement.

3.4.3 General procedures

(a) Synthetic process for the preparation of PMMA macromonomer by CCTP in emulsion.

For a standard CCTP in emulsion, bis[(difluoroboryl) dimethylglyoximato]cobalt(II) (CoBF, 7.5 mg) and a stirring bar were charged into a 100 mL round bottom flask. Nitrogen was purged in the flask for at least 1 h. Subsequently, MMA (20 mL, 18.72 g, 186.98 mmol) previously deoxygenated for at least 30 min was added to the flask *via* a deoxygenated syringe. The mixture was stirred under nitrogen atmosphere until total dissolution of the solid. Meanwhile, 4,4'-azobis(4-cyanovaleric acid) (CVA, 0.5 g, 1.7839 mmol), sodium dodecyl sulphate (SDS, 0.3 g, 1.0403 mmol) and 130 mL of deionised water were charged into a three-neck, 500 mL double jacketed reactor, equipped with a RTD thermometer and an overhead stirrer. The mixture was bubbled with nitrogen and stirred at 325 rpm for at least 30 min. Subsequently, the mixture was heated under inert atmosphere. When the temperature of the mixture reached 70 °C, the addition of the MMA-CoBF solution started by the use of a deoxygenated syringe and a syringe pump (feeding rate = 0.666 mL min⁻¹, feeding time = 30 min). After the end of the addition, stirring continued for another 30 min under the same temperature and stirring rate. Then, the temperature settings were adjusted to 107 °C in order to achieve a temperature higher than 80 °C in the mixture. Stirring continued for 60 min at 325 rpm. The number average molecular weight of the macromonomer was calculated by analysing the ¹H NMR spectra.

(b) General process for the application of methacrylic macromonomers as CTA agents in Free-Radical polymerisation of methacrylic monomers in emulsion. The amount of monomer to be subsequently added to the methacrylic macromonomer was calculated according to the targeted DP . For each addition, the volume of aqueous KPS solution added was equal to that of monomer. The reactions were stopped and the latexes were diluted with water, when solid content reached values above which coagulation was considered likely to occur. After every dilution, the solid content was measured (in g mL^{-1}) by gravimetry and the value was taken into account for calculating the amounts of monomer, initiator and water of the next addition.

3.4.4 Numerical data

Table 3.17: Characterisation data for the macromonomers synthesised *via* CCTP in emulsion and subsequently employed as CTAs in free radical polymerisation of BMA ($DP_n=80$) in emulsion.

Monomer	Catalyst	Mass of catalyst (mg)	[catalyst] (ppm)	Conv. ^a (%)	M_n^b ¹ H-NMR	$M_{n, SEC}$ ($\text{g}\cdot\text{mol}^{-1}$)	\mathcal{D}	Particle Diameter ^c (nm)	\mathcal{D}_{DLS}
MMA	CoBF	3	42	>99	4,300	5,200	1.52	108	0.050
EMA	CoBF	4.0	65	99	4,300	5,000	1.57	111	0.086
BzMA	Co(MePh)BF	32.5	400	>99	4,400	3,400	1.78	161	0.025
BMA	Co(MePh)BF	29.5	340	>99	4,200	8,500	1.42	52	0.040

[a]: conversion was measured by diluting the polymer latex with a mixture of deuterated solvents (chloroform/deuterated acetone=3/2)

[b]: DP_n and M_n by ¹H NMR were measured by dissolving the isolated polymer in deuterated chloroform

[c]: polymer particle size, expressed as hydrodynamic diameter, measured by DLS

Table 3.18: Experimental conditions used for the preparation of the undecablock copolymer in emulsion at 85 °C with potassium persulfate as initiator, utilising PBMA macromonomer as CTA.

Cycle	Monomer	DP_n targeted	M monomer added (g)	M_{CTA} added (g)	m_{KPS} added (mg)	V_{H_2O} added (mL)	V_{total} (mL) ^[a]	S.C. (g·mL ⁻¹)	% wt solids
2	BzMA	10	1.884	4.62	9.055	1.811	112.691	0.058	5.46
3	EHMA	10	2.039	6.347	11.52	2.304	112.295	0.075	6.95
4	BMA	10	1.402	8.184	7.84	1.568	111.163	0.086	7.94
5	BzMA	10	1.770	9.354	8.51	1.702	110.165	0.101	9.17
6 ^b	EHMA	10	0.851	4.75	4.8	0.961	114.961	0.049	4.65
7	BMA	10	0.585	5.469	3.27	0.654	112.915	0.054	5.09
8	BzMA	10	0.738	5.908	3.545	0.709	110.924	0.060	5.65
9	EHMA	10	0.795	6.484	4.49	0.898	109.122	0.067	6.25
10	BMA	10	0.546	7.098	3.055	0.611	107.033	0.071	6.67
11	BzMA	10	0.688	7.452	3.305	0.661	104.994	0.078	7.19

[a]: after the end of each cycle, a sample of 2.7 mL was taken. The amount of CTA removed from the system was taken into account for the calculations of the next cycle

[b]: 50 mL of the latex of cycle 5 were diluted to 4 % wt of solids by adding 64.0 mL of H₂O

Table 3.19: Experimental conditions used for the preparation of the nonablock copolymer in emulsion at 85 °C with potassium persulfate as initiator, utilising PEMA macromonomer as CTA.

Cycle	Monomer	DP_n targeted	M monomer added (g)	M_{CTA} added (g)	m_{KPS} added (mg)	V_{H_2O} added (mL)	V_{total} (mL) ^[a]	S.C. (g·mL ⁻¹)	% wt solids
2	EHMA	25	6.263	5.2	35.39	7.077	88.544	0.129	11.46
3	BMA	25	4.145	10.728	23.18	4.636	87.480	0.170	14.53
4	BzMA	25	4.984	13.904	23.96	4.792	86.572	0.218	17.91
5	EHMA	25	5.190	17.645	29.32	5.864	86.736	0.263	20.84
6 ^b	BMA	25	2.654	16.575	14.85	2.969	262.644	0.073	6.82
7	BzMA	25	3.346	18.813	16.09	3.217	260.161	0.085	7.85
8	EHMA	25	3.631	21.675	20.52	4.103	258.564	0.098	8.91
9	BMA	25	2.499	24.747	13.98	2.795	255.659	0.107	9.63

[a]: after the end of each cycle, a sample of 5.7 mL was taken. The amount of CTA removed from the system was taken into account for the calculations of the next cycle

[b]: 75 mL of the latex of cycle 5 were diluted to 6 % wt of solids by adding 184.675 mL of H₂O

Table 3.20: Experimental conditions used for the preparation of the nonablock copolymer in emulsion at 85 °C with potassium persulfate as initiator, utilising PBzMA macromonomer as CTA.

Cycle	Monomer	DP_n targeted	M monomer added (g)	M_{CTA} added (g)	m_{KPS} added (mg)	V_{H_2O} added (mL)	V_{total} (mL) ^[a]	S.C. (g.mL ⁻¹)	% wt solids
2	BMA	50	5.591	3.46	31.27	6.254	118.127	0.077	7.12
3	BzMA	50	6.873	8.612	34.04	6.808	119.035	0.130	11.51
4	EHMA	50	7.348	14.744	41.52	8.303	121.638	0.182	15.37
5 ^b	BMA	50	1.488	6.32	8.32	1.664	100.677	0.078	7.20
6	BzMA	50	1.869	7.597	8.98	1.797	99.774	0.095	8.67
7	EHMA	50	2.021	9.210	11.42	2.284	99.358	0.113	10.16
8 ^c	BMA	50	0.554	4.36	3.1	0.620	102.56	0.047	4.46
9	BzMA	50	0.696	4.787	3.34	0.669	103.229	0.053	5.04

[a]: after the end of each cycle, a sample of 5.7 mL was taken. The amount of CTA removed from the system was taken into account for the calculations of the next cycle

[b]: 40 mL of the latex of cycle 4 were diluted to 6 % wt of solids by adding 59.013 mL of H₂O [c]: 40 mL of the latex of cycle 7 were diluted to 4 % wt of solids by adding 64.640 mL of H₂O

Table 3.21: Experimental conditions used for the preparation of the tetrablock copolymer in emulsion at 85 °C with potassium persulfate as initiator, utilising high M_n PMMA macromonomer as CTA.

Cycle	Monomer	DP_n targeted	M monomer added (g)	M_{CTA} added (g)	m_{KPS} added (mg)	V_{H_2O} added (mL)	V_{total} (mL) ^[a]	S.C. (g.mL ⁻¹)	% wt solids
2	BMA	10	0.638	5.25	3.57	0.714	97.764	0.059	5.54
3	BzMA	10	0.803	5.729	3.86	0.772	98.536	0.066	6.22
4	EHMA	10	0.863	6.354	4.88	0.976	96.812	0.075	6.94

[a]: after the end of each cycle, a sample of 2.7 mL was taken. The amount of CTA removed from the system was taken into account for the calculations of the next cycle

Table 3.22: Experimental conditions used for the preparation of the pentablock copolymer in emulsion at 85 °C with potassium persulfate as initiator, utilising PBMA macromonomer as CTA.

Cycle	Monomer	DP_n targeted	M monomer added (g)	M_{CTA} added (g)	m_{KPS} added (mg)	V_{H_2O} added (mL)	V_{total} (mL) ^[a]	S.C. (g.mL ⁻¹)	% wt solids
2	BzMA	10	3.561	13.97	17.12	3.424	129.154	0.136	11.95
3	EHMA	10	3.859	17.164	21.8	4.360	130.814	0.161	13.85
4	BMA	10	2.661	20.588	14.89	2.977	131.091	0.177	15.06
5 ^b	BzMA	10	2.752	18.59	13.23	2.646	169.956	0.126	11.16

[a]: after the end of each cycle, a sample of 2.7 mL was taken. The amount of CTA removed from the system was taken into account for the calculations of the next cycle

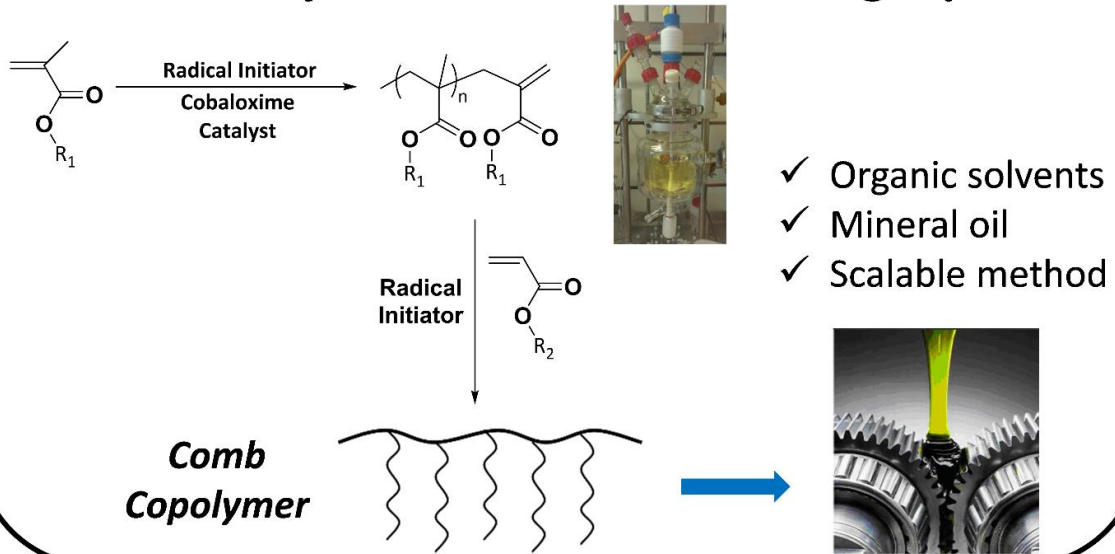
[b]: 110 mL of the latex of cycle 4 were diluted to 10 % wt of solids by adding 57.31 mL of H₂O

3.5 References

1. J.-F. Lutz, *Polym. Chem.*, 2010, **1**, 55-62.
2. R. B. Merrifield, *J. Am. Chem. Soc.*, 1963, **85**, 2149-2154.
3. S. Ida, T. Terashima, M. Ouchi and M. Sawamoto, *J. Am. Chem. Soc.*, 2009, **131**, 10808-10809.
4. M. Zamfir, and J.-F. Lutz, *Nat. Comm.*, 2012, **3**, 1138.
5. J. Vandenbergh, G. Reekmans, P. Adriaensens and T. Junkers, *Chem. Sci.*, 2015, **6**, 5753-5761.
6. J. Vandenbergh, G. Reekmans, P. Adriaensens and T. Junkers, *Chem. Commun.* 2013, **49**, 10358-10360.
7. K. Nakatani, Y. Ogura, Y. Koda, T. Terashima and M. Sawamoto, *J. Am. Chem. Soc.*, 2012, **134**, 4373-4383.
8. S. Ida, M. Ouchi and M. Sawamoto, *J. Am. Chem. Soc.*, 2010, **132**, 14748-14750.
9. S. Pfeifer and J.-F. Lutz, *J. Am. Chem. Soc.*, 2007, **129**, 9542-9543.
10. Y. Guo, J. Zhang, P. Xie, X. Gao and Y. Luo, *Polym. Chem.*, 2014, **5**, 3363-3371.
11. N. Badi and J.-F. Lutz, *Chem. Soc. Rev.*, 2009, **38**, 3383-3390.
12. R. McHale, J. P. Patterson, P. B. Zetterlund and R. K. O'Reilly, *Nat. Chem.*, 2012, **4**, 491-497.
13. M. Minoda, M. Sawamoto and T. Higashimura, *Macromolecules*, 1990, **23**, 4889-4895.
14. M. Ueda, *Prog. Polym. Sci.* 1999, **24**, 699-730.
15. E. Bayer and M. Mutter, *Nature*, 1972, **237**, 512-513.
16. J. C. Barnes, D. J. C., Ehrlich, A. X. Gao, F. A. Leibfarth, Y. Jiang, E. Zhou, F. T. Jamison and J. A. Johnson, *Nat. Chem.*, 2015, **7**, 810-815.
17. J. Lawrence, S.-H. Lee, A. Abdilla, M. D. Nothling, J. M. Ren, A. S. Knight, C. Fleischmann, Y. Li, A. S. Abrams, B. V. K. G. Schmidt, M. C. Hawker, L. A. Connal, A. J. McGrath, P. G. Clark, W. R. Gutekunst and C. J. Hawker, *J. Am. Chem. Soc.*, 2016, **138**, 6306-6310.
18. B. van Genabeek, B. F. M. de Waal, M. M. J. Gosens, L. M. Pitet, A. R. A. Palmans and E. W. Meijer, *J. Am. Chem. Soc.*, 2016, **138**, 4210-4218.
19. J.-F. Lutz, M. Ouchi, D. R. Liu and M. Sawamoto, *Science*, 341, 1238149 (2013), DOI:10.1126/science.1238149
20. M. Ouchi, N. Badi, J.-F. Lutz and M. Sawamoto, *Nat. Chem.*, 2011, **3**, 917-924.
21. A. H. Soeriyadi, C. Boyer, F. Nyström, P. B. Zetterlund and M. R. Whittaker, *J. Am. Chem. Soc.*, 2011, **133**, 11128-11131.
22. C. Boyer, A. H. Soeriyadi, P. B. Zetterlund and M. R. Whittaker, *Macromolecules*, 2011, **44**, 8028-8033.
23. C. Boyer, A. Derveaux, P. B. Zetterlund and M. R. Whittaker, *Polym. Chem.*, 2012, **3**, 117-123.

24. A. Anastasaki, V. Nikolaou, G. S. Pappas, Q. Zhang, C. Wan, P. Wilson, T. P. Davis, M. R. Whittaker and D. M. Haddleton, *Chem. Sci.*, 2014, **5**, 3536-3542.
25. A. Anastasaki, V. Nikolaou, N. W. McCaul, A. Simula, J. Godfrey, C. Waldron, P. Wilson, K. Kempe and D. M. Haddleton, *Macromolecules*, 2015, **48**, 1404-1411.
26. Y.-M. Chuang, A. Ethirajan and T. Junkers, *ACS Macro Lett.*, 2014, **3**, 732-737.
27. F. Alsubaie, A. Anastasaki, P. Wilson and D. M. Haddleton, *Polym. Chem.*, 2015, **6**, 406-417.
28. G. Gody, T. Maschmeyer, P. B. Zetterlund and S. Perrier, *Nat. Commun.*, 2013, **4**.
29. G. Gody, T. Maschmeyer, P. B. Zetterlund and S. Perrier, *Macromolecules*, 2014, **47**, 639-649.
30. G. Gody, M. Danial, R. Barbey and S. Perrier, *Polym. Chem.*, 2015, **6**, 1502-1511.
31. G. Gody, T. Maschmeyer, P. B. Zetterlund and S. Perrier, *Macromolecules*, 2014, **47**, 3451-3460.
32. A. P. Haehnel, M. Schneider-Baumann, K. U. Hildebrandt, A. M. Misske and C. Barner-Kowollik, *Macromolecules*, 2013, **46**, 15-28.
33. J. M. Asua, S. Beuermann, M. Buback, P. Castignolles, B. Charleux, R. G. Gilbert, R. A. Hutchinson, J. R. Leiza, A. N. Nikitin, J.-P. Vairon and A. M. van Herk, *Macromol. Chem. Phys.*, 2004, **205**, 2151-2160.
34. S. Beuermann, M. Buback, T. P. Davis, R. G. Gilbert, R. A. Hutchinson, A. Kajiwara, B. Klumperman and G. T. Russell, *Macromol. Chem. Phys.*, 2000, **201**, 1355-1364.
35. S. Beuermann, M. Buback, T. P. Davis, R. G. Gilbert, R. A. Hutchinson, O. F. Olaj, G. T. Russell, J. Schweer and A. M. van Herk, *Macromol. Chem. Phys.*, 1997, **198**, 1545-1560.
36. S. M. Chin, H. He, D. Konkolewicz and K. Matyjaszewski, *J. Polym. Sci., Part A: Polym. Chem.* 2014, **52**, 2548-2555.
37. A. Anastasaki, C. Waldron, P. Wilson, C. Boyer, P. B. Zetterlund, M. R. Whittaker and D. M. Haddleton, *Acs Macro Lett.*, 2013, **2**, 896-900.
38. A. Anastasaki, V. Nikolaou, G. S. Pappas, Q. Zhang, C. Wan, P. Wilson, T. P. Davis, M. R. Whittaker and D. M. Haddleton, *Chem. Sci.*, 2014, **5**, 3536-3542.
39. A. Anastasaki, V. Nikolaou, N. W. McCaul, A. Simula, J. Godfrey, C. Waldron, P. Wilson, K. Kempe and D. M. Haddleton, *Macromolecules*, 2015, **48**, 1404-1411.
40. N. G. Engelis, A. Anastasaki, G. Nurumbetov, N. P. Truong, V. Nikolaou, A. Shegiwal, M. R. Whittaker, T. P. Davis and D. M. Haddleton, *Nat. Chem.*, **2017**, **9**, 171-178.
41. D. M. Haddleton, D. R. Maloney and K. G. Suddaby, *Macromolecules*, 1996, **29**, 481-483.
42. L. Hutson, J. Krstina, C. L. Moad, G. Moad, G. R. Morrow, A. Postma, E. Rizzardo and S. H. Thang, *Macromolecules*, 2004, **37**, 4441-4452.
43. C. L. Moad, G. Moad, E. Rizzardo and S. H. Thang, *Macromolecules*, 1996, **29**, 7717-7726.
44. K. G. Suddaby, D. M. Haddleton, J. J. Hastings, S. N. Richards and J. P. O'Donnell, *Macromolecules*, 1996, **29**, 8083-8091.
45. J. P. A. Heuts and N. M. B. Smeets, *Polym. Chem.*, 2011, **2**, 2407-2423.
46. G. Gody, P. B. Zetterlund, S. Perrier and S. Harrisson, *Nat. Commun.*, 2016, **7**.
47. G. Nurumbetov, N. Engelis, J. Godfrey, R. Hand, A. Anastasaki, A. Simula, V. Nikolaou and D. M. Haddleton, *Polym. Chem.*, 2017, **8**, 1084-1094.
48. A. Bakac and J. H. Espenson, *J. Am. Chem. Soc.*, 1984, **106**, 5197-5202.

Oil soluble comb-like polymers *via* CCTP as viscosity modifiers for lubricating liquids

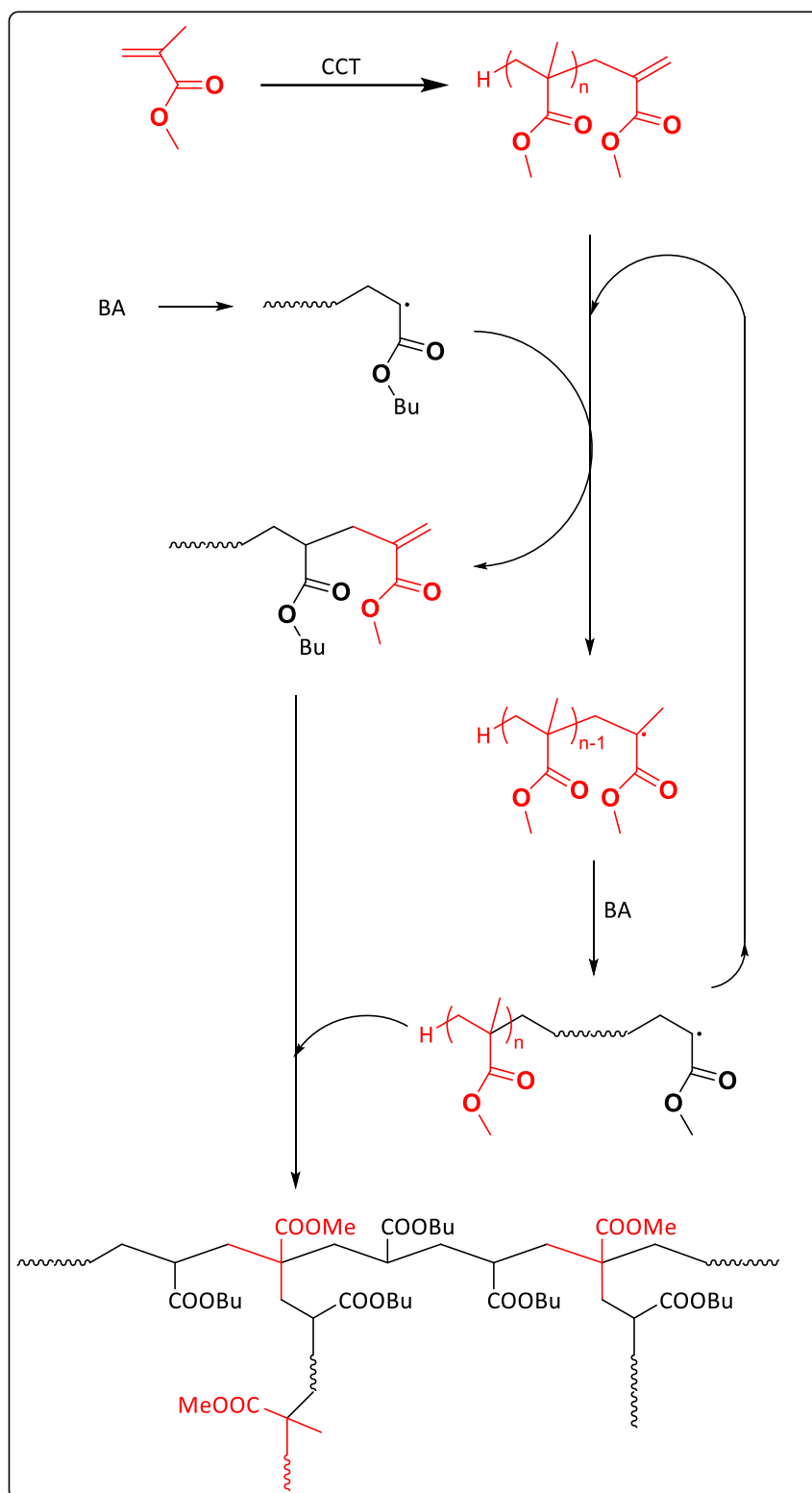


Oils provide essential functions for the smooth running of an engine and viscosity is one of the key functions. When the latter is too low, excessive wear will result as well as heat generation caused by mechanical friction. Similarly, if the viscosity is high the flow of the oil will be restricted, obstructing its ability to lubricate. Viscosity typically reduces with increasing temperature; while an ideal lubricant should maintain a constant viscosity across the temperature range in which the engine operates. Viscosity modifiers (VM) are employed as to reduce the extent of viscosity increase at lower temperatures and reduce the extent of viscosity decrease at higher ones. When large molecules such as polymers are dissolved in a solvent, the motion of smaller molecules (including those of the solvent) is constrained thus increasing the internal friction of the fluid and finally the viscosity. The higher the molecular weight of the added molecule, the greater the viscosity increase.

4.1 Introduction

Complex polymeric architectures such as star, comb, cyclic, hyperbranched polymers and dendrimers have attracted interest as they provide considerably diverse properties compared to linear structures. These diverse properties may include melting temperatures, hydrodynamic volumes *etc.* Mechanical properties of such polymers are also of interest as comb and brush copolymers have demonstrated resistance to compression and aggregation as well as dissipation to shear stress.¹

Comb-shaped polymers consist of a main polymer chain (backbone) and side chains attached to it, the branches. Usually, the composition as well as the physicochemical properties of the backbone and the branches differ. Although in most cases the distribution of branches across the main chain is random, studies have also focused on the synthesis of well-defined structures.² Generally, for the preparation of random comb copolymers, three strategies have been developed. “Grafting from”, “grafting onto” and “grafting through” (also referred to as the macromonomer method). In the “grafting from” method, active sites along an already synthesised backbone initiate the polymerisation of a second monomer thus, resulting in the formation of branches.² The “grafting onto” method is based on the separate preparation of the main chain and the branches and the subsequent reaction between functional groups of the chain and active chain ends of the branches.³ Finally, in the “grafting through” method, preformed macromonomers are copolymerised with another monomer. The polymerisation of the latter is going to form the backbone while the copolymerisation of the macromonomers active chain ends (vinyl ω -ends) leads to the incorporation of the branches. This description is rather an oversimplification and a proposed mechanism is shown in Scheme 4.1.⁴



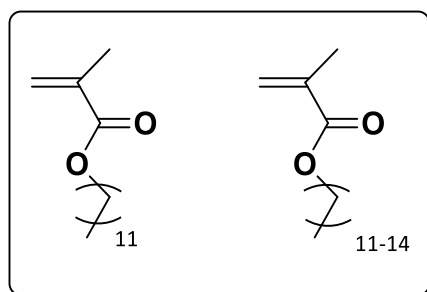
Scheme 4.1: Proposed mechanism for the graft copolymerisation of *n*-BA with methyl methacrylate macromonomer.⁴

Lubrizol as sponsors of this work are particularly interested in the mechanical properties of comb copolymers and as such had a request for the optimisation of the synthesis of combs utilising the “grafting through” method. The macromonomers employed for the synthesis of combs would preferably be prepared by CCTP and consisting of hydrophobic monomers as the optimisation of the process was considered by Lubrizol in organic media. Specifically, the study would focus on a mixture of long chain methacrylic monomers (C_{12} - C_{15}) used in industry. The aim was to optimise the parameters in order to be able to target a specific range of molecular weights for the macromonomers. Moreover, for the formation of the backbone, an acrylic monomer had to be considered, as, acrylates are known for forming combs when reacting with methacrylic macromonomers,⁴⁻⁶ and thus *n*-butyl acrylate (*n*-BA) was chosen. In parallel, there was particular interest in performing the synthesis in mineral oil as an alternative to conventional organic solvents making the method appealing for industrial applications. Ultimately, comb copolymers are considered as an additive to lubricating liquids. It should be noted here that the main focus of this chapter is the presentation of a general overview of the project, which is ongoing and funded by the Lubrizol Corporation. As such, its applications as well as some other parameters will not be discussed in detail. Nevertheless, some aspects of the optimisation of the synthesis of combs, as well as the corresponding synthesis in mineral oil will be discussed.

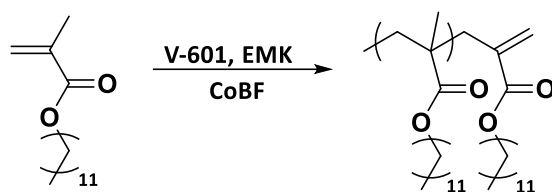
4.2 Initial Results

4.2.1 Attempts in organic solvent

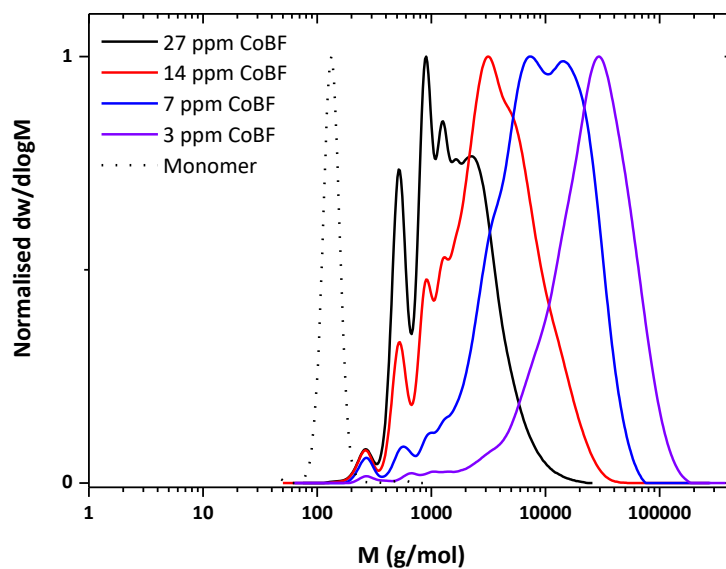
Following the “grafting through” method, low molecular weight macromonomers ($M_n \approx 2000 \text{ g mol}^{-1}$) were targeted, consisting of a mixture of long chain methacrylic monomers (C_{12} - C_{15}), later to serve as teeth in the comb structures. Initially, solution polymerisation was considered and studies employed lauryl methacrylate as a model monomer due to its structural similarities to the aforementioned mixture of monomers (Scheme 4.1). Moreover, ethyl methyl ketone and V-601 (2.8 % in respect to monomer concentration) were employed as the solvent and an oil soluble initiator respectively. Different amounts of bis(boron difluorodimethylglyoximate)cobalt (CoBF) were tested in order to estimate its efficiency. As predicted, higher amounts of catalyst resulted in polymeric products of lower molecular weight (Table 4.1, Figure 4.1).



Scheme 4.2: Chemical structures of lauryl methacrylate (LMA) and mixture of methacrylic monomers used in industry.

Table 4.1: Characterisation data for the synthesis of PLMA macromonomers in EMK.

[CoBF] (ppm)	Time (h)	Conversion (%)	$M_{n,SEC}$ (g.mol ⁻¹)	\bar{D}
3	1	74	23000	1.56
	2	91	20500	1.65
	5	99	17300	1.88
	24	100	17400	1.87
7	1	69	9000	1.69
	2	87	6100	2.15
	5	98	5300	2.37
	24	99	4400	2.82
14	1	61	2800	2.07
	2	81	2400	2.14
	5	96	2200	2.20
	24	99	1900	2.43
27	1	54	1600	2.02
	2	73	1300	1.65
	5	91	1200	1.67
	24	99	1100	1.74

**Figure 4.1:** SEC analysis of different MWt PLMA macromonomers, synthesised by diverse amounts of catalyst. The dot line shows the trace of the monomer.

Encouraged by the successful synthesis of macromonomers of M_n close to the desired value using lauryl methacrylate, the next step was the synthesis of macromonomers employing the mixture of long chain methacrylates (C_{12} - C_{15}) provided by Lubrizol. One of the particularities of the mixture is that the exact amount of each monomer is not accurately known. As a result, a relative catalyst concentration, estimated in mg per mL (mg mL^{-1}) of monomer was employed instead of a more precise expression such as ppm. Due to the aforementioned issue, the initiator concentration was also roughly estimated. At first, the reaction was performed using a stock solution with a concentration of 0.031 mg mL^{-1} . The obtained product had a molecular weight of 1800 g mol^{-1} and a dispersity of 1.59, close to the targeted value (2000 g mol^{-1}). The same reaction was then repeated in a higher scale (200 mL of monomer) yielding a large amount of macromonomer solution, later to be used for comparative studies in the copolymerisation stage. In order to secure efficient stirring for the scaled-up reaction, a reactor equipped with overhead stirrer was employed (Figure 4.2) SEC traces of the macromonomers confirmed that both scales provided identical products (Figure 4.3).



Figure 4.2: The 0.5 L reactor equipped with overhead stirrer, used for the synthesis of the methacrylic macromonomer in large scale.

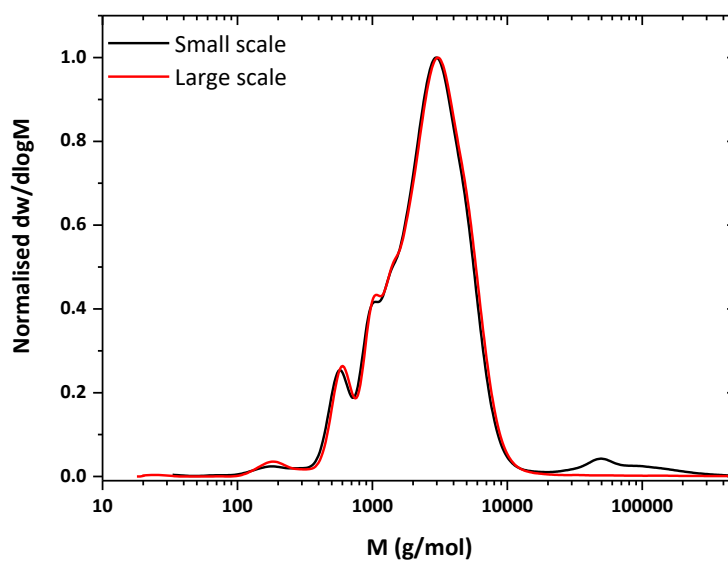


Figure 4.3: SEC analysis of PLMA macromonomers, synthesised in 20 and 200 mL monomer scale using the same amount of catalyst.

Subsequently, the macromonomer was reacted in a series of experiments with different amounts of an acrylic monomer each time. Notably, at this stage initiators generating oxygen-centred radicals were necessary as these species are known for deactivating cobaloximes.⁷ Thus, the catalyst would not be active anymore and due to low concentration employed, there would be no need for purification. The polymerisation of the latter, acrylic monomer would form the backbone and *n*-BA was employed. In order to estimate the effect of the ratio between macromonomer and acrylic monomer, macromonomer aliquots were reacted with 20, 40, 60, 80 and 100 eq of *n*-BA.

As seen on Table 4.2, full monomer conversion was achieved in all cases. Concerning the molecular weight of the obtained polymers, unexpectedly, the highest value was observed for the addition of 60 eq (Figure 4.4), higher than the one observed for the 100 eq addition (33900 to 23500 g mol⁻¹). This result could possibly be attributed to a higher teeth density throughout the backbone, in other words to the formation of a comb copolymer with more teeth. With respect to dispersity, comb-like structures are generally characterised by high values. However, the extremely high values obtained for samples prepared by 80 and 100 eq of *n*-BA indicated the formation of chemical species with very different molar masses during the reaction.

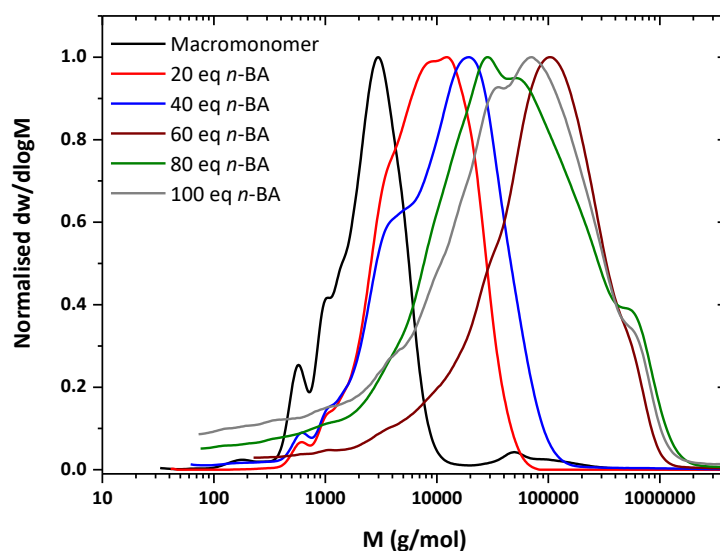


Figure 4.4: CHCl_3 SEC traces of the combs produced by different ratios of *n*-BA to macromonomer.

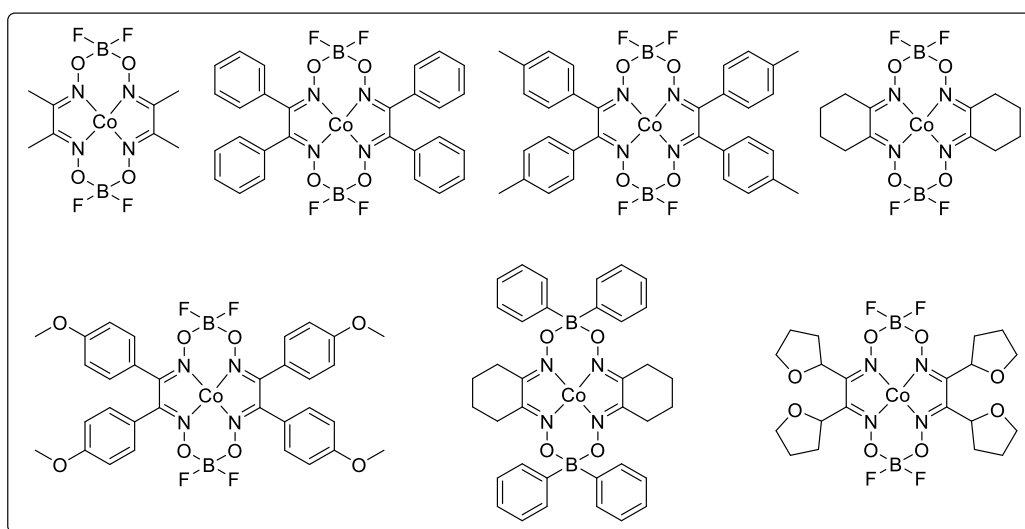
Table 4.2: Summary of results for the synthesis of combs.

Eq. of <i>n</i> -BA	Conversion (%)	M_n ($\text{g}\cdot\text{mol}^{-1}$)	\mathcal{D}
20	100	5100	2.3
40	100	7000	2.9
60	100	33900	4.4
80	100	12000	10.1
100	100	23500	5.3

4.2.2 Attempts in mineral oil

After successfully synthesizing combs with branches consisting of methacrylic macromonomers with long pendant aliphatic chain in organic solvent, the next target was to repeat the process in a solvent widely applied in industry and more appropriate for the desired applications. Specifically, it was thought that by performing the same process in mineral oil instead of EMK, the wider application of comb copolymers as additives in lubricants would be facilitated as such products are often based on mineral oils.

Initially, it was hypothesised that the whole process could be identical to the one performed in EMK. However, solubility issues of the catalyst in the mineral oil had detrimental effects on the employed process and a new method had to be designed. Initially, the solubility of various cobaloximes was tested. Theoretically, this would allow the synthesis to be performed as in EMK, as the different side groups of the catalyst govern the solubility of the molecule without affecting the catalytic cycle/mechanism. However, as none of the tested derivatives (Scheme 4.2) was soluble in the new reaction medium, the process had to be appropriately altered. It was then assumed that the catalyst could be introduced into the reaction mixture by dissolving it in the monomer. Subsequently, the solubility of the catalyst in the mixture of monomers was tested. Among the catalysts tested, only $\text{Co}(\text{MePh})\text{BF}$ was soluble in the monomer mixture, allowing the synthesis in mineral oil, with V-601 being employed as initiator.



Scheme 4.3: Structures of the cobaloximes tested for solubility in mineral oil.

The macromonomer synthesis method should be robust and reliable even when different monomers would be employed or higher molecular weights would be targeted. In order to ensure catalyst dissolution for various conditions, the introduction of MMA in the monomer mixture was considered. This monomer is known for solubilising several cobaloxime catalysts of different hydrophobicity such as CoBF,⁸ cycCoBF,⁹ CoPhBF,¹⁰⁻¹² and its ratio in the mixture would be limited. In detail, the new mixture would consist of 15 % MMA and 85 % mixture of long chain methacrylic monomers (w/w). This new mixture could also solubilise the catalyst. Although the molecular weight of the produced macromonomer was close to the desired range of values (2300 g mol⁻¹), full conversion was not achieved (Figure 4.5). Nonetheless, this was not considered as a major drawback since any residual monomer or macromonomer were expected to copolymerise in the second step which is the comb formation.

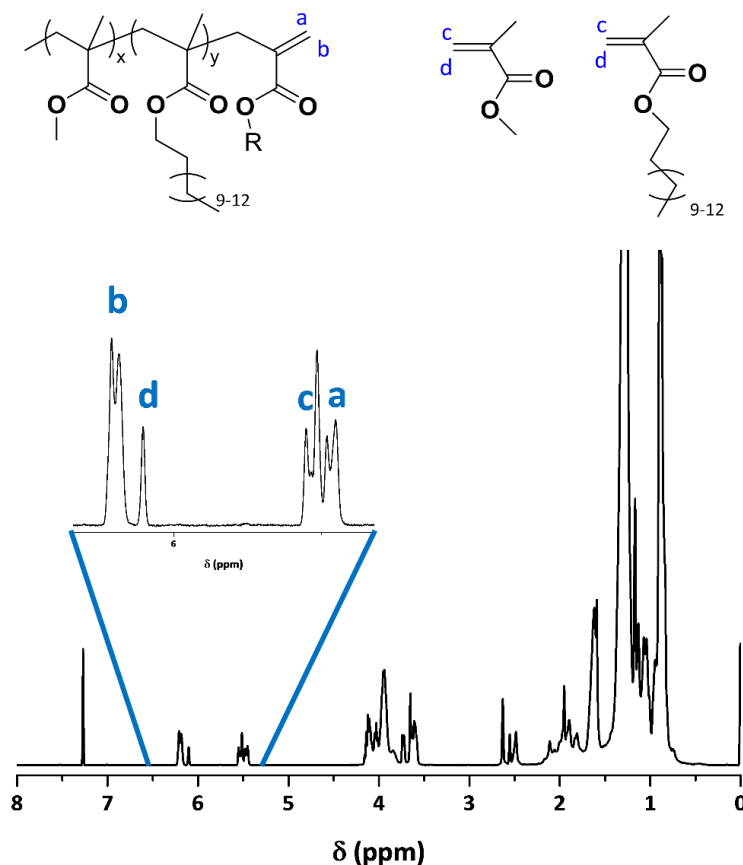


Figure 4.5: ^1H NMR spectrum of the reaction mixture of the macromonomer synthesis. Residual monomer peaks are visible.

Subsequently, comb synthesis was attempted. Following the change of solvent, the reaction process had to be modified. Again, the use of an initiator that would generate oxygen-centred radicals was considered necessary as such species deactivate Co^{II} catalysts that remain in the reaction mixture. Benzoyl peroxide was again chosen as the initiator. Previously, it was dissolved in the solvent (EMK) and the solution was added simultaneously with the acrylic monomer into the macromonomer solution under stirring. However, as benzoyl peroxide was insoluble in the mineral oil, it was dissolved in the acrylic monomer (*n*-BA) and fed with it in the reaction mixture.

As previously in EMK, different amounts of *n*-BA to macromonomer were tested in order to assess the effect of acrylic monomer to macromonomer ratio on the final product.

Reactions with 20, 40, 60, 80 and 100 eq. of *n*-BA were performed. Quite importantly, in all cases, the final monomer as well as macromonomer conversion were full, as proved by the complete absence of vinyl peaks on the ^1H NMR spectrum in the 6.5-5 ppm area (Figure 4.6). With regards to molecular weights and dispersities, it was noted that increased amount of acrylate resulted in higher weight average molecular weights (M_w) and \mathcal{D} values as, in all cases, number average molecular weight (M_n) had very similar values (8600-10000 g mol^{-1} , Table 4.3, Figure 4.7).

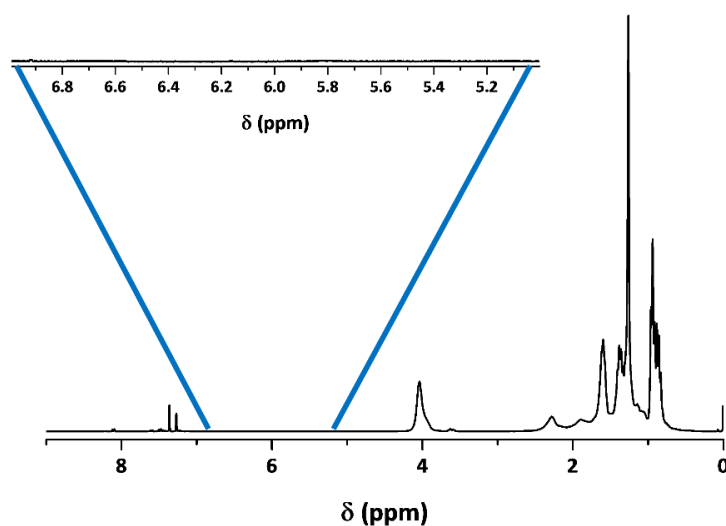


Figure 4.6: ^1H NMR spectrum of the final product of comb synthesis. The absence of peaks between 5 and 6.5 ppm indicate the complete conversion of all monomers and the macromonomer.

Table 4.3: Summary of results for the synthesis of combs in mineral oil.

Eq. of <i>n</i> -BA	M_n ($\text{g}\cdot\text{mol}^{-1}$)	M_w ($\text{g}\cdot\text{mol}^{-1}$)	\mathcal{D}
20	8600	16700	1.9
40	9300	67000	7
60	10000	183000	18
80	9400	171000	18
100	9500	282000	29

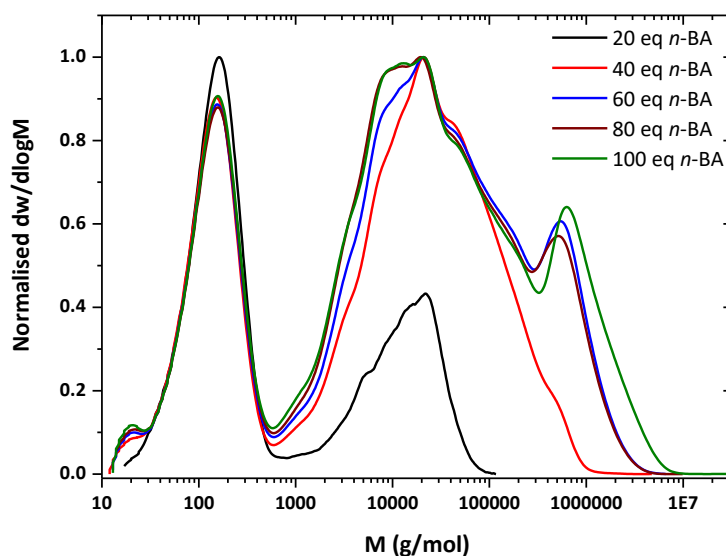


Figure 4.7: CHCl_3 SEC traces of comb copolymers synthesised in mineral oil. The low molecular weight, narrow peak is the mineral oil employed as solvent.

The extremely high dispersity values obtained by CHCl_3 SEC led to the conclusion that the product was a mixture of structures of massively different molecular weights and the reaction process would be rather inconsistent. Judging by the results presented in Table 4.3, it was considered that the macromonomer was fully consumed relatively early during the reaction and subsequently homopolymerisation of *n*-BA as well as unavoidable crosslinking was taking place. As a result, the amount of *n*-BA that would be enough to cause full macromonomer consumption was considered as the key parameter for the synthesis of combs of narrower dispersity. In order to point out that exact amount of *n*-BA, necessary to quantitatively react with the macromonomer, kinetic experiments were planned. Moreover, it was considered that the amount of *n*-BA would probably differ to some extent, depending on the rate of addition. Therefore, three different addition rates were tested, 0.5, 0.25 and 0.1 mL min^{-1} . The accuracy of the addition rate was secured by the use of a syringe pump, as depicted in previous chapter. Monitoring would be based on ^1H NMR spectroscopy as the

statistical macromonomer generates a distinguishable peak at 6.21 ppm (Figure 4.8). Thus, disappearance of that peak would indicate full consumption of the macromonomer. It has to be noted that in order to achieve more accurate results, sampling frequency was adjusted according to the addition rate each time. The ultimate target of this kinetic study would be to enable the synthesis of combs by ceasing *n*-BA addition slightly before full macromonomer consumption. This would allow the preparation of products with similar structures and similar molecular weights.

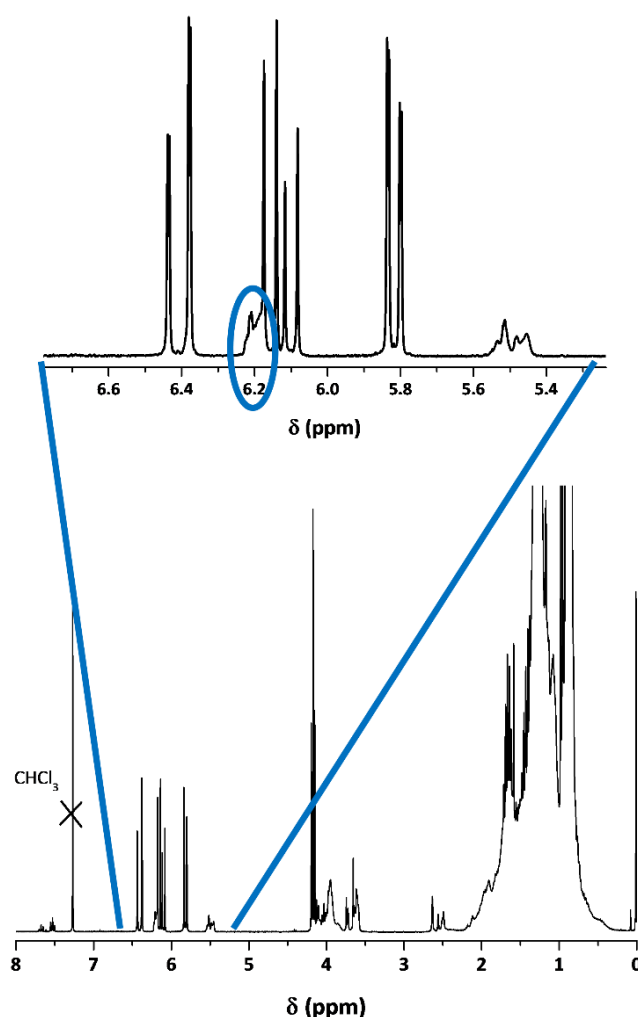


Figure 4.8: ¹H NMR spectrum of the reaction mixture during the addition of *n*-BA. The narrow peak at 6.21 ppm corresponding to the macromonomer allowed monitoring during the kinetic study.

4.2.3 Kinetics of synthesis (feeding rate 0.1 mL min⁻¹)

Initially feeding rate was 0.1 mL per minute and sampling was performed every 30 min. As shown on Table 4.4 M_n is evolving until a certain timepoint (210 min). Subsequently, this value remains practically constant (within the error of the instrument) while M_w increases (Table 4.4, Figure 4.9). The macromonomer peak at 6.21 ppm was not observed at the 180 min sample. By that time, 14.9 eq of *n*-BA were added. Notably, \mathcal{D} increases considerably on later samples. Finally, values become extremely high thus, indicating that rather uncontrolled reactions are taking place.

Table 4.4: Summary of results for the synthesis of combs in mineral oil (feeding rate 0.1 mL min⁻¹).

Sample	M_n (g.mol ⁻¹)	M_w (g.mol ⁻¹)	\mathcal{D}
30	2000	2600	1.4
60	2200	3100	1.4
90	3200	5500	1.7
120	5700	12300	2.2
150	10800	26700	2.5
180	14800	48300	3.3
210	16100	66900	4.1
240	15300	75000	4.0
270	13200	81000	6.1
300	13500	88000	6.5
330	12600	97000	7.7
360	13000	106000	8.2
390	11200	121000	11
420	10700	138000	13

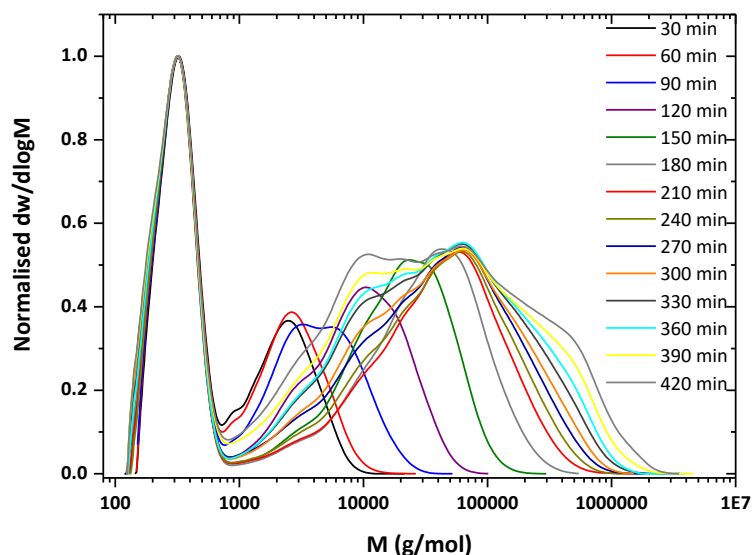


Figure 4.9: CHCl_3 SEC traces showing the evolution of molecular weight during the addition of acrylate by 0.1 mL min^{-1} rate.

4.2.4 Kinetics of synthesis (feeding rate 0.25 mL min^{-1})

Sampling for 0.25 mL min^{-1} feeding rate was performed every 20 min. The results in this case are very similar to those obtained by applying the slower addition rate (Table 4.5). In detail, considerable increase in \mathcal{D} is noted just after the total consumption of the macromonomer (Table 4.5, Figure 4.10). However, macromonomer consumption was observed earlier in this case, at 80 min when 16.5 eq of *n*-BA had been added.

Table 4.5: Summary of results for the synthesis of combs in mineral oil (feeding rate 0.25 mL min^{-1}).

Sample	$M_n \text{ (g.mol}^{-1}\text{)}$	$M_w \text{ (g.mol}^{-1}\text{)}$	\mathcal{D}
Macromonomer	1300	1900	1.4
20	1800	2500	1.4
40	2200	3300	1.6
60	4200	9500	2.3
80	11100	32000	2.9
100	20600	79000	3.8
120	21900	115000	5.3
140	20100	130000	6.5
160	20900	139000	7.1
180	21900	176000	8

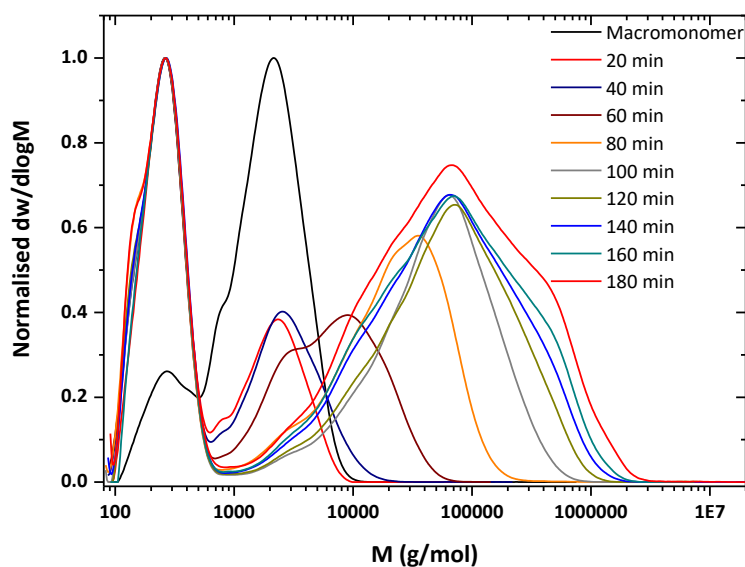


Figure 4.10: CHCl_3 SEC traces showing the evolution of molecular weight during the addition of acrylate by 0.25 mL min^{-1} rate.

4.2.5 Kinetics of synthesis (feeding rate 0.5 mL min^{-1})

Sampling for 0.5 mL min^{-1} feeding rate was performed every 10 min. Observations are in accord with the aforementioned feeding rates with regards to molecular weight evolution and \mathcal{D} values (Table 4.6, Figure 4.11). In this case, ^1H NMR spectroscopy showed that total macromonomer consumption occurred at 50 min, by the addition of 20.7 eq of *n*-BA.

Table 4.6: Summary of results for the synthesis of combs in mineral oil (feeding rate 0.5 mL min⁻¹).

Sample	M_n (g.mol ⁻¹)	M_w (g.mol ⁻¹)	\bar{D}
Macromonomer	1300	1900	1.4
10	1900	2600	1.3
20	2100	3000	1.4
30	3100	5600	1.9
40	7200	18900	2.6
50	15500	44800	2.9
60	28100	88000	3.1
70	30300	108000	3.6
80	23400	108000	4.6
90	21300	118000	5.5
100	21600	134000	6.2
110	20600	144000	7

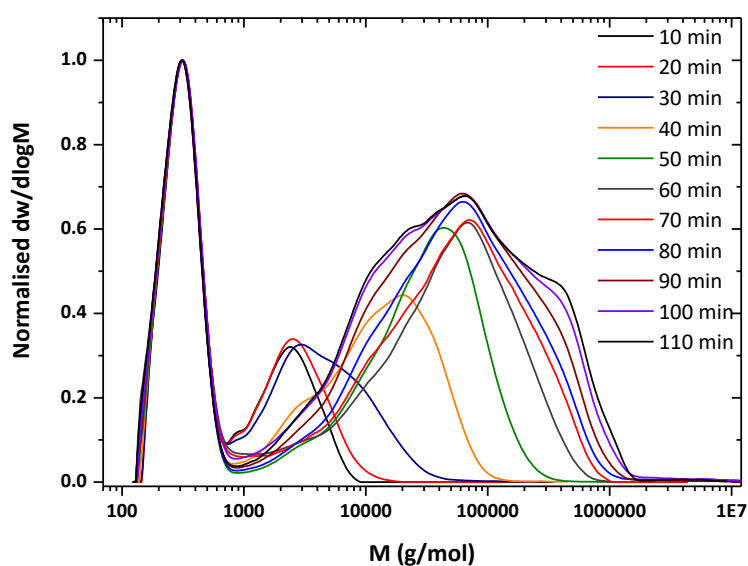


Figure 4.11: CHCl₃ SEC traces showing the evolution of molecular weight during the addition of acrylic monomer by 0.5 mL min⁻¹ rate.

4.2.6 Summary for the kinetic studies (0.1, 0.25 and 0.5 mL min⁻¹)

In all three kinetic experiments, the observations were in agreement in terms of the evolution of molecular weights and molecular weight distributions. After the disappearance of the free macromonomer species from the reaction mixture, M_n remained practically constant while M_w increased significantly thus, causing increased \mathcal{D} values. As shown in Figure 4.14, \mathcal{D} values increase in an exponential manner after macromonomer consumption. This fact supports the assumption that homopolymerisation of *n*-BA and uncontrolled chain transfer to polymer (intermolecular as well as intramolecular) are taking place. An interesting observation however, was that full macromonomer consumption occurred at different times (also meaning different amounts of *n*-BA added) for different feeding rates. This indicates that the rate of addition was higher than the rate of propagation of the acrylate, at least for the two higher rates of addition, if not for all.

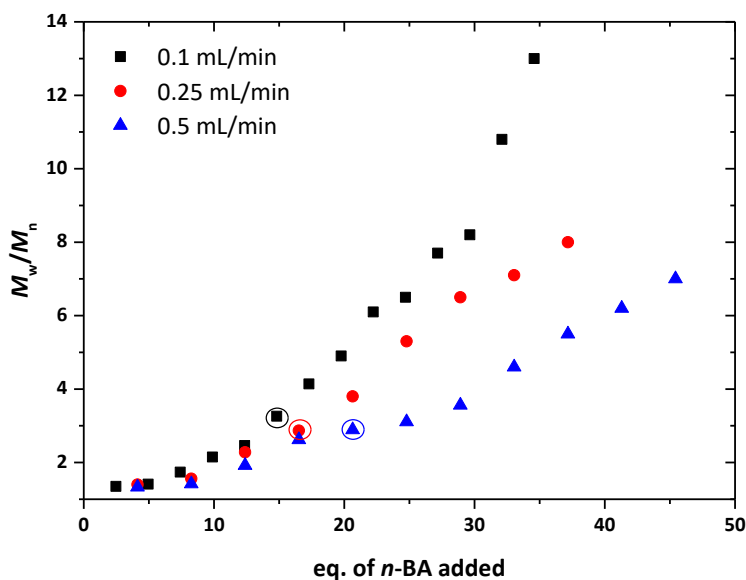


Figure 4.12: Evolution of \mathcal{D} in function with the eq of *n*-BA added for the three different addition rates. The cycles on the graph indicate the point where full macromonomer conversion was observed.

Table 4.7: Summary of results for the kinetic experiments. Characterisation data correspond to the samples taken at points of full macromonomer conversion.

Rate (mL.min ⁻¹)	Eq/min	Time (min)	Volume (mL)	Eq of <i>n</i> -BA	<i>M_n</i> (g.mol ⁻¹)	<i>M_w</i> (g.mol ⁻¹)	<i>D</i>
0.1	0.083	180	18	14.9	14800	48900	3.3
0.25	0.207	80	20	16.5	11100	32200	2.9
0.5	0.413	50	25	20.7	15500	44900	2.9

4.3 Conclusions & future work

This chapter is an ongoing work in collaboration with the Lubrizol Corporation. Therefore, only a few initial findings are presented and discussed. Further characterisation and testing for the synthesised comb copolymers are currently carried out in the Lubrizol site. Moreover, further studies on the optimisation of comb copolymer synthesis in mineral oil need to take place as to facilitate its application in industry. It was demonstrated that comb synthesis can be performed in mineral oil although modifications on the process are necessary to yield similar results as observed for traditional organic solvent systems.

4.4 Experimental

4.4.1 Materials and Methods

Chemicals were purchased from Sigma Aldrich and used as received unless otherwise stated. The mixture of long-chain methacrylic monomers (C₁₂-C₁₅) was provided by the Lubrizol Corporation. Monomers were passed through a column of basic alumina prior to use in polymerisations to remove inhibitors and other impurities. Bis(boron difluorodimethylglyoximate)cobalt (CoBF) and bis(boron difluorodimethylphenylglyoximate)cobalt [Co(MePh)BF] were synthesised as described

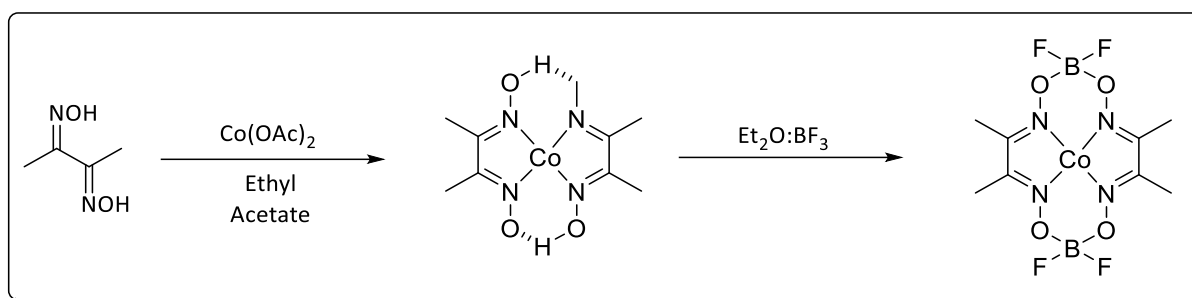
below, while other cobaloximes were previously synthesised in the Haddleton Group according to procedures described in literature.¹³

4.4.1.1 Synthesis of Bis(boron difluorodimethylglyoximate)cobalt (CoBF)

The synthesis was adapted from a reported procedure. In order to obtain anhydrous cobalt(II) acetate, cobalt(II) acetate tetrahydrate (22 g) and a stirrer bar were charged to a 100 mL round bottom flask, topped with a connector containing glass wool and cotton wool (as to avoid contaminating the vacuum line). The round bottom flask was then placed in an oilbath (100 °C) under vacuum (10^{-2} mbar) and the salt was stirred overnight. 14.8 g of anhydrous cobalt(II) acetate were obtained.

In a Schlenk tube equipped with a magnetic stirring bar, anhydrous cobalt acetate (CoAc, 12.200 g, 68.92 mmol) and dimethylglyoxime (12.805 g, 110.272 mmol) were mixed and degassed by bubbling with N₂ for 1 h. Subsequently, ethyl acetate (100 mL) was added and the mixture was vigorously stirred. Boron trifluoride diethyl etherate (BF₃Et₂O, 29.77 mL, 34.236 g, 241.22 mmol) was added dropwise and the mixture was heated up to 50 °C for 30 min. The mixture was allowed to cool down to room temperature and sodium hydrogen bicarbonate (9.032 g, 107.513 mmol) was added in portions as to avoid excessive frothing. Subsequently, the mixture was placed in an icebath and stirred for 1 h to allow the product to crystallize. Filtering was followed by washing with water methanol and ethyl acetate. Ethyl acetate was then removed at the rotary evaporator and the product was dried in vacuum oven.

Product: 10.5 g (39.6 % yield)



Scheme 4.4: General scheme for the synthesis of CoBF.

4.4.1.2 Synthesis of Bis(boron difluorodimethylphenylglyoximate)cobalt [Co(MePh)BF]

Preparation of 4,4'-dimethylbenzyl glyoxime

In a 250 mL round bottom flask placed in icebath, an aqueous solution of sodium hydroxide (40 g, 1009.7 mmol, 196.3 mL H₂O) was mixed with an aqueous solution of hydroxylamine hydrochloride (22 g, 2.33 mmol, 41.7 mL). The mixture was stirred for 30 min and subsequently ethanol (1 mL) and 4,4'-dimethylbenzyl (22 g, 92.33 mmol) were added. The resulting yellow solution was heated at 80 °C for 3 h in an oilbath. Subsequently, it was cooled down to 30 °C, transferred to a three neck round bottom flask and bubbled with carbon dioxide (CO₂) for 2 h by the use of dry ice and air blow. The white precipitate was dispersed in water (100 mL) and stirred for 30 min. Then was filtered, washed with water (2x40 mL) and dried in vacuum. The solid was then dispersed in methanol (160 mL) and was allowed to stir at ambient temperature for 12 h. The insoluble E:E isomer was then filtered, washed with methanol and redispersed in water for 1 h. Subsequently, the white solid was filtered, washed with water (2x20 mL) and methanol (2x20 mL). The volatiles were removed *in vacuo*. The product was obtained in 50.9 % yield (12.6 g).

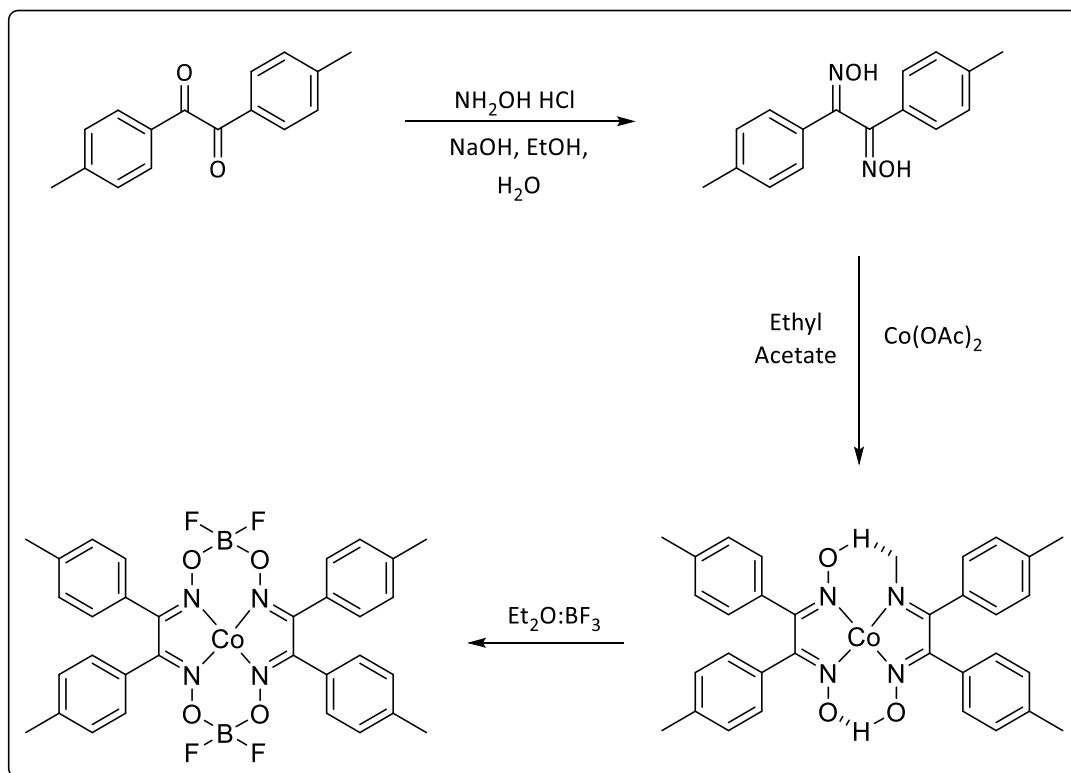
¹H -NMR (AcD₆, 298 K, MHz): δ 10.14 (s, 2 H), 7.08 (d, 4 H), 6.92 (d, 4 H), 1.77 (s, 6 H)

Co(MePh)BF

The synthesis was adapted from a reported procedure. In order to obtain anhydrous cobalt(II) acetate, cobalt(II) acetate tetrahydrate (10 g) and a stirrer bar were charged in a 100 mL round bottom flask, topped with a connector containing glass wool and cotton wool (as to avoid contaminating the vacuum line). The round bottom flask was then placed in an oilbath (100 °C) and the salt was stirred overnight. 6.9 g of anhydrous cobalt(II) acetate were obtained.

In a Schlenk tube equipped with a magnetic stirring bar, anhydrous cobalt acetate (CoAc, 4.982 g, 28.14 mmol) and 4,4'-dimethylbenzyl glyoxime (10.733 g, 45.04 mmol) were mixed and degassed by bubbling with N₂ for 1 h. Subsequently, ethyl acetate (100 mL) was added and the mixture was vigorously stirred. Boron trifluoride diethyl etherate (BF₃Et₂O, 12.23 mL, 14.06 g, 99.09 mmol) was added dropwise and the mixture was heated up to 50 °C for 30 min. The mixture was allowed to cool down to room temperature and sodium hydrogen bicarbonate (3.69 g, 43.92 mmol) was added in portions as to avoid excessive frothing. Subsequently, the mixture was placed in an icebath and stirred for 1 h to allow the product to crystallize. Filtering was followed by washing with water methanol and ethyl acetate. Ethyl acetate was then removed at the rotary evaporator and the product was dried in vacuum oven.

Product: 11.7 g (60.3 % yield)



Scheme 4.5: General scheme for the synthesis of $\text{Co}(\text{MePh})\text{BF}$.

4.4.2 Instrumentation

^1H NMR spectra were recorded on a Bruker DPX-300 or DPX-400 using deuterated chloroform (CDCl_3) obtained from Aldrich. Chemical shifts are given in ppm downfield from the internal standard tetramethylsilane. Size exclusion chromatography (SEC) measurements were conducted using an Agilent 1260 GPC-MDS system fitted with differential refractive index (DRI), light scattering (LS) and viscometry (VS) detectors equipped with 2 x PLgel 5mm mixed-D columns (300 x 7.5 mm), 1 x PLgel 5 mm guard column (50 x 7.5 mm) and autosampler. Narrow polydispersity linear poly(methyl methacrylate) standards in range of 200 to $1.0 \times 10^6 \text{ g mol}^{-1}$ were used to calibrate the system. All samples were passed through a $0.45 \mu\text{m}$ PTFE filter before analysis. The mobile phase was chloroform with 2% trimethylamine eluent at a flow rate of 1.0 mL min^{-1} . SEC data was analysed using Cirrus v3.3

software with calibration curves produced using Varian Polymer Laboratories Easi-Vials linear poly(methyl methacrylate) standards ($200\text{--}4.7 \times 10^5 \text{ g mol}^{-1}$). Controlled rate additions were performed using a Harvard Apparatus PHD ULTRA double syringe pump.

4.4.3 General procedures

4.4.3.1 Preparation of CCT agent stock solution for solution polymerisation

In a typical CCTP procedure, an amount of CoBF higher than 15 mg was weighted and placed in a 100 mL round bottom flask together with a stirring bar. Nitrogen was purged in the flask for at least 1 h. Subsequently, an accurate volume of previously degassed solvent was added to the flask using a degassed syringe. The mixture was vigorously stirred under inert atmosphere until total dissolution of the catalyst.

4.4.3.2 CCTP in solution for the synthesis of PMMA macromonomer

Ethyl methyl ketone (20 mL), lauryl methacrylate (20 mL, 17.36 g, 68.23 mmol), V-601 initiator (204 mg, 0.88699 mmol) and a stirrer were charged in a 100 mL round bottom flask. The mixture was purged with nitrogen for at least 45 min. An appropriate amount of previously degassed CCT agent stock solution was added using a degassed syringe and the mixture was immersed in a pre-heated oilbath (73 °C) for 24 h. A sample was taken for $t=0$ just before the flask was placed into the oil bath.

4.4.3.3 Comb copolymer synthesis in solution

Benzoyl peroxide (2 g, 8.256 mmol) was dissolved in ethyl methyl ketone (60 mL) and the mixture was purged with nitrogen for 30 min. The macromonomer solution was used as obtained by CCTP (42.5 mL containing 21.75 mmol of macromonomer) and purged with nitrogen for 30 min. *n*-Butyl acrylate (60 mL, 53.64 g, 418.5 mmol) was also purged with nitrogen for 30 min. Subsequently, the macromonomer solution was placed in a pre-heated oil bath (73 °C) and the addition of the monomer and the initiator solution started by the use of a syringe pump (feeding rate: 1 mL min⁻¹, feeding time: 1 h). Stirring under constant T continued for 90 min after the end of the addition.

4.5 References

1. P. Tian, D. Uhrig, J. W. Mays, H. Watanabe and S. M. Kilbey, *Macromolecules*, 2005, **38**, 2524-2529.
2. N. Hadjichristidis, M. Pitsikalis, S. Pispas and H. Iatrou, *Chem. Rev.*, 2001, **101**, 3747-3792.
3. R. Barbey, L. Lavanant, D. Paripovic, N. Schüwer, C. Sugnaux, S. Tugulu and H.-A. Klok, *Chem. Rev.*, 2009, **109**, 5437-5527.
4. J. P. A. Heuts and N. M. B. Smeets, *Polym. Chem.*, 2011, **2**, 2407-2423.
5. P. Cacioli, D. G. Hawthorne, R. L. Laslett, E. Rizzardo and D. H. Solomon, *J. Macromol. Sci., Part A: Pure Appl. Chem.*, 1986, **23**, 839-852.
6. K. J. Abbey, D. L. Trumbo, G. M. Carlson, M. J. Masola and R. A. Zander, *J. Polym. Sci., Part A: Polym. Chem.*, 1993, **31**, 3417-3424.
7. A. A. Gridnev and S. D. Ittel, *Chem. Rev.*, 2001, **101**, 3611-3660.
8. R. A. Sanayei and K. F. O'Driscoll, *J. Macromol. Sci., Part A: Pure Appl. Chem.*, 1989, **26**, 1137-1149.
9. D. M. Haddleton, D. R. Maloney, K. G. Suddaby, A. V. G. Muir and S. N. Richards, *Macromol. Symp.*, 1996, **111**, 37-46.
10. J. P. A. Heuts, D. J. Forster, T. P. Davis, B. Yamada, H. Yamazoe and M. Azukizawa, *Macromolecules*, 1999, **32**, 2511-2519.
11. J. P. A. Heuts, D. J. Forster and T. P. Davis, *Macromolecules*, 1999, **32**, 3907-3912.
12. J. P. A. Heuts, D. J. Forster and T. P. Davis, *Macromol. Rapid Commun.*, 1999, **20**, 299-302.
13. A. Bakac and J. H. Espenson, *J. Am. Chem. Soc.*, 1984, **106**, 5197-5202.

Conclusions & Outlook

The main focus of this thesis was to expand the employment of methacrylic macromonomers, derived from CCTP as CTAs. Initially, the use of PMMA macromonomers was considered in emulsion polymerisation. The preparation of methacrylic multi block copolymers was achieved by exploiting the compartmentalisation effect, as expressed in dispersed systems and the consequent fast polymerisation of methacrylates. After synthesising a heneicosablock multi block homopolymer deriving from BMA with narrow molecular weight distribution ($M_n=27800 \text{ g mol}^{-1}$, $\mathcal{D}=1.20$), the preparation of a true multi block copolymer ($M_n=29500 \text{ g mol}^{-1}$, $\mathcal{D}=1.35$) of 21 blocks was achieved by the inclusion of BzMA and EHMA in the primary structure. Subsequently, the efficiency of the technique was proved by the synthesis of an undecablock copolymer, comprising of blocks with ever increasing DP_n , from 5 to 50. Moreover, all employed monomers supported equally well the propagation of the subsequent block, proving the versatility of the system. Last but not least, another complex structure comprised of 7 long blocks ($DP_n=45$, $M_n=41300 \text{ g mol}^{-1}$, $\mathcal{D}=1.24$) was prepared in large scale thus highlighting the potential of the technique with regards to industry.

Despite the successful preparation of multi block copolymers, there were still doubts about the range of monomers that could be employed both for the preparation of the CTA as well as for the chain extensions. Emulsion polymerisation is known for requiring sparingly water-soluble monomers and thus, the compatibility of the monomers with the present system was also investigated. The monomer pool that allowed successful CCTP in emulsion for the synthesis of macromonomers (CTAs) was expanded (from MMA initially) to include EMA, BMA and BzMA. Importantly, all four macromonomers proved to be equally efficient as

CTAs and allowed very similar levels of control over polymerisations ($1.20 < \bar{D} < 1.28$ for equal DP_n). Although the demonstrated structures were limited to 11 blocks, the similarity of the obtained results allows the consideration that even if more chain extensions were performed (as in the case of the PMMA macromonomer), the level of control would still be comparable. Regarding chain extensions, *i*BMA sets the limits of hydrophobicity/hydrophilicity, as its blocks demonstrated broader molecular weight distributions compared to *n*BMA, despite reaching full conversion and showing clear shifts to higher molecular weights. Notably, for all complex structures mentioned above, NMR, SEC and DLS characterisations were performed for each block. In all cases, monomer conversions were quantitative or nearly quantitative (> 98 %) and there were clear shifts of the chromatograms to higher molar masses. Interestingly, DLS demonstrated a constant increase of the polymer particle sizes which followed an almost linear mode related to the molecular weight of the polymeric species.

Notably, the mechanism of interaction between methacrylic macromonomers and methacrylic monomers during the free radical polymerisation of the latter, had been previously reported. Its similarity to RAFT, combined with the lack of any sulphur-containing species (at least with regards to CTAs employed), allowed for the creation of the term Sulphur-Free RAFT.

The current status of the art for SF-RAFT allows for the synthesis of well-defined multi block copolymers derived from methacrylates. However, the fast polymerisation rates observed are mainly achieved thanks to the compartmentalisation effect. As such, obtaining similar results for methacrylates in solution seems unlikely. Nonetheless, performing SF-RAFT in solution, would enable the expansion of the monomer pool, as the limitation regarding specific hydrophobicity/hydrophilicity would no more apply. In addition, further research

should be conducted to investigate the effect of sequence-controlled polymers derived from methacrylates, as all studies up to date have been focusing on acrylates and acrylamides. The considerably higher T_g values of methacrylic homopolymers compared to their acrylic counterparts, are promising for new possibilities in both materials and biological applications.